

# THE TRANSITION

DESIGN AND ENGINEERING OF A  
SUSTAINABLE SOLAR CARPORT FOR  
THE 'NEDERLANDSE SPOORWEGEN'

J.A. DIJKEMA  
4652487



TU DELFT UNIVERSITY OF TECHNOLOGY  
ARCHITECTURE, URBANISM AND BUILDING SCIENCES  
BUILDING TECHNOLOGY TRACK  
YEAR 2018-2019



# ACKNOWLEDGEMENTS

First of all I would like to express my gratitude to my main mentor in this master thesis, Prof. dr. ir. A.A.J.F. van den Dobbelsteen, professor Climate Design & Sustainability at TU-Delft University, who guided my master thesis with his knowledge of sustainability and provided insights when needed. His enthusiasm in the field of solar design and sustainability were the motivation why I selected this master thesis. Secondly, I would like to thank, ir. P. Eigenraam, docent structural mechanics, who guided my through the structural analyses/calculations and parametric design. His guidance was of the greatest importance to me during this very crucial part of my graduation thesis. Without the guidance and supervision of both, this graduation thesis wouldn't be realized.

Also, I would like to thank my third mentor, Z. Haghghi MSc. His expertise in the field of solar design and insights on design aspects greatly contributed to the end result presented in this thesis.

Finally, I would like to thank Dr. Ir. Machteld Lamers for presenting, with great enthusiasm, this topic to me and for her helpful advice on the technical side of solar module design.



# ABSTRACT

The energy transition is a hot topic, businesses also need to think about manners to transition to sustainable energy. Within this graduation thesis, a stakeholder is involved named the 'Nederlandse Spoorwegen', in short NS. The stakeholder has the ambition to make their station's energy neutral. To achieve this, electricity generating assets needs to be implemented on every asset they own. One of these assets is the P+R parking plots near stations. An easy way of implementing solar into the parking plots is by integrating the solar panels into a carport structure. Current solar carport designs which have been constructed so far, are purely focusing on the aspect of generating the maximum amount of electricity and neglecting the aspect of design. The NS has the ambition to make the carport design sustainable in appearance and material use. Besides the sustainable appearance of the design, the design should be applicable in every P+R parking plots. This results in a modular sustainable carport design that is orientation independent.

For the design, a solar cell technology was needed. Three generations of solar cells were found in literature, but the third generation was not further researched since this generation isn't commercially available yet. The remaining two generations of solar cell technologies (1st and 2nd generation) were researched on the following topics; performance, design, and sustainability. The information found in this literature research directly fed the multi-criteria analysis (MCA) method called the analytical hierarchy process. With this MCA method, polycrystalline silicon solar cell technology was selected to be the best suitable for the design. Another downside to the current solar carport designs is that these designs don't fully exploit the structural capabilities of the solar panels. In the final design, a connection is designed and analyzed to exploit the structural capabilities of the solar panels, whilst still keeping the transparent nature of the solar panels intact.

The final design features recycled rail tracks in the structure of the carport. Besides being made from high-grade steel and the shape of the rail tracks suits their integrating into the structure, the direct link to the stakeholder was also recognized as a benefit for the final selection of this material. To further enhance the sustainable appearance/function of the carport, a green wall is implemented to absorb the rainwater. Thus, improving the water absorption in the asphalt dominated landscape of the P+R parking plots.

In particular, the design of the sustainable solar carport for the NS is analyzed on solar radiation performance and structural performance (on carport scale and on connection scale). To gain an understanding if the new connection is beneficial on a carbon footprint scale, the newly designed connection is compared to a standard aluminum transom and mullion system.



# content

<b>1 </b>	<b>Introduction.....</b>	<b>[p. 9-19]</b>
	1.1. General topic and scope of the study	
	1.2. Solar cell technology	
	1.3. Analysis of solar carport designs	
	1.4. Bibliography	
<b>2 </b>	<b>Research Definition.....</b>	<b>[p. 20-32]</b>
	2.1. Nederlandse Spoorwegen	
	2.2. Problem statement	
	2.3. Research questions	
	2.4. Approach and methodology	
	2.5. Role of stakeholder	
	2.6. Timeplanning	
	2.7. Bibliography	
<b>3 </b>	<b>Solar technologies.....</b>	<b>[p. 33-54]</b>
	3.1. Introduction	
	3.2. First generation	
	3.3. Second generation	
	3.4. Performance	
	3.5. Design	
	3.6. Sustainability	
	3.7. Bifacial	
	3.8. Electrical connection	
	3.9. Bibliography	
<b>4 </b>	<b>Structural solar modules.....</b>	<b>[p. 55-71]</b>
	4.1. Introduction	
	4.2. Glass as load bearing material	
	4.3. Solar cell wafer	
	4.4. Structural capabilities PV	
	4.5. Mechanical connection	
	4.6. Mechanical connection integration in PV	
	4.7. Bibliography	
<b>5 </b>	<b>Pilot study.....</b>	<b>[p. 72-81]</b>
	5.1. Introduction	
	5.2. Design	
	5.3. Analysis design	
	5.4. Conclusion	
<b>6 </b>	<b>Case studies.....</b>	<b>[p. 82-93]</b>
	6.1. Introduction	
	6.2. Case studies	
	6.3. Conclusion	

<b>7 </b>	<b>Conceptual designs</b> .....	[p. 94-109]
	7.1. Introduction	
	7.2. Design brief	
	7.3. Structural materials	
	7.4. Conceptual designs	
	7.5. Design evaluation & choice	
	7.6. Bibliography	
<b>8 </b>	<b>Final design</b> .....	[p. 110-156]
	8.1. Introduction	
	8.2. Multi-criteria analysis	
	8.3. Final design	
	8.4. Design analysis	
	8.5. Connection analysis	
	8.6. Comparison connection with existing connection	
	8.7. Final conclusions and recommendations	
	8.8. Bibliography	
<b>9 </b>	<b>Personal reflection</b> .....	[p. 157-160]
	9.1. Personal reflection	



# **1. INTRODUCTION**

## 1.1 GENERAL TOPIC AND SCOPE OF THE STUDY

Maximizing the output of solar implemented designs often conflicts with the design parameter. These designs often angle the solar panels 35 degrees to the south (in the Netherlands) and neglect the aspect of design. Particularly solar carports use this design philosophy. This philosophy results in most of the solar carports having the same appearance.

Current carport designs don't fully exploit the structural capabilities of the glass in the solar panels. In those designs, the solar panels only act as an enclosure of the design, whilst the glass of the solar panels is more than capable to handle loads. Current research of structural capabilities of solar panels focuses on the ability to transfer wind- and snow load to the structure behind, whilst the integration of solar panels in a structural member is neglected.

The stakeholder in this graduation, the 'Nederlandse spoorwegen' (NS), is planning to integrate solar generating devices into their park and ride plots across the Netherlands. After analyzing the current products on the market the NS came to the conclusion that the current designs of solar carports don't reflect the image that is wished for by the NS.

This study focusses on a solar carport design for the application in park and ride plots aside NS stations across the whole Netherlands.

## 1.2 SOLAR CELL TECHNOLOGY

To gain understanding about solar cell technologies, the basics regarding the element of which a solar panel consists, how solar panels convert sunlight to energy and the basic terminology is explained in this chapter.

A photovoltaic module consists of smaller photovoltaic cells (fig. 1.2.2). These cells are connected to each other to create a cell string. This results in the cells being connected in series. By connecting the cells in series, the voltage rises whilst the ampere remains the same. This has the benefit that the cabling for the solar module can remain thinner and therefore less costly/heavy.

Photovoltaic cells convert the energy from the sun, photons, into electric energy, electrons. This is done by allowing the photons to extract electrons from atoms, generating a flow of energy. This flow of energy is directed to the front electrode towards the back electrode of the next cell in the string. Photovoltaic cells generate direct current, this DC current is often converted into alternating current. This AC current is what regular households use.

The energy produced in a panel exits the panel via a junction box. This junction box is a piece of technology that connects panel A to panel B and creates a string of panels. As previously mentioned, the panels create DC current and this is often converted in AC current. To convert this current a converter is used. This converter can be integrated at panel level into the junction box or at the end of a PV string.

The most commonly known solar cell technology is silicon wafer based. In (fig. 1.2.1.) a schematic view is given of how a silicon wafer-based solar cell works. A new generation of solar cells consists of thin film solar modules. As the name suggests, the conductor is applied in a thin layer. This has the benefit that the panels can be made flexible.

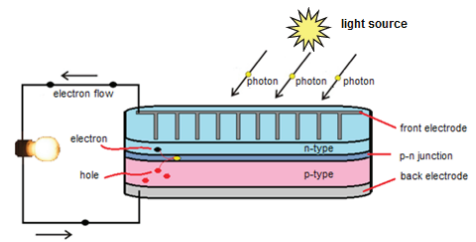


fig. 1.2.1: schematic structure of a silicon solar cell (source: InTech)

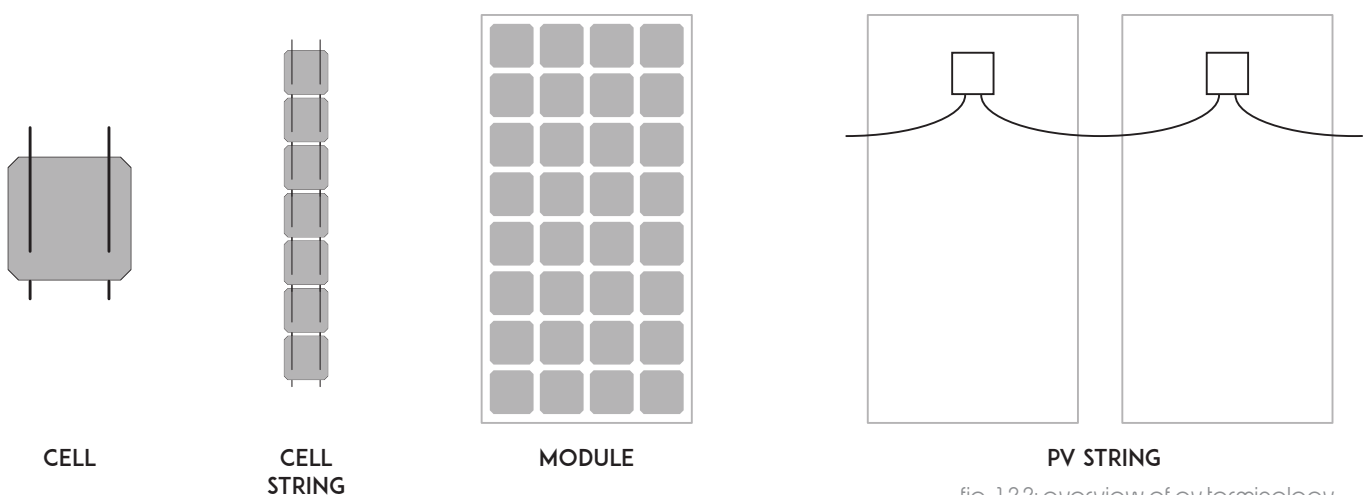


fig. 1.2.2: overview of pv terminology

The most commonly used structures of solar modules are either glass-back sheet (fig. 1.2.3) or glass-glass (fig. 1.2.4) structures. Both structures are the same except for the back sheet material. The structure goes as follows: Glass, EVA (encapsulant for lamination), Solar cells, EVA and back sheet material. In the glass-back sheet structure, the back sheet is made out of plastic and glass-glass out of glass. The benefits of a glass-glass module are the option for transparency and the added strength.

As previously mentioned there are flexible thin-film solar modules available. The active layers of these solar cell technologies are deposited on flexible substrates. The application thickness varies from a few nanometers to tens of micrometers, much thinner than the previously mentioned silicon wafer-based technologies (around 200 micrometers thick). The material of the substrate varies from steel, aluminum to plastic. Although the benefit of this technology is that it can be made flexible, rigid modules also exist.

To prevent dust accumulation and make us of the self cleaning possibilities of the solar panels, the minimal tilt to prevent major dust build up is 15 degrees<sup>[1.1]</sup>.

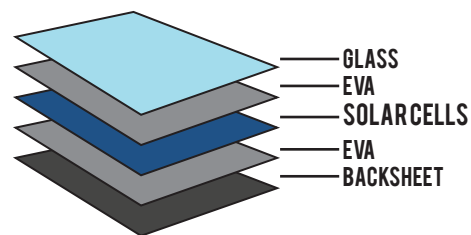


fig. 1.2.3: schematic structure of glass-backsheet solar module

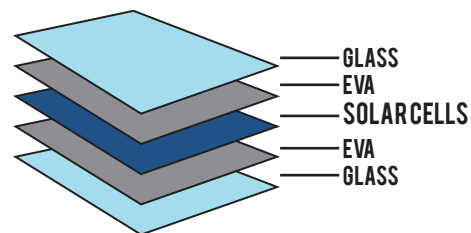


fig. 1.2.4: schematic structure of glass-glass solar module

## 1.3 ANALYSIS OF SOLAR CARPORT DESIGNS

In this section selected samples of current designs of carports are analyzed on their PV technology used, structural material, transparency, orientation, function and impact on the context surrounding the designs. The aim of this analysis is to gain knowledge of current carport designs and their intentions.

### Michigan state university carports



(source: MSU today)

### analysis

pv tech:	mono c-Si <sup>[1,2]</sup>
orientation:	East-West
function:	shelter for cars
structural material:	metal
impact on surrounding:	creates smaller space

### description

The Michigan State University (MSU) solar carports are the largest solar carport project in North America. In total 5000 parking spaces are covered by the design<sup>[1,2]</sup>. The design is mainly focused on electricity production. The east and west orientation in combination with a small inclination results in a high output of the structure. Other than the function of generating electricity, it also provides shelters for the cars below. The structure is made out of metal. The structural design of the carport makes the space look smaller. This is due to the crowded metal structure, the diagonal columns, the metal beams that extrude out of the design. By placing the foundation parallel to the parking spot, the impact on the functionality is kept to a minimum.

# Airport Weeze



(source: Airport weeze)

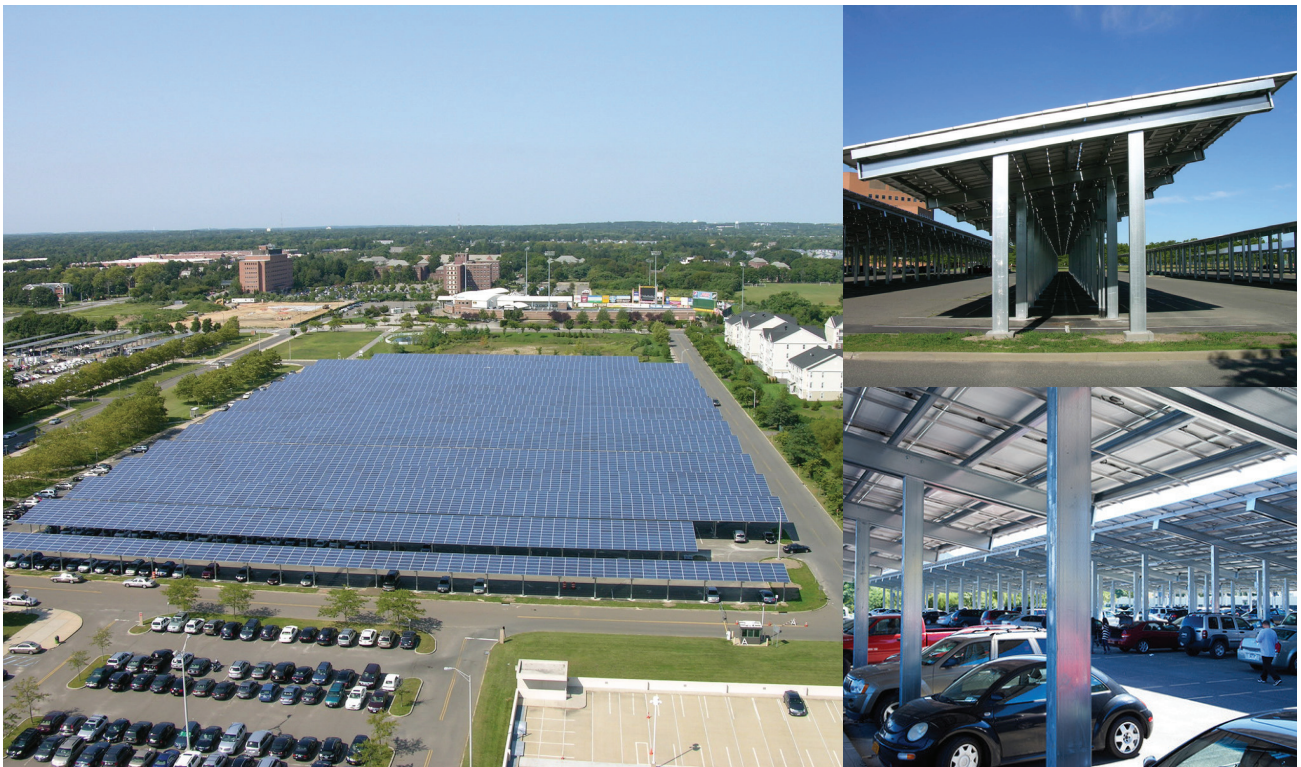
## analysis

pv tech:	c-Si
orientation:	SouthWest
function:	shelter for cars
structural material:	metal
impact on surrounding:	creates smaller space

## description

The parking plot of Airport Weeze consists of 15296 solar panels that cover 1350 parking spots <sup>[1.4]</sup>. The design is mainly focussed on electricity production. The southwest orientation results in a high output of the solar panels. Other than the function of generating electricity, it also provides shelters for the cars below. The structure is made out of metal. The structure of this design is comparable to that of the MSU design. In this design, the metal beams on the back side of the solar panels are covered with a plate. This creates a more calm image. The structure's foundation is placed in the middle of two parking spots. This does result in a smaller area that is available for the parking spot but has no influence on the functionality of the parking spot.

## Eastern long island carpark by BlueOakEnergy



(source: Blue Oak energy)

### analysis

pv tech:	mono c-Si <sup>[1.4]</sup>
orientation:	unknown
function:	shelter for cars
structural material:	metal
impact on surrounding:	creates smaller space

### description

The Eastern long island project is a project of the Suffolk County and consists out of six different car-parks with over 8,5-hectare solar panels installed <sup>[1.4]</sup>. This is the largest solar project in the state of New York. The design is mainly focused on electricity production. Other than the function of generating electricity, it also provides shelters for the cars below. The structure is made out of metal. The structural design of the carport makes the space look smaller. This is due to the crowded metal structure, the repetitive columns and the aluminum beams. The color used in the design makes the design looks cold and not inviting.

# USVA sacramento by BlueOakEnergy



(source: Blue Oak energy)

## analysis

pv tech:	poly c-Si <sup>[1,3]</sup>
orientation:	east & west & south
function:	shelter for cars
structural material:	metal
impact on surrounding:	unknown

## description

This design is placed at three parking plots at the Sacramento Outpatient VA Hospital. Each of the parking spots implement a different orientation of the solar panels. One is orientated East, the other West and the final South. This allows for a divided energy production across a day. The east orientated panels will provide maximum power during the morning, the south orientated panels during midday and the West orientated panels during the evening. This allows for a divided energy production across a day.

## conclusion

As seen in the analysis of current designs, they are all focused on maximum solar gain. Every design needs to be altered for the ideal tilt for the different orientations. All of the structures are made from steel or aluminum. These materials are easily made into profiles and therefore cost-effective.

The purpose of these designs is to generate as much electricity as possible, without compromising the functionality of the parking plot. The columns are placed on a concrete base, which is placed parallel to the parking spot. The repetitiveness of the columns makes the space look small and crowded.

When the analyzed designs are compared to each other, the conclusion can be made that they are all alike. The appearance of the solar cells, the structural material and structure all are similar. This are typical examples of engineered carports that lack a influence of design.

Besides the functionality of a shelter for cars and generating electricity, these designs do not add any value to the context or the experience of the parking plot. Therefore the conclusion is drawn that these designs are purely focusing on maximum solar gain and maintaining the function of the parking plot, whilst neglecting the aspect of design.

## 1.4 BIBLIOGRAPHY

- [1.1] IEA (2014, 14 january). Photovoltaics in Buildings: A Design Handbook for Architects and Engineers [http://www.iea-shc.org/Data/Sites/1/publications/task16-photovoltaics\\_in\\_buildings-full.pdf](http://www.iea-shc.org/Data/Sites/1/publications/task16-photovoltaics_in_buildings-full.pdf)
- [1.2] Inovateus Solar (n.d.). Michigan State University Retrieved from <https://inovateus.com/portfolio-items/michigan-state-university/>
- [1.3] Airport Weeze (2016, 21 september). Carports met zonnepanelen op Airport Weeze. Retrieved from [http://m.airport-weeze.com/nl/carports\\_met\\_zonnepanelen\\_op\\_airport\\_weeze.html](http://m.airport-weeze.com/nl/carports_met_zonnepanelen_op_airport_weeze.html)
- [1.4] BlueOakEnergy(n.d.). Eastern Long Island Solar Project. Retrieved from <https://www.blueoakenergy.com/solar-portfolio/eastern-long-island-solar-project>
- [1.5] BlueOakEnergy(n.d.). USVA - Sacramento. Retrieved from <https://www.blueoakenergy.com/solar-portfolio/usva-sacramento-solar-case-study>



## **2.** RESEARCH DEFINITION

## 2.1 NEDERLANDSE SPOORWEGEN

As previously mentioned in this graduation project a stakeholder is involved. The 'Nederlandse Spoorwegen' (NS) is a company that facilitates public transport and especially trains. Besides managing the trains the scope of the company also involves building and maintaining railway stations. This graduation project is for the real estate division of the NS, named 'NS Stations'.

In 2017 a sustainable ambition of the stakeholder was reached by making climate neutral traveling possible. This was accomplished by signing a deal with an energy corporation to provide them with 100% wind energy and therefore reaching their ambition to allow the passengers of their trains to travel climate neutral <sup>[2.1]</sup>. The next ambition of the NS is to generate enough energy on assets in their real estate portfolio to accomplish energy neutrality of their railway stations. To accomplish this energy generating devices need to be implemented on every asset. One of these assets is the park and ride (P+R) plots. The NS wants to explore the option of implementing solar panels into the carport because these are easily accessible places to integrate solar panels without major adjustments to the asset. These plots are bare parking spots across the whole Netherlands.

The aim of the NS is to start a pilot project of the NS Solar Carport. This pilot will take place in a visible place beside a station. If this pilot meets the expectations of the NS, the next step is the implementation of the design on the other 228 P+R plots scattered across the Netherlands.



fig. 2.1.1: NS stations logo  
(source: NS Stations)



fig. 2.1.2: Number of P+R locations in The Netherlands  
(source: Own image, information: ANWB)

## 2.2 PROBLEM STATEMENT

Due to the ambition of the stakeholder to make their railway station energy neutral by 2025 the necessity to integrate energy generating devices onto their assets arises.

The P+R plots are accessible places for solar modules to be integrated. The integration of the solar modules should be done in such a way that the functionality of the parking plots is kept to a maximum. Therefore the integrating the solar modules into car shelter structures is wished for.

The analysis of the current solar carport products showed that there is a trend to engineer the solar carport for maximum solar gain and neglect the aspect of design. The stakeholder has a certain image that they want to project onto this design, which current carport designs on the market do not fulfill. Additionally, these designs don't offer orientation independently, meaning the designs have to be altered when applied in a different P+R plot with a different orientation, which will lead to a rise of cost for the design.

The current designs don't fully exploit the structural capabilities of solar panels. Most solar panels are integrated into the structure as enclosure and only transfer the loads of the wind and snow load to a structure behind the solar panel. The possibility of exploiting the structural capabilities of the glass of the solar panel to transfer the load to the foundation of the structure is often not explored.

## 2.3 RESEARCH QUESTIONS

By studying the current carport designs and the wishes of the stakeholder the following research question arises:

“What would the design of a modular shelter for cars be when taken into account the integration of solar panels into the structure with maximum solar gain in different orientations and the image of the NS whilst keeping the function as parking lot?”

Current designs are limited in the design by the maximum gain of solar power and integration of the solar panel. therefore the aim is to create a design of a carport that integrates the solar panels fully into the structure. Furthermore, this research will produce a design that reflects the sustainable image the NS wants to represent with this design.

To answer the research question it is divided into multiple sub-research questions:

1. What solar cell technology are currently available for integration into a carport structure?
2. What are the structural parameters of integration the solar modules into the structure of the carport?
3. What is the image of the NS?
4. What is the best suiting solar technology to be integrated into the carport?
5. How can the carport be designed in such a manner that the functionality of the parking lot is kept to a maximum?
6. What are the parameters for the design of a modular carport?
7. How can the solar panels be integrated into the structure of the solar carport?
8. What is the optimal design in regard of solar gain when taken into account the different orientations?

## 2.4 APPROACH AND METHODOLOGY

This research will be based on the concepts of research for design and research through design, whereby the design will acquire new knowledge. The research will be divided in to four different phases:

1. Knowledge
2. Conceptual design
3. Design
4. Digital design optimization

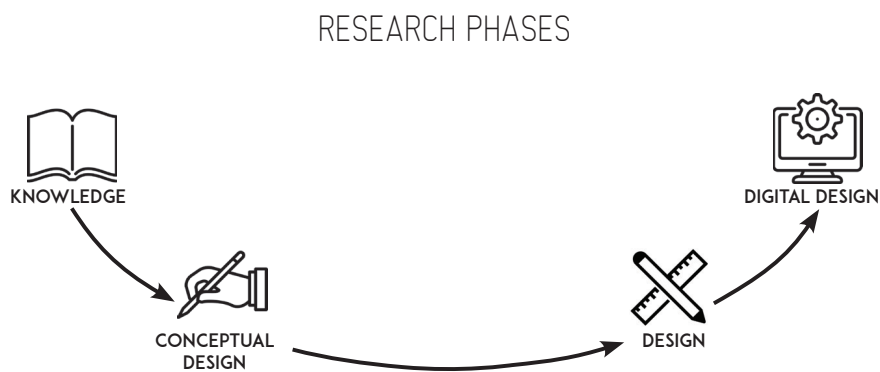


fig. 2.4.1: Research phases

Each of these four research phases has his own methodologies and goals. These methodologies and goals will be further elaborated in the coming sub-chapters.

# knowledge phase

The goal of this phase is to gather knowledge that can be applied during the design of the carport. The knowledge will result in input for the design brief. Another function of this phase is to generate input for the Multi-criteria analysis.

During the knowledge phase literature study will be conducted to gather information on the following topics:

- Solar cell technologies and their design parameters
- Structural integration of solar cells

From research the following three generations of solar panels have been found <sup>[2.2][2.3]</sup>:

**1st generation**, wafer-based crystalline silicon technology:

- Mono crystalline silicon cell (mono c-Si)
- Poly crystalline silicon cell (poly c-Si)

**2nd generation**, Thin film technology:

- Amorphous silicon solar cell (a-Si and a-Si/ $\mu$ c-S)
- Cadmium Telluride (Cd-Te)
- Copper-Indium-Selenide (CIS) and Copper-Indium-Gallium-Disele-nide (CIGS)

**3rd generation**:

- Dye-sensitized (DSSC)
- Organic solar cells (OPV)
- Perovskite cell
- Concentrating PV (CPV)

During this research, the first and second generation of solar panels will be researched. The third generation of solar panels will be out of scope since the technologies are not commercially available yet and the stakeholder wishes the design to be realizable.

For the research into the design parameters of different solar cell technologies the following aspects of the solar cells will be researched to ensure the right selection of solar cell technology:

**Performance:**

- Efficiency
- Performance drop off per kelvin

**Design:**

- Cell customizability
- Flexibility of the cell

**Sustainability:**

- Recyclability
- Energy pay back time (EPBT)

Literature will be studied to gather information regarding the structural capabilities and/or complexities of integrating the solar modules into the structure of the carport.

To gain understanding about current novelties in solar designs, case studies are done. The designs selected will be analyzed on the following aspects: PV tech used, manner of integration of the PV, Structural material, structural connection, smart design and when applicable other factors of the design worth mentioning.

The last part of the knowledge phase is a pilot study. This pilot study will involve the integration of solar panels into the structure of an already existing carport design. During the integration of the solar panels into the carport, the following topics will be discussed.

- Structural connection
- Structural calculations

After the integration of the solar cells into the existing carport is realized the process and end product will be analyzed. The analysis out of the pilot study will provide input for the design brief of the conceptual designs and final design.

## conceptual design phase

The stakeholder, NS, has provided a list of requirements for the design of the solar carport. The goal of the conceptual designs is to get a scope of different designs to get a broader point of view for the final design. The conceptual designs will consist of three designs with different topics which will be designed to an extreme version of these topics. The three topics are:

- Cost effective design (costs reduction of design& performance)
- Sustainable design (additional function & low embodied energy)
- Architectural Design (maximum design)

Various structural materials will be researched to further enhance the designs. The materials that are selected are recycled aluminum, glu-lam, bamboo, hardwood (oak) and end of life rail tracks. The reason these materials are selected is either their low embodied energy and/or their structural capabilities.

After the conceptual designs are made, the student will make a decision on which conceptual design to elaborate on further. A combination of conceptual designs aspects is also an option.

## design phase

In this phase, one out of the three conceptual designs or aspects of the conceptual designs are combined to create the final design. The choice for which conceptual design to elaborate on will be done by the student. Afterward, the final design parameters will be set. This will result in a MCA to conclude the right solar technology is selected for the design. The priorities of the MCA will be selected by the needs for the design.

In this phase, the individual components such as solar panel, structure, and connections will be designed in detail. These individual components will be integrated into each other to form the base for the digital design phase.

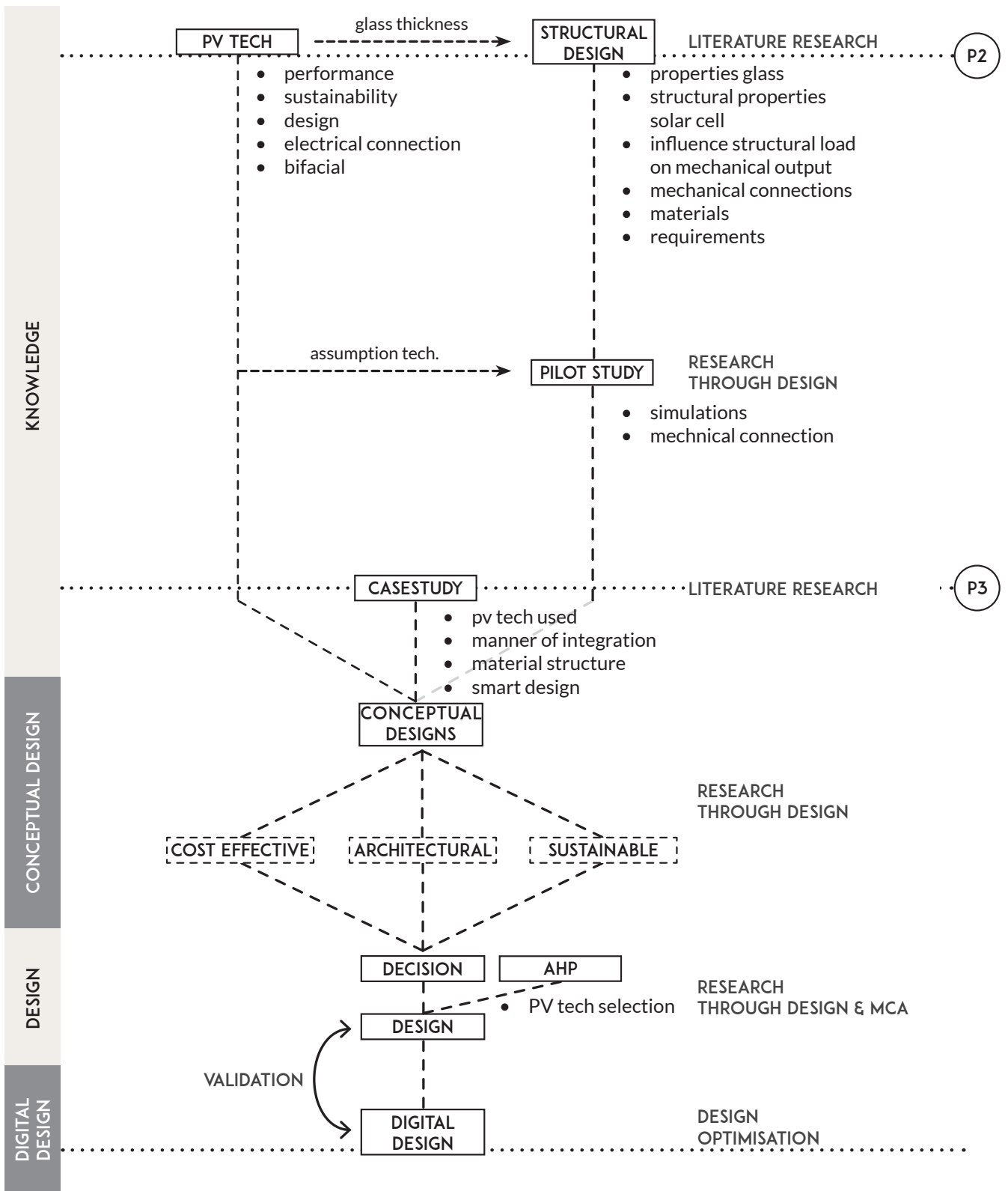
## digital design

In the digital design phase, the concept will be digitally modeled and validated using Grasshopper with the following plug-ins: Karamba, Ladybug, Honeybee, and Galapagos.

The structural design of the carport will be validated through deflection and tensile stress in the structure. When these values exceed their maximum allowable value, the parameters in the design phase are altered to allow these values to drop below the maximum threshold.

The solar performance of the design is also validated. The design is simulated in 5 different orientations (N, NE, E, SE, S) to see the performance of the design in these different circumstances. The goal of the final design is to be an orientation in depend.

# methodology scheme



## 2.5 ROLE OF STAKEHOLDER

The role of the stakeholder on the research into solar cell technologies is the exclusion of the third generation of solar cells. As previously mentioned the stakeholder wishes the design to be realizable for the pilot and eventually the role out of the design onto the other P+R plots. The research into the structural integration of solar modules has no interference of the stakeholder.

The design of the solar carport will be influenced by the stakeholder via the list of requirements for the design and the image that the NS wants to achieve. The final selection of the design will be made by the student.



## 2.7 BIBLIOGRAPHY

- [2.1] Nederlandse spoorwegen. (2018, 11 27). Duurzaamheid bij de NS. Retrieved from NS: <https://www.ns.nl/over-ns/duurzaamheid/duurzaamheid-bij-ns.html>
- [2.2] IRENA. (2012). Renewable energy technologies: Cost analysis series: Solar Photovoltaics. Bonn: International Renewable Energy Agency.
- [2.3] Ranabhat, K., Patrikeev, L., Revina, A., Andrianov, K., Lapshinsky, V., & Sofronova, E. (2016). An introduction to solar cell technology. *Journal of Applied Engineering Science*.



**3.** **SOLAR  
TECHNOLOGIES**

## 3.1 INTRODUCTION

As mentioned in 'Approach and methodology' the research will focus on solar cell technologies and the structural integration of solar cells. In this chapter the solar technologies will be discussed. In literature three different generations of solar cell technologies were found:

1st generation, wafer-based crystalline silicon technology:

- Mono crystalline silicon cell (mono c-Si)
- Poly crystalline silicon cell (poly c-Si)

2nd generation, Thin film technology:

- Amorphous silicon solar cell (a-Si and a-Si/ $\mu$ c-S)
- Cadmium Telluride (Cd-Te)
- Copper-Indium-Selenide (CIS) and Copper-Indium-Gallium-Diselenide (CIGS)

3rd generation:

- Dye-sensitized (DSSC)
- Organic solar cells (OPV)
- Perovskite cell
- Concentrating PV (CPV)

In this research, the first and second generation will be discussed. The third generation is out of scope due to not being commercially available as mentioned in the 'Approach and methodology'.

The goal of this chapter is to gain knowledge about the different technologies on the following topics:

**Performance:**

- Efficiency
- Performance drop off per kelvin

**Design:**

- Cell customizability
- Flexibility of the cell

**Sustainability:**

- Recyclability
- Energy pay back time (EPBT)

## 3.2 FIRST GENERATION

The first generation of solar cell technologies are wafer-based crystalline silicon (c-Si) technology, either mono crystalline silicon or poly crystalline silicon solar cell <sup>[3.1]</sup>. Both will be discussed below.

Both of the solar cell technology share the same two main structures; Glass-glass or glass-back sheet. Both structures consist of the same materials except for the back sheet (fig. 3.2.1 & 3.2.2). The following parts are used in the panels; Aluminum frame (optional, frameless panels are on the market), front glass, EVA film, solar cell, EVA film, and back sheet or glass.

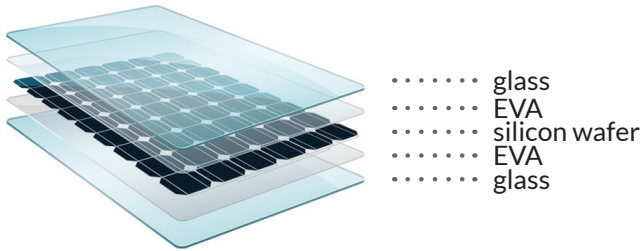


fig. 3.2.1: glass-glass structure  
(source: Jentsys)

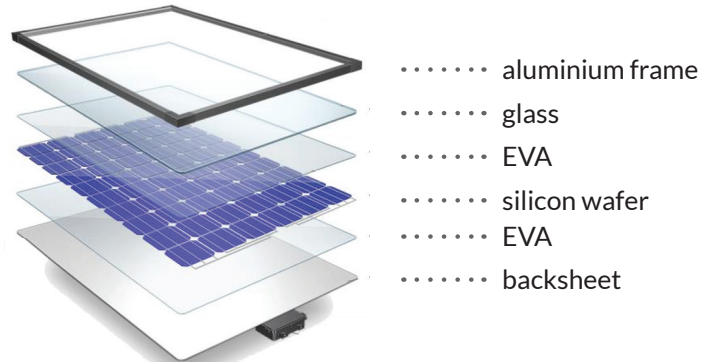


fig. 3.2.2: glass-backsheet structure  
(source: Trina solar)

### mono crystalline silicon (mono c-Si)

Mono crystalline is the oldest existing solar cell technology. The first practical silicon solar cell dates from 1954 which had an efficiency of 6% <sup>[3.2]</sup>. From then to now the market share of mono crystalline is grown to about 35% <sup>[3.3]</sup>. The global annual production in 2017 of m-Si panels was 32,2 GWp <sup>[3.4]</sup>. The solar cell itself is made out of silica which is converted to high-purity silicon. The cells are manufactured through the Czochralski process. This process creates cylindrical shaped ingots. These ingots are then sliced into wafers and from the wafers, cells are made. The production process can be seen in (fig.3.2.4). Most of the mono crystalline solar cells are made into pseudo squares, the reason for this being to reduce the waste in the manufacturing process but still allow the maximum amount of solar cells to be integrated into the standard rectangular shape solar module. The appearance of a mono c-Si solar cell is uniform (-fig. 3.2.3).

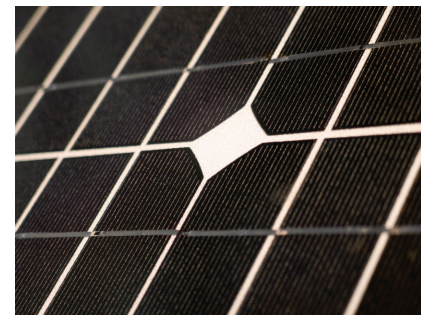


fig. 3.2.3: mono c-Si solar panel close up  
(source: semprus)

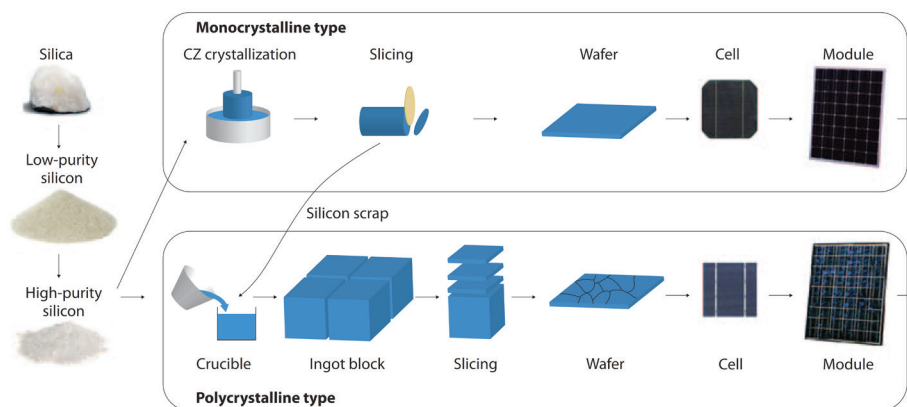


fig. 3.2.4

fig. 3.2.4: manufacturing silicon solar cell  
(source: bibliography 3.5)

## poly crystalline silicon (poly c-Si)

Poly crystalline solar panels have the biggest market share of all solar cell technologies currently available; 56%<sup>[3.3]</sup>. This market share resulted in a 60,8 GWp annual production globally<sup>[3.4]</sup>. The structure of the poly crystalline cells is identical to the mono crystalline solar cells. The manufacturing process (fig. 3.2.4) is as follows: silica is upgraded to high purity silicon and made into square silicon substrates. These square silicon substrates are then sliced into wafers<sup>[3.5]</sup>. The benefit of this manufacturing process is that there is less waste when compared to mono crystalline, due to the ingots being produced in squares instead of round ingots. Poly c-Si is easily recognizable from mono c-Si by its camouflage-like pattern of the crystals in the wafer (fig. 3.2.5)



fig. 3.2.5: close-up poly c-Si solar module  
(source: semprius)

### 3.3 SECOND GENERATION

The second generation of solar cells consists out of thin film solar cells. These thin film solar cells have three technologies<sup>[3.1]</sup>:

- Amorphous (a-Si) or micromorph silicon (a-Si/ $\mu\text{c-Si}$ )
- Cadmium-telluride (CdTe)
- Copper-Indium-Selenide (CIS) or Copper-Indium-Gallium-Disele-nide (CIGS)

These three technologies will be further elaborated on below.

#### Amorphous (a-Si) or micromorph silicon (a-Si/ $\mu\text{c-Si}$ )

Amorphous silicon solar (a-Si) is part of the thin film solar cell family. The attractive feature of this material is its ability to absorb sunlight within a thin layer of micrometers due to the fact that it is a direct bandgap material<sup>[3.6]</sup>. This allows the absorbing material to be applied in such a thin layer that the solar module becomes flexible (when applied on a flexible substrate). The global production of a-Si panels in 2017 according to the photovoltaics update of Fraunhofer (2018) is 0,3 GWp, making it the least producing solar cell technology. A high volume manufacturing plant in Michigan, USA, operated by United Solar Ovonic, a-Si solar cells are produced by depositing solar cells on steel rolls. The flexible steel roll acts as the substrate for the solar cell. The steel roll is processed by four different machines to complete the production of the a-Si solar cell. The first machine deposits the back-reflector on the steel roll, followed by the second machine depositing the layers of a-Si. The final machine applies a layer of anti-reflection coating onto the solar cell<sup>[3.7]</sup>. The structure of an a-Si solar cell is based on two different technologies; single junction or multijunction p-i-n layer. In (fig. 3.3.1) a single junction and double (multi) p-i-n layer(ed) a-Si module is schematized. In (fig. 3.3.2) a triple junction a-Si module is schematized. As seen in this image there are different types of coated a-Si being implemented into the module.

#### Cadmium Telluride (CdTe)

With a production of 2,3 GWp globally in 2017 CdTe is the highest producing thin-film solar technology<sup>[3.4]</sup>. CdTe is a direct bandgap material, similar to a-Si silicon technology. H.W. Schock states that CdTe is a material with nearly ideal photovoltaic properties with the negative side of this material being its toxicity<sup>[3.8]</sup>. This material can be made in a wide range of different manners. The high-efficiency cells are manufactured using the close-spaced sublimation (CSS) technique<sup>[3.9]</sup>. Besides offering the highest efficiency cells, CSS also offers a high deposition rate.

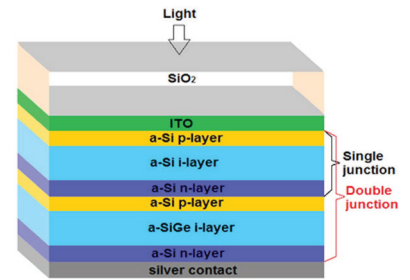


fig. 3.3.1: structure of single and double (multi) junction a-Si module (source: bibliography 3.6)

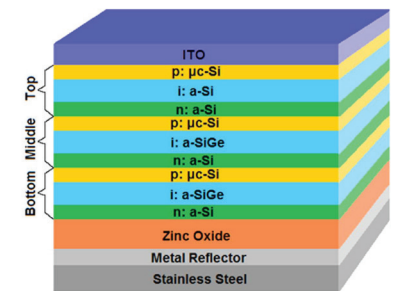


fig. 3.3.2: structure of triple (multi) junction a-Si module (source: bibliography 3.6)

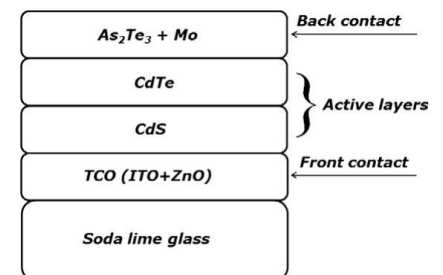


fig. 3.3.3: Structure of CdTe cell on soda lime glass (source: bibliography 3.9)

## Copper-Indium-Gallium-Diselenide (CIGS)

Like all thin film materials CI(G)S is a direct bandgap material. This allows the semiconductive layer to be applied in a thin layer. The semiconducting layer of CIGS panels is thin 1.2–4.04  $\mu\text{m}$  compared to 170–200  $\mu\text{m}$  of c-Si panels <sup>[3.6]</sup>. The disadvantage of CI(G)S is its toxicity. One of the ways to produce CI(G)S panels is by a roll-to-roll production process. Global solar, one of the manufactures of CIGS solar cells, uses this batch manufacturing process<sup>[3.10]</sup>. This production process involves a roll of the substrate. This substrate material is then unrolled and passes by a couple of evaporators. These evaporators apply small layers of materials that make the CIGS panel. The production of CI(G)S panels in 2017 was 1,9 GWp <sup>[3.4]</sup>. Making it the second largest producing thin-film solar technology.

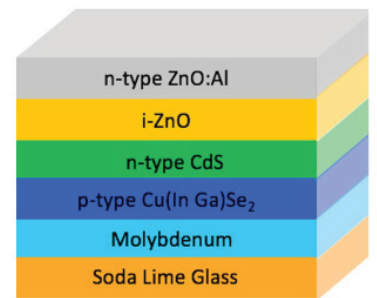


fig. 3.3.4: structure of CIGS solar cell  
(source: bibliography 3.6)

## 3.4 PERFORMANCE

In this chapter the performance of the solar cell technologies reviewed in this paper will be discussed. The technologies discussed (in order): mono c-Si, poly c-Si, a-Si or a-Si/ $\mu$ c-Si, CdTe, CIS or CIGS. The following topics will be discussed:

- Efficiency in %
- Performance drop off / Celsius (thermal coefficient of Pmax) in %/°C

At the end of the performance chapter a summarizing table will be shown to give an overview of the performance of all the technologies discussed.

### efficiency

The ability of the solar panel to convert the energy of the sun into electrical energy is discussed in this chapter. This number is given in percentages. The difference in the efficiency of lab tested solar cells and commercial modules is explained by the losses due to the interconnections of the cells.

Mono crystalline has the highest efficiency of all solar cell technologies researched in this paper. Crystalline has, when compared to other solar cell technologies, the advantage of a stable, non-toxic, abundant and well-understood absorber material. Due to the fast amount of R&D put into the panels, this technology is reaching its modeled efficiency of 29,4%<sup>[3.3]</sup>. The highest efficiency achieved in a lab is 26,7%<sup>[3.4]</sup>, whilst most commercially available mono crystalline cells have an efficiency of 16-18%, with some high-efficiency modules with an efficiency of over 20%<sup>[3.5]</sup>.

The highest performing poly crystalline solar cell reached an efficiency of 22,3%<sup>[3.11]</sup>. Although most commercially available poly crystalline cells have an efficiency of 15-17% which is slightly less than the mono crystalline solar cells. On a module level, poly crystalline performs almost the same as mono crystalline modules, due to the higher packing factor of the square poly cells versus the pseudo mono cells<sup>[3.5]</sup>.

The maximum tested efficiency of the triple junction a-Si/nc-Si/nc-Si cell is 14% at 25 °C<sup>[3.12]</sup>. Whilst commercially available a-Si solar panels have an efficiency of 7-10,4%<sup>[3.13]</sup>. The strength of this technology isn't its maximum efficiency but its ability to cope with low light conditions. A triple junction module performs 40% better under low light conditions (50-100 W/m<sup>2</sup>) than most present crystalline based technologies<sup>[3.7]</sup>.

The maximum tested efficiency of a CdTe cell is 21,0 ± 0,4 % at regular test circumstances<sup>[3.12]</sup>. The highest commercially available CdTe module is from First Solar with an efficiency of 18,6%<sup>[3.6]</sup>. In the last 10 years the average efficiency of commercially available CdTe modules went up from 8% to 16%<sup>[3.4]</sup>

CI(G)S has the highest efficiency of all thin film technologies. Reason for this being that Copper indium diselenide ( $\text{CuInSe}_2$ ) has a high absorption value that allows almost all of the available light to be absorbed in the first micrometer of the material. When small amounts of gallium are added to the  $\text{CuInSe}_2$  it will enhance its light absorbing band gap, meaning it's voltage and efficiency increases<sup>[3.7]</sup>. The highest laboratory cell efficiency reached by a CIGS cell is 22,3% that is achieved by Solar Frontier<sup>[3.6]</sup>. Another benefit of CIGS panels is that the efficiency over time is stable due to their self-repairing capabilities. Some chemical bonds break easily but the wandering copper molecules will spread evenly meaning that they will fill up damaged spots of the cell<sup>[3.7]</sup>. NREL tested this in 1988 during a time period of 7 years with an ARCO CIS module and the module didn't have any significant degradation over that period<sup>[3.8]</sup>. The commercially available CI(G)S panels have an efficiency that ranges from 7% to 16%<sup>[3.1]</sup>.

## performance drop off / celsius

The temperature of a solar cell can have an impact on its output. The technologies ability to cope with this temperature is discussed in this chapter. This is also called the thermal coefficient  $P_{max}$  and is expressed in  $\%/^{\circ}\text{C}$ . This number represents the percentage maximum power loss per Celsius increase.

Although mono crystalline has the highest efficiency of the first generation solar cells, the ability to cope with temperature is less than poly crystalline. In a research different solar cell wafers are tested on the influence of temperature on the output of the solar cell. In this research, it showed that on average mono crystalline has a temperature coefficient of  $-0,446 \%/^{\circ}\text{C}$ <sup>[3.14]</sup>. Whilst poly crystalline has a temperature coefficient of  $-0,387 \%/^{\circ}\text{C}$ <sup>[3.14]</sup>. Therefore the temperature of the poly crystalline cell has less impact on the performance of the cell than the temperature of a mono crystalline cell.

Different commercially available a-Si solar panels technical sheets were researched for this paper. The temperature coefficient of the commercial available a-Si solar panels is  $-0,3\%/^{\circ}\text{C}$ <sup>[3.15]</sup> and  $-0,2\%/^{\circ}\text{C}$ <sup>[3.16]</sup>. In a research, an a-Si cell is tested with a thermal coefficient of  $-0,234\%/^{\circ}\text{C}$ <sup>[3.14]</sup>.

The influence of temperature on the nominal maximum power output of commercially available CdTe panels is  $-0,32\%/^{\circ}\text{C}$  to  $-0,21\%/^{\circ}\text{C}$ <sup>[3.17]</sup><sup>[3.18]</sup><sup>[3.19]</sup><sup>[3.20]</sup>. Research showed that a temperature coefficient  $P_{max}$  of  $-0,172\%/^{\circ}\text{C}$  is possible<sup>[3.14]</sup>. This performance drop off per Celsius is slightly better than a-Si solar panels and performs better than c-Si solar under high-temperature circumstances. This was evaluated by a research done by A.H. Munshi et al. (2018)<sup>[3.21]</sup>. This research showed that CdTe had a higher power output over the entire day than poly c-Si solar panels under the same circumstances. The conclusion was made that this was due to the better temperature coefficient of CdTe.

The influence of temperature on the nominal maximum power output of commercially available CIGS panels is  $-0,36\%/^{\circ}\text{C}$  to  $-0,26\%$ <sup>[3.22]</sup><sup>[3.23]</sup>.

## conclusion

A summary of the performance of the discussed technologies can be seen in (table 3.4.1). Mono crystalline has the highest efficiency in the lab as well as in the commercially available solar cells. Research showed that mono c-Si also had the highest performance drop off per Celsius increase. Meaning that this cell technology loses the most efficiency when the temperature of the cell increases. The second generation of solar cell technology, thin film generation, showed that they have the ability to handle temperatures better than the first generation of solar cell technologies. CdTe, in particular, has a low thermal coefficient Pmax, almost three times as low as mono c-Si. Research showed that a-Si cells have the lowest efficiency of all the technologies. Although the technology has a low efficiency it performs 40% better under low light conditions.

Technology	Efficiency	Performance drop off / Celsius
mono c-Si:		-0.45% /°C
- max. lab	26,7%	
- commercial	16-18%	
poly c-Si:		-0.39% /°C
- max. lab	22,3%	
- commercial	15-17%	
amorp. Si:		-0.23% /°C
- max. lab	14%	
- commercial	7-10,4%	
CdTe:		-0.17% /°C
- max. lab	21,0%	
- commercial	avg. 16%	
Cl(G)S:		-0,36% °C - 0,26%/°C
- max. lab	22,9%	
- commercial	7-16%	

table. 3.4.1: summary performance

## 3.5 DESIGN

In this chapter the design possibilities of the technologies are discussed. The ability to customize the cell in size, shape and color together with the flexibility of the solar cell is reviewed. The following topics will be discussed:

- Cell customizability
- Flexibility

### cell customizability

To allow integration of the solar cell into the design the possibilities of cell customizability are researched.

The ability to customize the color isn't technology-dependent but structure dependent. Current customizability options are focused on the front pane of glass. Some technologies have structures where there is no front pane of glass and therefore the customizability options are limited.

The following technologies are possible:

- Ceramic ink
- Optical filters

Ceramic ink print patterns on the front glass of the solar module. By applying it with small gaps between the ink it allows the solar cell to still receive sunlight (fig. 3.5.1). When seen from a couple of meters the surface looks uniform as seen in (fig. 3.5.2). The print on the front glass is fully customizable to the wish of the designer.

Optical filters add another layer of filter on the glass of the solar cell. This layer still allows light to penetrate upon the solar cell with a lower impact on efficiency than ceramic ink. There is a great variety of high saturated colors possible, though only single colors can be applied. Another disadvantage is that the color is not consistent at different angles. The optical filter can be applied at cell level (fig. 3.5.3) or at the front side of the glass (fig. 3.5.4)

Normal sizing of the silicon-based solar cell technologies (mono c-Si & poly c-Si) are solar cells are 125 mm (5 inches) or 156 mm (6 inches) squares<sup>[3.5]</sup>. The color of the crystalline cells is mostly blue or in the cold/dark range of colors (black, purple green)<sup>[3.24]</sup>

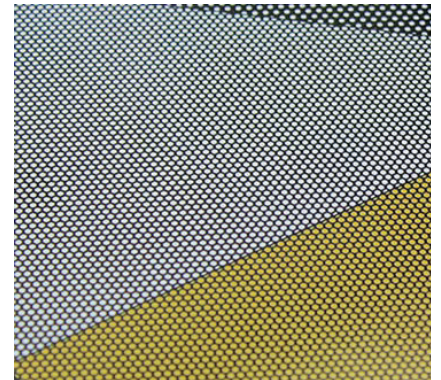


fig. 3.5.1: ceramic ink close-up  
(source: kameleon solar)



fig. 3.5.2: ceramic ink solar panels from a distance  
(source: kameleon solar)

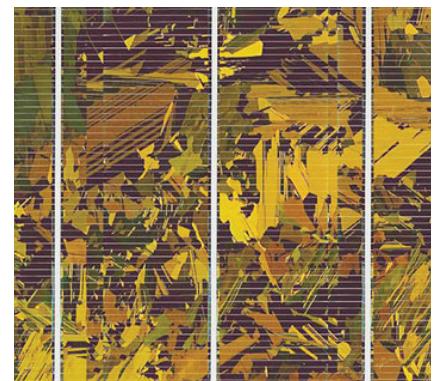


fig. 3.5.3: optical filter at cell level  
(source: kameleon solar)



fig. 3.5.4: optical filter on glass  
(source: kameleon solar)

Normal solar cells have front and back contacts to transmit electricity. This results in the thin metal bars across the solar cell. This not only shades the solar panel and influences the efficiency of the panel, but it also influences the aesthetics of the panel as seen in (fig. 3.5.5). New solar panel technology allows back contact only solar cells. This results in a flat surface without the metal strips going across the cell as seen in (fig. 3.5.6)

As previously mentioned the mono silicon cells are originally made in a cylindrical shape. To maximize the number of cells that can be integrated into a solar panel the cells are made into pseudo squares <sup>[3.5]</sup>. The edges are rounded to decrease the amount of waste produced by the process. Although pseudo squares are the most used shape for the mono crystalline cells it is possible to make a custom shape. The more that is divided from a round shape the more waste is produced by the process.

The manufacturing process of poly silicon cells is square. Same as with the mono silicon cell the shape of the cells can be customized but the more that is diverted from a square the more waste there will produce.

From the origin, the c-Si wafers are not transparent, but by applying the glass-glass structure and by adjusting the density of the c-Si solar wafers the transparency of the panels can be adjusted (fig. 3.5.7).



fig. 3.5.5: front contact c-Si cell (source: Oplii)



fig. 3.5.6: back contact c-Si cell (source: Oplii)



fig. 3.5.7

fig. 3.5.7: transparent c-Si solar panels (source: De Groene Bron)

The most common colors that manufacture produce a-Si solar cells are brown, blue, black or laminates in dark blue or magenta. The choice of color is still limited to a small number of manufactures.

Whilst the previously mentioned first-generation solar cell technologies are opaque, a-Si solar cell technology can be applied as semitransparent. The transparency can be tweaked to let more or less light pass through. The more transparency the cell has the less output the panel generates. An example can be seen in (fig. 3.5.8). This opens the possibility of invisible solar.

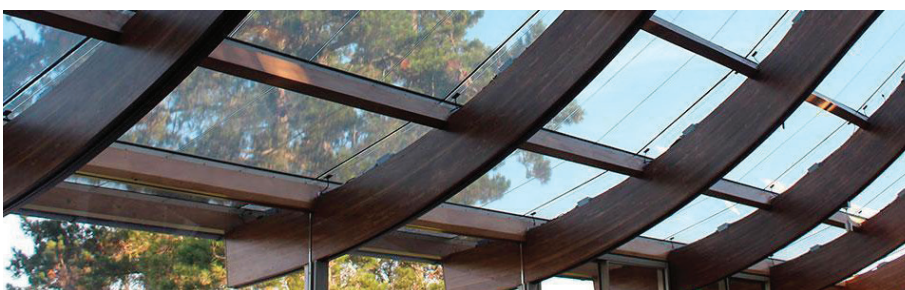


fig. 3.5.8

fig. 3.5.8: transparent a-Si solar panels (source: Onyx solar)

Also, CdTe has the possibility of being transparent. CdTe manufacturer Polysolar makes Photovoltaic glass CdTe modules with transparencies up to 50% (fig. 3.5.9)



fig. 3.5.9

fig. 3.5.9: transparent CdTe solar panels  
(source: Polysolar)

## flexibility

Due to the relatively thick solar cell of the c-Si technology, they are not flexible. The second generation of solar technology has the benefit that it can be applied in thin layers what makes the technology flexible. The flexibility of the panels are dependent on the substrate it is placed upon. The most common options are glass, metal or plastic. One of the main benefits of this technology it's flexible and therefore applicable to different shapes of surfaces.

## conclusion

The customizability of the color solar cell is more dependent on the structure of the solar cell than the technology itself. The first generation of solar cells have standard dimensions but custom dimensions and shapes are possible if desired. The transparency of c-Si panels is realized by applying a glass-glass structure and adjusting the density of c-Si cells in a panel. A-Si and CdTe technology can be transparent. The transparency can be adjusted but the more transparent the panel is the lesser power it will generate. The second generation of solar panels can be flexible, this depends on the substrate it is applied on.

Technology	Customizability	Flexibility
mono c-Si:	Optical filters, colored encapsulant, ceramic ink <sup>[1]</sup> , transparency <sup>A</sup>	No
poly c-Si:	Optical filters, colored encapsulant, ceramic ink <sup>[1]</sup> , transparency <sup>A</sup>	No
amorp. Si:	Optical filters <sup>B [2]</sup> , ceramic ink <sup>B [2]</sup> , transparency <sup>[3]</sup>	Yes
CdTe:	Optical filters <sup>B [2]</sup> , ceramic ink <sup>B [2]</sup> , transparency <sup>[4]</sup>	Yes
Cl(G)S:	Optical filters <sup>B [2]</sup> , ceramic ink <sup>B [2]</sup> , transparency <sup>[5]</sup>	Yes

<sup>A</sup> = Cell itself is not transparent, dependend on structure of cell & cell density

<sup>B</sup> = Only on glass substrate

table 3.5.1: summary design

## 3.6 SUSTAINABILITY

In this chapter sustainability of the technologies will be discussed. In this research sustainability consists out of:

- Recyclability
- Energy pay back time

The energy pay back time means the amount of years of energy generating it takes to pay back the energy of production of the solar panel.

### recyclability

Silicon solar cells are recyclable. Yan Xu et al. state in 'Global status report of recycling waste solar panels: A review'(2017)<sup>[3.25]</sup> that there are multiple ways to recycle a silicon solar cell. One of them is to separate the components of the solar cell; Aluminum frame, glass, back material, junction box, and cell. The solar cell is then processed into a chemical bath to extract the silicon. Mentioned in the same research is a method to extract an undamaged silicon wafer from a module with the use of organic solvents. The only downside of this process that it takes ten days to dissolve the EVA to extract the silicon wafer.

The a-Si solar cells can be recycled by crushing the panel into small fragments. These fragments are then separated and recycled. About 70-85% of the glass can be recovered by the process of physical operations<sup>[3.26]</sup>.

One of the manufactures of CdTe solar panels, First Solar, has developed a recycling process for end of life (EOL) modules. The company will set aside sufficient funds for recycling at every sale. The recycling procedure of First Solar starts with shredding the module in large pieces, followed by shredding it into small pieces (5mm or less) using a hammer mill. Then the semiconductor is removed by passing it through a slow leaching drum. Afterward, the glass is separated through a chemical solid-liquid separation. Via a vibrating screen, the glass is separated from the larger ethylene vinyl acetate (EVA) pieces<sup>[3.27]</sup>. According to the website of First Solar, this process allows them to reuse up to 90% of semiconductor material into new modules and 90% of glass into new glass products<sup>[3.28]</sup>. CdTe technology consist out of significant amount of Cadmium, which is a relatively toxic material. Therefore it present an environmental problem that have to be take into account during recycling<sup>[3.27]</sup>.

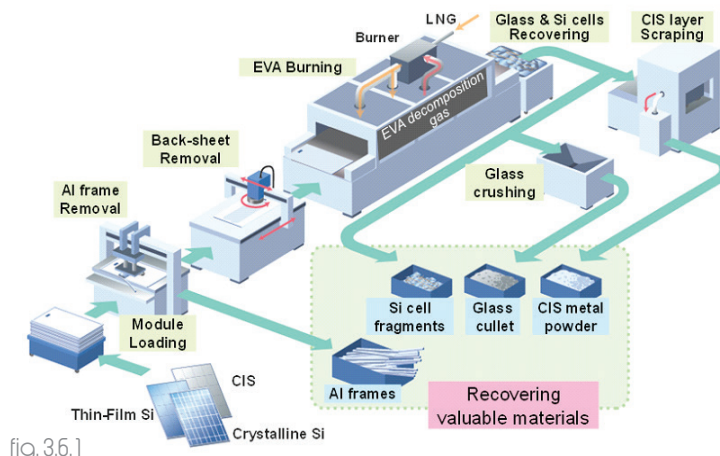


fig.3.6.1: overview of recycling process of different technologies of solar modules (source: google images)

The company Loser Chemie has developed a method of recycling CI(G)S panels by first crushing and separate the materials mechanically. The next stage of recycling uses a chemical treatment to recover the semiconductor metals. At last, the aluminum metallization is recovered and can be used for producing wastewater treatment chemicals<sup>[3.27]</sup>. Extra care has to be taken for the toxicity of the panel.

## energy payback time (EPBT)

In the research of K.P. Bhandari, et al. (2015)<sup>[3.29]</sup> a review and meta-analysis is done to gather information regarding the EPBT of all the technologies mentioned in this paper.

Due to the high energy needed for the conversion of silica to the purity of silicon needed for the manufacturing of the mono c-Si solar cell and the waste created by converting a cylindrical shape ignot to a pseudo-square solar cell, it has the highest embodied energy of all the technologies mentioned. Even though it also has the highest efficiency it still takes the longest time of all the technologies to pay back the energy invested. According to the meta-analysis, mono c-Si has a harmonized mean of 4,1 years and a standard deviation of 2 years<sup>[3.29]</sup>. In the photovoltaic update of 27 August 2018 from Fraunhofer ISE<sup>[3.4]</sup>, the EPBT is shown for Germany located technologies (Germany has the same global irradiation as The Netherlands, 1000 kWh/m<sup>2</sup>/year). In this report, the EPBT of mono c-Si including mounting, cabling and inverter is 3,3 years respectively. This is consistent with the data found in the meta-analysis.

Due to the lesser energy demanding manufacturing process of poly c-Si the EPBT of this technology is lower than mono c-Si. The meta-analysis showed a harmonized mean of 3,1 years with a standard deviation of 1,3 years [3.29]. The photovoltaic updated showed an EPBT in Germany of 2,1 years including mounting, cabling and inverter<sup>[3.4]</sup>.

Amorphous silicon has a low embodied energy but due to the low efficiency of the technology, the mean energy pay back time is 2,3 years with a standard deviation of 0,7 years<sup>[3.29]</sup>. The photovoltaic report of Fraunhofer ISE (2018), states that in Germany a-Si modules including mounting, cabling and inverter has an energy payback time of 2,4 years.

Together with a high efficiency for thin film technology and relatively low embodied energy of CdTe resulting in an energy pay back time of 1 year with a standard deviation of 0,4<sup>[3.29]</sup>. This is further backed by the photovoltaic report of Fraunhofer ISE (2018), where it states that in Germany CdTe modules including mounting, cabling and inverter has an energy payback time of 1,2 years.

CI(G)S has the highest embodied energy of all thin film technologies. The efficiency of CI(G)S ensures that the embodied energy of the module is payed back in 1,7 years with a standard deviation of 0,7. The photovoltaic report of Fraunhofer ISE (2018) shows that a CI(G)S module including mounting, cabling and inverter placed in Germany has an energy pay back time of 1,7 years.

## conclusion

Every technology reviewed in this paper can be recycled. Crystalline silicon wafer-based solar panels are the only one where the wafer can be extracted to be reused in another panel. The other technologies can all be recycled via crushing to extract the materials. The toxicity of CdTe and Cl(G)S means that during recycling extra caution needs to be taken. Due to the high embodied energy mono c-Si has the highest energy payback time of all technologies. The reason c-Si technologies have a longer EPBT is due to the relatively thick layer of the wafer in comparison to the thin film generation. The thin layer applied in thin film technologies means that the energy payback time of these technologies is low.

Technology	Recyclability	EPBT (years)
mono c-Si:	Yes, possibility to extract silicon wafer and re-use	3,3
poly c-Si:	Yes, possibility to extract silicon wafer and re-use <sup>[1]</sup>	2,1
amorp. Si:	Yes, via crushing of panel	2,4
CdTe:	Yes, via crushing of panel	1,2
Cl(G)S:	Yes, via crushing of panel	1,7

table 3.6.1: summary sustainability

## 3.7 BIFACIAL

Traditional solar panels capture sunlight on one light absorbing side of the solar panel, light which is not able to be absorbed is reflected away without further use. Bifacial solar panels have the ability to trap sunlight on both sides of the solar module, resulting in power generation on both sides, increasing the efficiency of the panel. Trinasolar claims that the backside of the panel can generate up to 25% more energy when the modules are installed above highly reflective surfaces<sup>[3.31]</sup>. A research compared the output of a bifacial solar module to a regular monofacial solar modules at a 45-degree incline and facing southwards. This result was measured during a period of 4 weeks with a mean increase in energy yield of 13,96%<sup>[3.30]</sup>.

The application of bifacial modules is best suitable for applications like pergolas or other ground-mounted systems where the solar panels are elevated from the ground. This allows the surface behind the solar panel to reflect the light onto the backside of the bifacial module and thereby generate more electricity. In residential sloped roof applications, bifacial modules aren't beneficial for performance and will only drive up the costs without an improvement in performance.

The structure of bifacial solar modules is always glass-glass. Besides the transparent backside of the solar panel is also lets sunlight penetrate through the gaps between the solar cell wafers. This extra light will reflect on the surface behind and therefore generate more power.



fig. 3.7.1: Bifacial solar modules  
(source: Power from Sunlight)

## 3.8 ELECTRICAL CONNECTION

The junction box is a simple box often applied at the back of a solar panel. This piece of technology has two important roles, one being to protect the electronic parts from the environment and two being to connect multiple solar panels to each other (fig 3.8.1). Another function of the junction box is to prevent part of the solar panel consuming power when in a partially shaded state. To prevent this from happening every string has a bypass diode attached to it. At the event of shading of one of the strings, the bypass diode will offer a different path for the current to follow and allow the remaining strings to operate in a normal manner.

In principle the junction box is a simple piece of technology, connecting the solar modules to each other in series, though more functionalities can be added into the junction box. An option is to add power optimizers to the junction box, allowing the power output of the solar panel to be optimized.

Different types/shapes of junction boxes are possible. The most used junction box is a square junction box on the backside of the panel (fig 3.8.2). This type is mostly used in glass-backsheet structure solar modules. In a glass-glass structured solar module, mostly slim designs of junction boxes are applied. An example of this is the pen shape junction box from Almaden (fig 3.8.3). A slim design of the junction box is especially important when applied on a bifacial solar module. The slimness of the junction box allows for less shade to fall on the backside of the module what results in more output.

Placement of the junction box is also variable on the structure, type, and layout of the solar module. On a glass-backsheet structured solar module, the junction box is mostly placed on the backsheet towards the end of the solar module (fig 3.8.2). Reason for this being to facilitate the shorter cables and ease of installation. On glass-glass structured solar modules, there are multiple options. By cutting a hole in the glass the junction box can be placed on the glass backsheet towards the edge (fig 3.8.3). This has the disadvantage initial glass pane is weakened by the hole of the junction box. Extra precautions need to be taken to ensure the waterproofing of the connection between the solar module and the junction box. The other option is to place the junction box on the side of the solar panel. This allows the pane of glass to be kept whole and, when applied in a bifacial application, lesser shade to the backside of the solar module (fig 3.8.4).

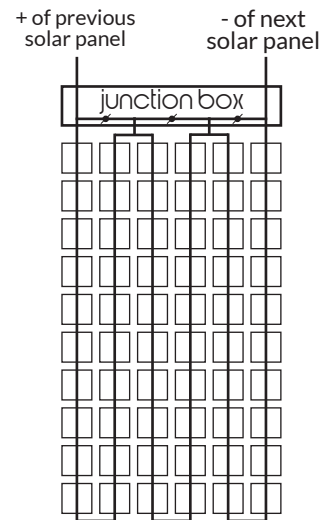


fig. 3.8.1: scheme of function junction box



fig. 3.8.2: junction box on the back of a glass-backsheet module (source: ebay)



fig. 3.8.3: pen shape junction box on the edge of a glass-glass module (source: almaden)



fig. 3.8.4: edge junction box (source: staubli)

## 3.9 BIBLIOGRAPHY

- [3.1] IRENA. (2012). Renewable energy technologies: Cost analysis series: Solar Photovoltaics. Bonn: International Renewable Energy Agency.
- [3.2] Chodos, A. (2009, April). This month in Physics history. Retrieved from APS News: <https://www.aps.org/publications/apsnews/200904/index.cfm>
- [3.3] Battaglia, C., Cuevas, A., & De Wolf, S. (2016). High-efficiency crystalline silicon solar cells: status and perspectives. Royal Society of Chemistry.
- [3.4] ©Fraunhofer ISE: Photovoltaics Report, updated: 27 August 2018. Retrieved from ISE Fraunhofer: <https://www.ise.fraunhofer.de/content/dam/ise/de/documents/publications/studies/Photovoltaics-Report.pdf>
- [3.5] Saga, T. (2010). Advances in crystalline silicon solar cell technology for industrial mass production. Japan: NPG Asia materials.
- [3.6] Lee, T. D., & Ebong, A. U. (2017). A review of thin film solar cell technologies and challenges. *Renewable and Sustainable Energy Reviews*, 1286-1297. doi:10.1016/j.rser.2016.12.028
- [3.7] Pagliaro, M., Ciriminna, R., & Palmisano, G. (2008). Flexible Solar Cells. *ChemSusChem*, 880-891.
- [3.8] Schock, H. (1996). Thin film photovoltaics. *Applied Surface Science*.
- [3.9] Bosio, A., Menossi, D., Mazzamuto, S., & Romeo, N. (2011). Manufacturing of CdTe thin film photovoltaic modules. *Thin Solid Films*.
- [3.10] Britt, J., Wiedeman, S., Schoop, U., & Verebelyi, D. (2008). High-volume manufacturing of flexible and lightweight CIGS solar cells., 2008 33rd IEEE Photovoltaic Specialists Conference (pp. 1-4). San Diego: IEEE.
- [3.11] Schindler, F., Fell, A., Müller, R., Benick, J., Richter, A., Feldmann, F., Glunz, S. W. (2018). Towards the efficiency limits of multicrystalline silicon solar cells. Freiburg: Elsevier
- [3.12] Green, M. A., Emery, K., Hishikawa, Y., Warta, W., Dunlop, E. D., Levi, D. H., & Ho-Baillie, A. W. (2017). Solar cell efficiency tables (version 49). *Progress in Photovoltaics: Research and Applications*, 3-13.
- [3.13] Meillaud, F., Boccard, M., Bugnon, G., Despeisse, M., Hänni, S., Haug, F., ... Ballif, C. (2015). Recent advances and remaining challenges in thin-film silicon photovoltaic technology. *Materials Today*.
- [3.14] Dash, P., & Gupta, N. (2015). Effect of Temperature on Power Output from Different Commercially available Photovoltaic Modules. *Journal of Engineering Research and Applications* [www.ijera.com](http://www.ijera.com).

- [3.15] SHARP. (2010). 135 Watt Thin Film module NA-V135H1. Sharp.
- [3.16] SCHOTT Solar. (2009). Thin film solar modules. Alzenau: SCHOTT Solar
- [3.17] Advance Solar Power. (2019, 1 3). CdTe THIN FILM SOLAR MODULES. Retrieved from WCP Solar: [http://www.wcpsolar.com/files/DS-WCP\\_Modified\\_ASP\\_Specifications\\_12222014-150122.pdf](http://www.wcpsolar.com/files/DS-WCP_Modified_ASP_Specifications_12222014-150122.pdf)
- [3.18] Calyxo. (2019, 3 1). CX3-SERIES - CDTE THIN FILM SOLAR PANEL. Retrieved from Calyxo: <https://calyxo.com/en/cx-series.html>
- [3.19] DMSolar. (2019, 1 3). DM 77W CdTe Solar Modules. Retrieved from DMSolar: <http://www.dmsolar.com/cdte.html>
- [3.20] FIRST SOLAR. (2018). SERIES 6. First solar INC. Retrieved from <http://www.firstsolar.com/en-EMEA/-/media/First-Solar/Technical-Documents/Series-6-Datasheets/Series-6-Datasheet.ashx>
- [3.21] Munshi, A. H., Sasidharan, N., Pinkayan, S., Barth, K. L., Sampath, W., & Ongsakul, W. (2018). Thin-film CdTe photovoltaics – The technology for utility scale sustainable energy generation. In I. S. Society, *Solar Energy* (vol. 173 ed., pp. 511-516). Elsevier.
- [3.22] Stion. (2019, Januari 3). High Performance CIGS Thin-Film Solar Modules. Retrieved from Stion: [https://www.platendt.nl/pdf/300-007-000\\_rev\\_a\\_stion\\_sto\\_datasheet\\_module\\_135-150.pdf](https://www.platendt.nl/pdf/300-007-000_rev_a_stion_sto_datasheet_module_135-150.pdf)
- [3.23] Global Solar. (2019, Januari 3). PowerFLEX+ Flexible Solar Panels. Retrieved from Global solar: <http://www.globalsolar.com/sites/default/files/uploads/images/Copy%20of%20PowerFLEX%20BAPV%20Data-sheet%20%28PROD%20LIT%20-%201000781%20-%201%20-%20D%29.PD>
- [3.24] International Energy Agency. (2013). Task 41 - Designing Photovoltaic systems for architectural integration. Paris: International Energy Agency.
- [3.25] Xu, Y., Li, J., Tan, Q., Peters, A. L., & Yang, C. (2017). Global status of recycling waste solar panels: A review. Beijing: Elsevier.
- [3.26] Granata, G., Pagnanelli, F., Moscardini, E., Havlik, T., & Toro, L. (2014). Recycling of photovoltaic panels by physical operations. *Solar Energy Materials and Solar Cells*.
- [3.27] Lunardi, M. M., Alvarez-Gaitan, J., Bilbao, J. I., & Corkish, R. (2018). A Review of Recycling Processes for Photovoltaic Modules. Sydney: IntechOpen.
- [3.28] First Solar. (2019, 1, 3). Recycling. Retrieved from Firstsolar: <http://www.firstsolar.com/Modules/Recycling>
- [3.29] Bhandari, K. P., Collier, J. M., Ellingson, R. J., & Apul, D. S. (2015). Energy payback time (EPBT) and energy return on energy invested (EROI) of solar photovoltaic systems: A systematic review and meta-analysis. Toledo: Elsevier.
- [3.30] P. Sánchez-Friera, B. Lalaguna, D. Montiel, J. Gil, L.J. Caballero, J. Alonso, M. Piliouguine, M. Sidrach de Carmona (2007) Development and characterisation of industrial bifacial PV modules with ultra-thin screen-printed solar cells. 2008 22nd EUPVSEC conference. Milan.

[3.31] Trinasolar (2019, April 27). DUOMAX twin. Retrieved from <https://www.trinasolar.com/us/product/duomax-twin>



**4.** **STRUCTURAL  
SOLAR  
MODULES**

## 4.1 INTRODUCTION

Solar modules cope with wind and snow load in real-world applications. These loads are changing continually and are hardly ever the same. These forces are then distributed onto the mounting structure behind the solar panel. This structure will transfer the forces to the ground/foundation or in case of a roof mounted solar system to the structure of the building. An example of a regular supporting structure of solar panels is given in (fig. 4.1.1). The main concern when the solar modules are loaded with the loads mentioned above is deformation of the module. This deformation will result in extra stress at the solar cell level which will result in the cell cracking. When the silicon wafer is cracked it can affect the output of the panel in three ways. First, if the crack breaks an electrical connection within the cell itself the current cannot flow through the cell causing a 'dead zone'. Second, a cracked cell reduces the shunt resistance of the cell, resulting in reduced current output of the cell. Thirdly, cracks create traps and defects throughout the entire thickness of the cell reducing its efficiency. The goal of this research is to explore the possibilities of integrating the solar panels into a structure. Therefore discarding the need of a supporting structure.



fig. 4.1.1: supporting structure of regular ground mounted solar modules (source: Hi-tech)

The most used solar cell modules technologies; mono crystalline and poly crystalline solar cells, have two structures, one that has a front and back pane of glass, whilst the other has a back pane of plastic. The outermost layers of the solar module protect the solar cell from the environment. It protects the solar cells from; water, water vapor and gaseous pollutants. The cover glass is often made out of hardened tempered glass to protect from wind and hail damage.

Research showed the ability of a person of 90 kg walking on two different configuration of silicon modules, one was a glass-glass configuration and the other a glass-foil configuration<sup>[4.1]</sup>. The modules were placed horizontally on the ground and supported amongst side the edges to allow deflection to occur. An electroluminescence equipment was utilized to record any damages on the module after mechanical stress. The results showed that the glass-foil silicon cells were damaged after applying the load on the module. This resulted in physical cracks in the solar cells, as seen in (fig. 4.1.3). The glass-glass module did not present any damage after the mechanical load, as seen in (fig. 4.1.4). This research shows the structural capabilities of regular solar modules.

This is further backed by a finite model simulation of a glass-foil and glass-glass solar module by Gabor, et al. (2016). In this simulation the stress in the middle of the two structures is shown, as seen in (fig. 4.1.2). Because of the symmetrical construction of glass-glass the stress in the center is close to nothing when compared to glass-foil.

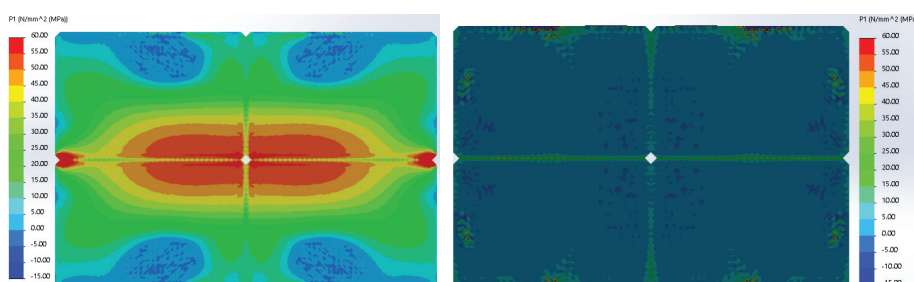


fig. 4.1.2: finite simulation of stress in solar module. left: glass-foil, right: glass-glass (source: bibliography 42)

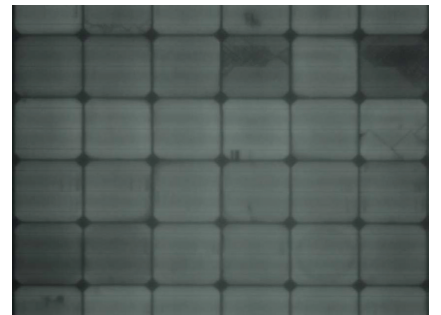
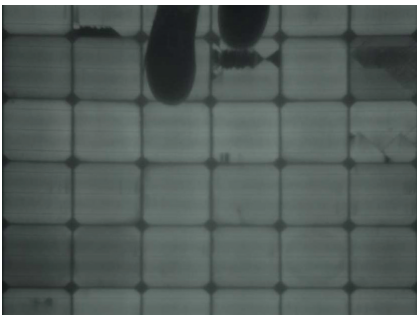
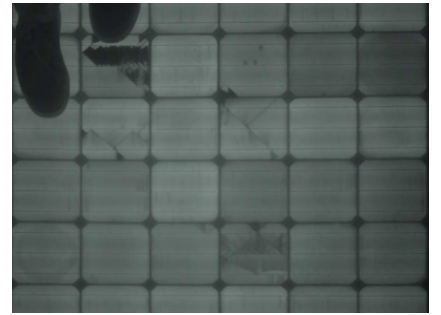
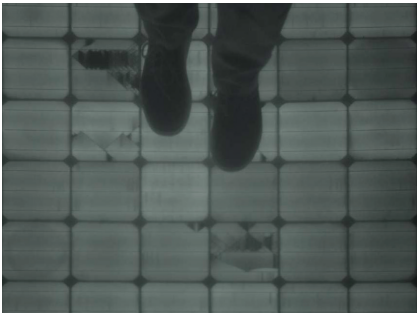
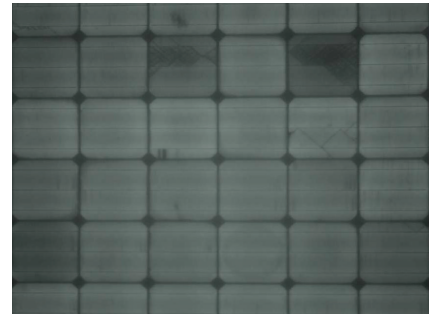
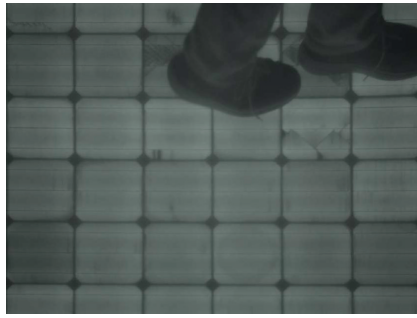


fig. 4.1.3: glass-foil module electroluminescence images  
(source: bibliography 4.1)

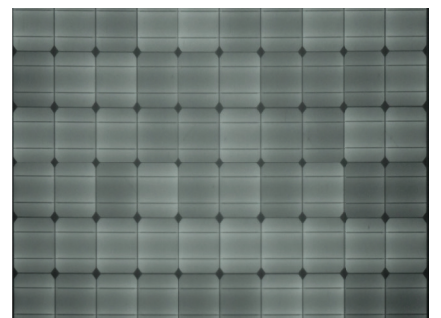
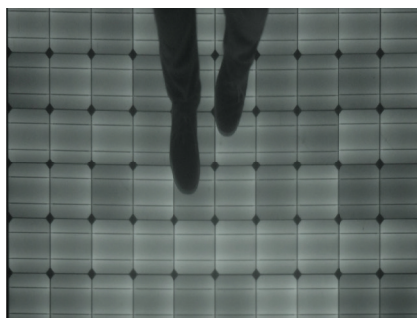


fig. 4.1.4: glass-glass module electroluminescence images  
(source: bibliography 4.1)

## 4.2 GLASS AS LOAD BEARING MATERIAL

Glass is a product of fusion. In a hot and viscous state glass can be formed into planar, linear or compact semi-finished products. Glass itself is a brittle material, meaning that when subjected to stress the material breaks without significant deformation (fig. 4.2.1). Due to this brittleness point loads need to be avoided to reduce stress in the glass. After the production of the glass, usually float glass, optional production processes follow to achieve better specific technical properties.

Almost all of the glass that is manufactured is used in float glass, only 10 percent is used in rolled or drawn<sup>[4,3]</sup>, therefore this chapter will focus on float glass.

After manufacturing of the basis float glass further processing steps can be applied to achieve different types of glass. From the basic float glass / annealed glass different types of glass can be produced. Each of these types has different characteristics. Tempering and heat-strengthening of the glass involves artificially introducing stresses into the glass to further enhance their structural properties. Tempered and heat-strengthened glass is manufactured in similar manner. Annealed/basic float glass is heated briefly up to 650 °C to be forced cooled afterwards. This process creates surface or edge compression in the glass. By controlling the rate of cooling the glass is either tempered or heat-strengthened. Tempered glass is created by increasing the rate of cooling, which increases the stresses in the glass and therefore increases the mechanical strength of the glass.

The introduced stress in the glass has enhanced the structural capabilities of heat-strengthened and tempered glass. In (table 4.2.1) the mechanical properties of the different types of glass are shown. The density and Young's modulus of tempered and heat-strengthened glass didn't alter after the introduction of surface stress. Although the tensile strength of heat-strengthened glass almost doubled, whilst tempered glass almost has triple the tensile strength when compared to annealed glass. When loaded until breaking point another characteristic of tempered glass shows. Where annealed and heat-strengthened glass fracture in large pieces, tempered glass fractures into smaller pieces (fig. 4.2.2). Which tends to lead to a safer situation when loaded until breaking point, although the fractured pieces may stay together until they fall out which could lead to injury.

	Annealed glass	Tempered glass	Heat-strengthened glass
Density (kg/m <sup>3</sup> )	25	25	25
Young's modulus (kN/cm <sup>2</sup> )	70	70	70
Tensile strength (kN/cm <sup>2</sup> )	4,5	7	12

table 4.2.1: overview mechanical properties different glass types

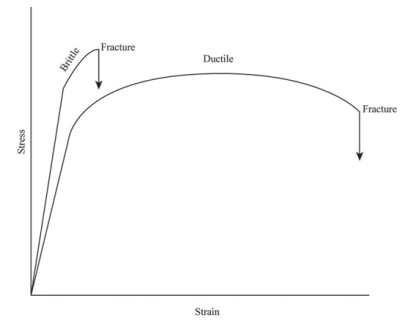


fig. 4.2.1: Brittle vs ductile material, stress vs strain (source: Chegg)

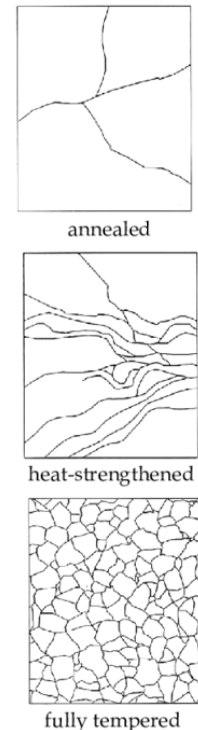


fig.4.2.2: fracture pattern different types of glass (source: Schittich)

## requirements glass

The requirements for the use of glass is dependent on the application of the glass. When the glass is applied non-vertical and is only accessible for maintenance and repairs and in the overhead application the following requirement is applicable. The glass applied in the structure should be layered glass according to specification 1B1 according to NEN-EN 12600. Glass is tested by fixing a glass plate in a frame and swinging a 50 kg weight into the glass. The number in the type indication means the height at which the weight is released, in this case, 1200 mm<sup>[4.4]</sup>. How the glass breaks are indicated by the letter (fig. 4.2.4), B meaning it shatters but sticks together by the intermediate layer in between the layered glass.



fig. 4.2.3: Glass testing for specification  
(source: GlasInBeeld)

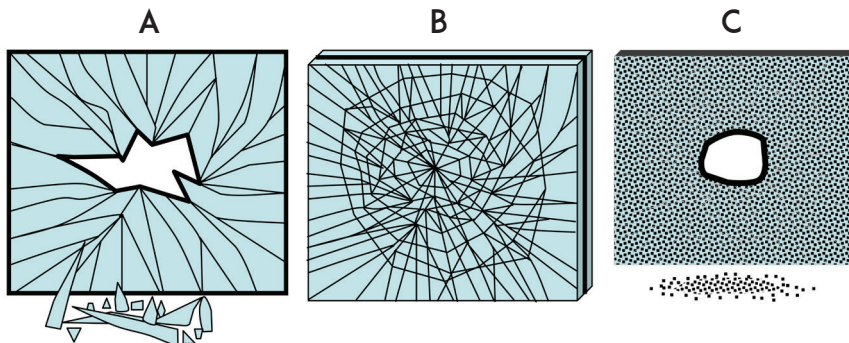
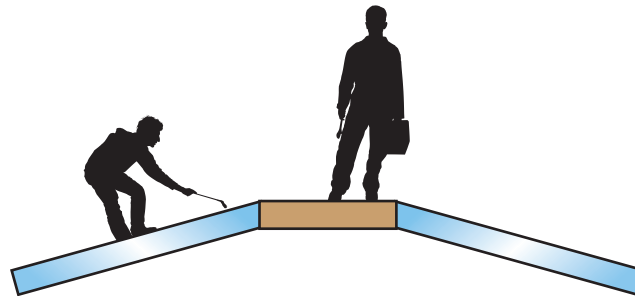
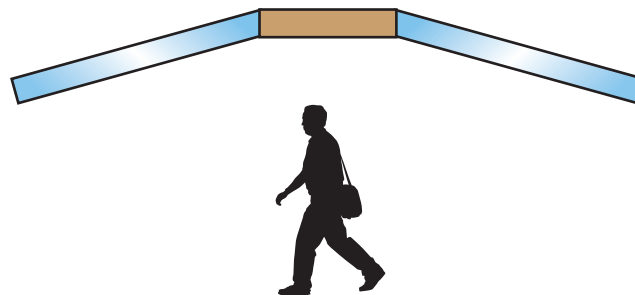


fig. 4.2.4: Breakage types glass  
(source: bibliography 4.4)

RISK OF BREAKING THROUGH GLASS  
NON VERTICAL, ACCESSIBLE FOR MAINTNANCE



RISK OF FALLING GLASS  
NON VERTICAL



## 4.3 SOLAR CELL WAFER

The solar cell wafer in the middle of the solar module is a fragile piece in the lamination. This chapter will discuss the silicon wafers ability to handle the load. The silicon wafer is a thin piece of silicon cut from a silicon ingot. The thickness of this wafer varies amongst different solar panel manufactures. To further reduce the costs the photovoltaic industries are decreasing the thickness to bring down prices of the solar module. This increases the change of cracked silicon wafers which have a great impact on the durability of the solar panel.

In unpublished work of the University of Central Florida has shown that maybe the magnitude of stress and strain gradients is strongly related to the location of the cracked cells in the module<sup>[4.2]</sup>. The ability of the wafer to handle stress is researched by S. Schoenfelder and A. Bohne (2007). In this research, 100 different pseudo square mono crystalline solar cell wafers from the PV industry were examined. The thickness of these wafers varies from 137  $\mu\text{m}$  to 209  $\mu\text{m}$ , with a mean of 176  $\mu\text{m}$ . These wafers had the most common used size being 156mmx156mm. These wafers were subjected to three different test methods, being; 4-point bending test, ball-on-ring test, and twist test, as shown in (fig. 4.3.1). For the ball-on-ring test, smaller samples were used to avoid buckling during loading.

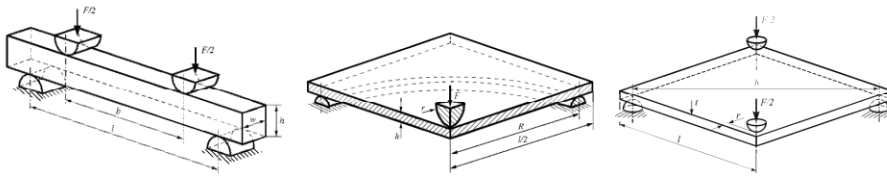


fig. 4.3.1: different test methods (left to right: 4-point bending, ball-on-ring and twist test (source: bibliography 4.5)

The results of this experiment can be seen in (table 4.3.1). The 4-point bending test showed the greatest fracture force and fracture deflection. These outcomes were transferred into a finite element simulation generate the fracture stress of the wafers. After the stress was calculated for every sample, the outcomes were statistically evaluated. The characteristic fracture stress  $\sigma_{\theta}$  represents the stress at which 63,2% of all the samples failed.

Test method	Fracture force (N)		Fracture deflection (mm)		Characteristic fracture stress $\sigma_{\theta}$ (MPa)
	mean	standard deviation	mean	standard deviation	
4-point bending	17,21	2,77	15,02	2,26	262 (255..269)
ball-on-ring	5,21	0,87	0,057	0,006	372 (365..380)
twist test	4,71	0,75	14,27	2,00	157 (153..162)

table 4.3.1: Experiment result of fracture force and fracture deflection (source: bibliography 4.5)

## 4.4 STRUCTURAL CAPABILITIES PV

Different methods have been used to test the modules capability to handle the load. Gabor, et al. (2018) mentions in their research that BrightSpot Automation built a new type of mechanical testing tool to load test solar modules, the Loadspot prototype. This tool applies vacuum/air-pressure to the rear side of the panel. As seen in (fig. 4.4.1) this tool has a transparent front side, which allows the relation of performance degradation and crack formation versus the load on the panel to be analyzed.



fig. 4.4.1: BrightSpot Automation mechanical testing tool (source: bibliography 4.2)

The first step in the experiment was to create an increasing load on a panel, as seen in (fig. 4.4.2). The panel had no cracks in the initial state. When the load was increased up top 1200 Pa significant cracks occurred. After increasing the pressure more cracks started occurring. When decreasing the pressure back to 0 Pa all the cracks fully closed and where undetectable via the EL images.

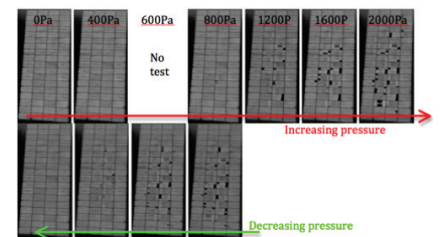


fig. 4.4.2: Electroluminescence images of solar panel when increasing and decreasing structural load (source: bibliography 4.2)

The following experiment had the goal to find the impact of loading in relation to the output of the panel. Increasing pressure was applied to the backside of the panel, increasing from 0 Pa to 2000 Pa. Additionally, different shading types were tested under loading. The module used in the previous experiment was re-used which had pre-existing cracks.

(fig. 4.4.3) shows the relationship with loading the solar module and the power degradation. With increasing the load on the solar panel the power output of the panel did drop. Gabor, et al. (2018) notes that the initial difference of 8,6% between the no shade level and narrow shade stick increases when the loading increases. This research also showed that in the phase from 0 to 400 Pa no decrease in output is noticed.

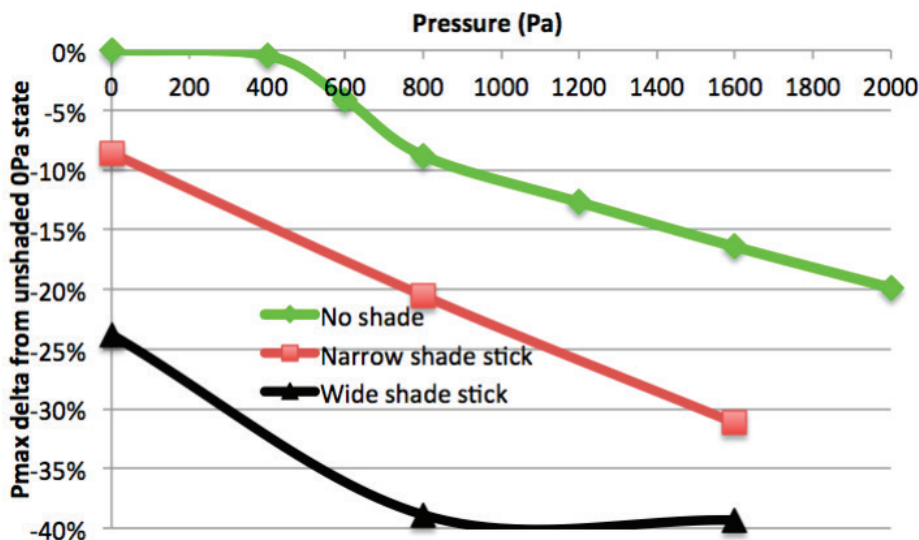


fig. 3.7.9

fig. 4.4.3: Power degradation in relationship with loading at different shade levels (source: bibliography 4.2)

## structural requirements solar panels

As previously mentioned in 'Requirements for glass' the use of overhead glazing is restrained to laminated glass. Therefore classifying glass-glass solar modules is desirable, but current building requirements are not adequate. Normally in laminated glass polyvinyl butyral (PVB) is used as an intermediate layer, in solar modules this layer normally consists out of Ethyleenvinylacetaat (EVA), although PVB is possible however EVA is more conventional. Another question is the influence of the integrated solar cells on the shear stiffness of the interlayer. In research done by Claudia Hemmerle (2017)<sup>[4,6]</sup> full-size glass-glass solar modules with PVB interlayers are compared to laminated safety glass with the same thickness PVB. In this experiment, the following aspects are tested; Residual resistance testing and shear testing.

In the residual resistance test post fracture capabilities of a solar module is compared to a laminated safety glass (LSG) at standard temperature (23 degrees) and increased temperature (50 & 68 degrees). The module and LSG were damaged by dropping a steel ball from a height of 2.5m. Integrating the solar cells into the lamination didn't significantly influence the breakage structure. Post breakage a load is applied to gain insight into the residual resistance. At the standard temperature scenario, none of the samples failed. The solar modules with embedded silicon wafers showed 20 - 25% less deflection at the center. The conclusion was made that the integration of PV cells improved the residual resistance of the lamination. In the increased temperature test the thickness of the PVB layer showed as a crucial parameter. Both PV and LSG samples with a 0.76 mm PVB layer failed as soon as the temperature exceeded 50 degrees Celsius. PV and LSG samples with 1.00mm PVB layer passed the test without failure. Again the solar modules had 20 to 25% less center deflection. In the second temperature test of 68 degrees, none of the PV samples failed whilst two out of three of the LSG samples failed. The interconnection of the solar cell wafer within the solar module reinforce the broken glass and provide support for tensile forces (fig. 4.4.4). The ability of solar modules to absorb solar energy results in a higher temperature than LSG. The research showed that solar modules with embedded silicon wafers could heat up 11 to 18 degrees more than the LSG to achieve the same deflection. The temperature rise of Integrating the solar modules into a building skin when compared to LSG is only 5 to 6 degrees.

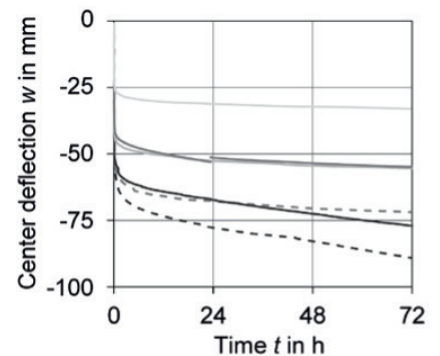
In the next experiment the influence of solar cell integration on the shear bond and adhesion. Cylindrical PV samples and LSG samples were compared to each other. First, a load of 400N was applied for 10 minutes, followed by an increase in load at a speed of 2mm/min. The test showed that integrating PV cells did not significantly influence the shear modulus. Yet, the solar cells failed at lower stresses than the LSG samples. The conclusion was made that by integrating the PV cells the adhesive bond within the laminate is reduced.

The final conclusion of the research is that the tested glass-glass solar wafer modules provided a safety level which is at least the equivalent to laminated safety glass.

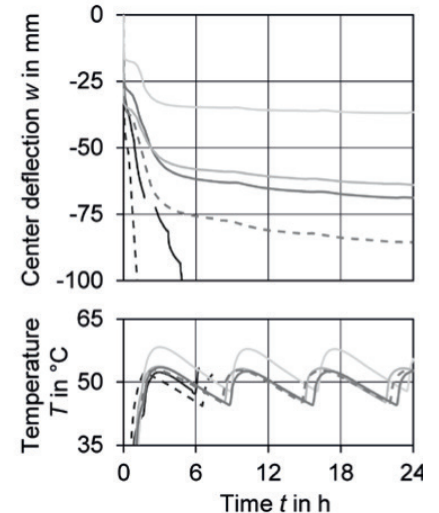


fig. 4.4.4: Improved residual resistance due to PV wafer cells' soldered inter-connectors  
(source: bibliography 4.5)

### NORMAL TEMPERATURE



### INCREASED TEMP.



- PV flexible thin-film
- PV wafer thin glass
- PV wafer float glass
- PV superstrate glass
- - - LSG 1 (1.00mm PVB)
- - - LSG 2 (0.76 mm PVB)

## 4.5 MECHANICAL CONNECTION

The mechanical connections within the structure transfer the load from the glass panels to other glass panels to the supporting structure below. Forces can be transferred either at the surface of the glass or at the edge of the glass. It is important that this connection doesn't cause stress concentration, because due to the brittleness of glass this can lead to failure of the panel without warning<sup>[4.3]</sup>. There are two main categories of connections; mechanical and adhesive connections. Within these two main categories different types of subcategories are recognized (fig 4.5.1)

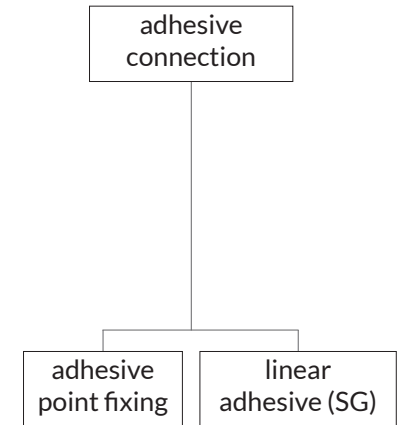
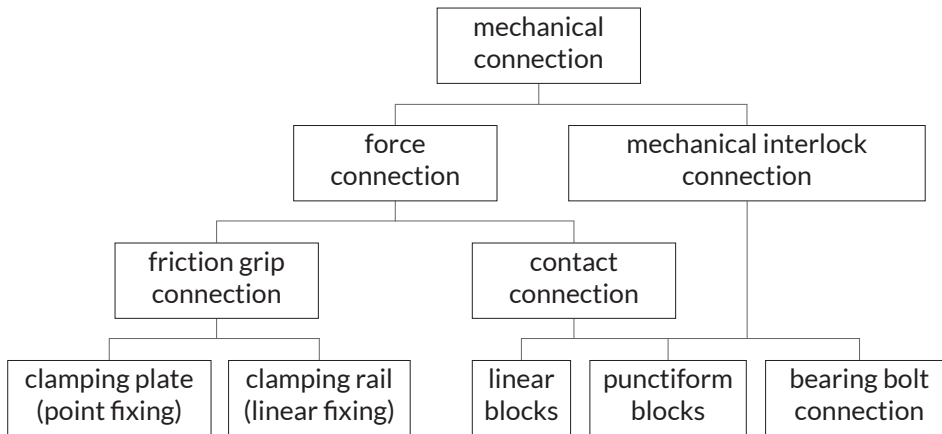


fig. 4.5.1: classification of connections (source: bibliography [4.3])

Due to the potential replacement of the PV panels and the complexity of replacing the panels when adhesive connections are applied, this connection type isn't further researched.

When point fixing is compared to linear fixing the conclusion can be made that point supports cause extra stress concentration. This is due to the more efficient use of the cross section by linear supports. This is substantiated by FEM simulations (fig 4.5.2). The FEM simulations show that when a plate is loaded in plane and uses punctiform supports the stress distribution is higher than when the same force is applied on linear support. Therefore the punctiform supports are rejected as a choice for the mechanical connection between the solar panels.

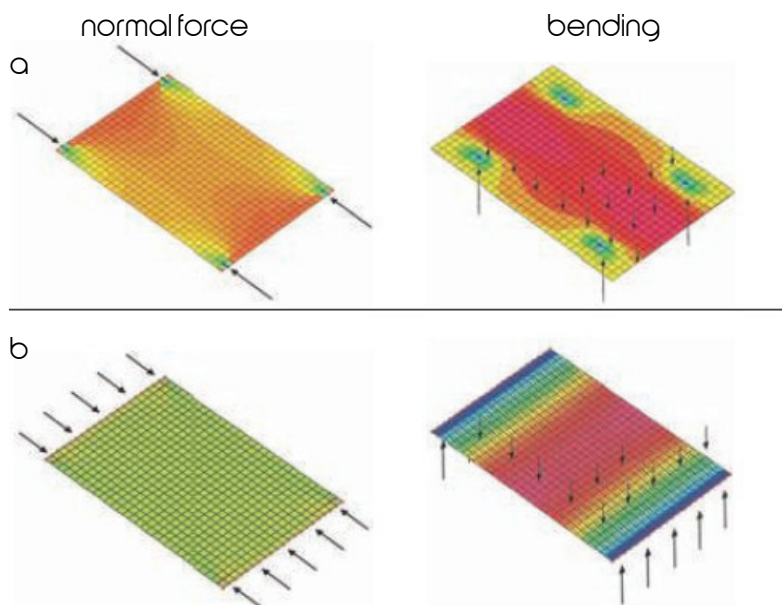


fig. 4.5.2: Qualitative comparison of the stress distribution in panes and plates with punctiform (a) or linear supports (b) based on FEM models (source: bibliography [4.3])

## analysis of existing linear mechanical connection

To gain an understanding of a possible mechanical connection for the glass carport different cases will be analyzed. From every case, the pro's and the con's will be acknowledged to generate an overview of the possibilities and their strengths and weaknesses. The cases that will be studied are Glass dome by TU Delft and the graduation project of Niki Nikolaou.

## glass dome TU Delft

In 2003 a glass dome was designed as a showcase for the structural application of glass. A line joint was concluded to be an effective connection for the dome. The direct connection between the hard materials, glass, and aluminum had to be avoided, otherwise, local point loads couldn't be avoided which introduce local stresses on the edges of the glass. For joining the glass elements together a combination of adhesive and mechanical joining method was used. This was done by gluing a square aluminum rod to the edge of the glass panels using an adhesive. These aluminum rods are then clamped together using two strips and a bolt. The corners of the glass are kept free to allow for some tolerance.

### advantages

By gluing the connection to the glass, the glass elements can be unaltered and in full strength. No holes are necessary for this connection. The applying the adhesive there is no need for a soft intermediate material between the two hard, glass and aluminum, materials. The adhesive also has the benefit of distributing the stress across the joint.

### disadvantages

This kind of connection is ideal for a dome. In a dome the main type of loading is compression. If an alternate shape is introduced, tensile forces will occur. These tensile forces will try to delaminate the adhesive from the glass which will over time result in a failure of the connection. In the dome, every pane of glass has the same angle relative to each other. In a design where the curvature is not consistent this connection will be hard to realize since the angle at which the square aluminum rods are glued to the glass alters.

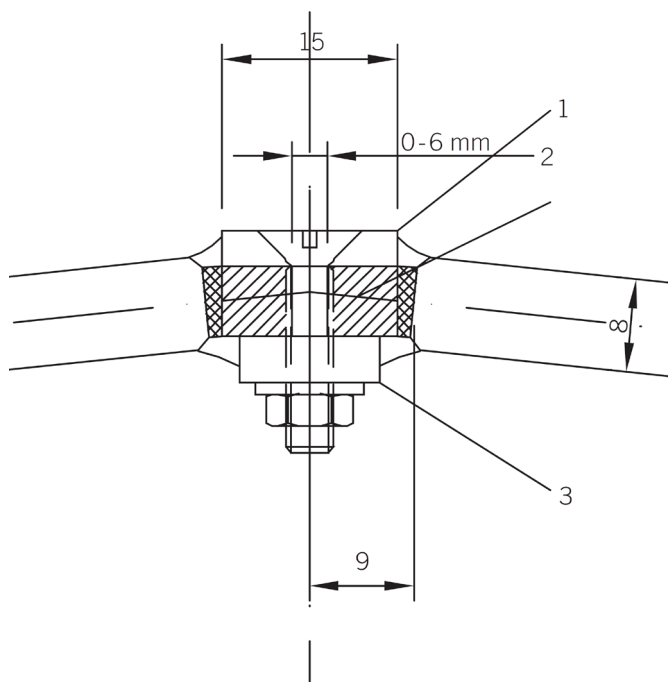


fig. 4.5.3: Overview glass dome TU Delft  
(source: bibliography 4.7)

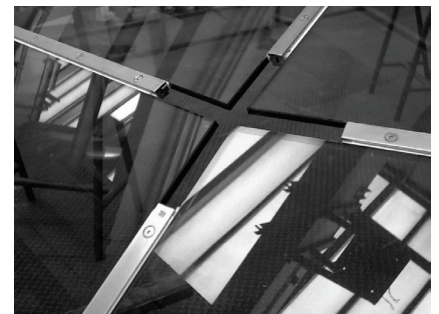


fig. 4.5.4: Close up connection  
(source: bibliography 4.7)

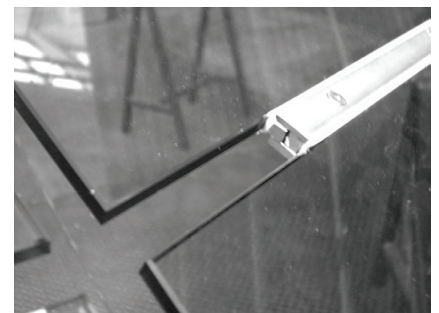


fig. 4.5.5: Close up connection  
(source: bibliography 4.7)

fig. 4.5.6: detail of glass connection TU Delft dome  
1: 15/3 flat steel  
2: 6/6 square rod  
3: 14/2 flat steel  
(source: bibliography 4.3)

# graduation project Niki Nikalaou

A mechanical connection by laminating the connection between the glass layers. This linear contact block connection consists of a composite material that is laminated into the glass. This cylindrical shaped composite joint is then clamped in a linear aluminum contact block. Between the composite element and the aluminum contact block, a PCM sleeve is placed for added friction.

## advantages

The joint allows for an alternation of the angle between two panes. This is due to the cylindrical shape of the composite element and the contact block not completely closing the element. Therefore this connection is better suitable for free from structures. By laminating the connection into the glass the area at which the load is transferred to is bigger, therefore distributing the forces.

## disadvantages

By applying this connection the manufacturing process of the solar panels needs to be altered, although the current solar panels already are laminated. This will result in a rise in costs. The contact block has quite a substantial size, therefore reducing the transparency of the whole structure. The embedded reinforcement protrude into the glass structure. This will result in less area at which solar cells can be placed and therefore reducing the overall efficiency of the solar panel.

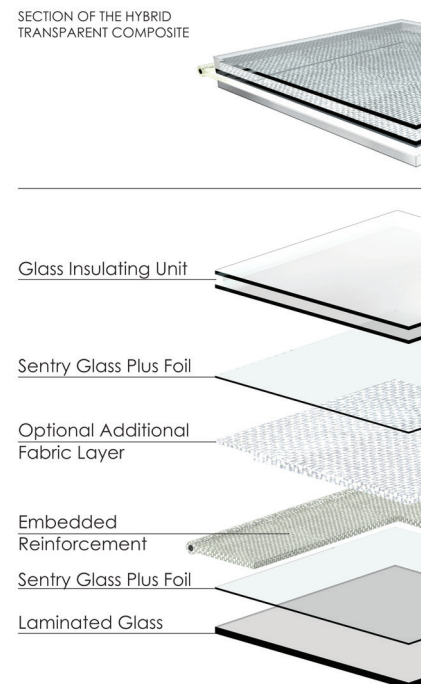


fig. 4.5.7: Exploded view of the connection (source: bibliography 4.8)

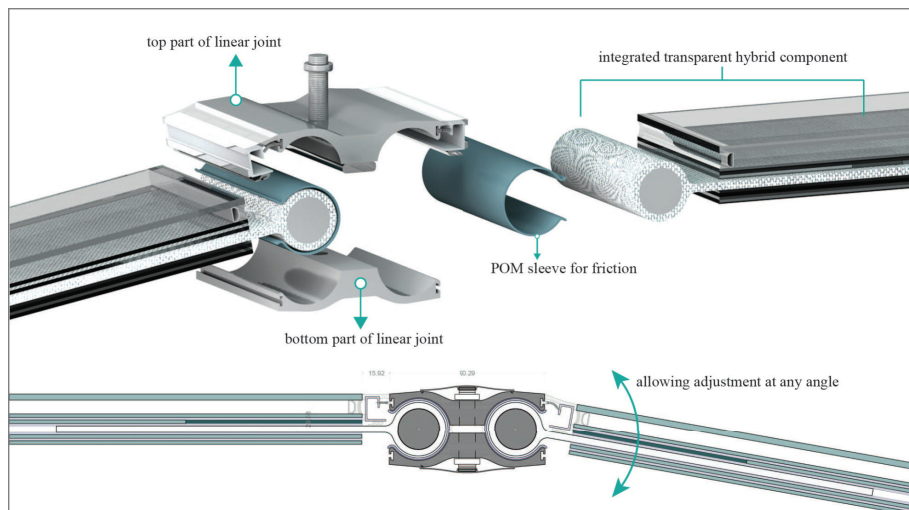


fig. X.X.X

fig. 4.5.8: Detail of the connection (source: bibliography 4.8)

## conclusion

From the different connection typologies acknowledged by J. Wurm, a selection is made. Adhesive connections are not desirable due to the possibility of replacement of the PV panels either by failure or due to the option of replacing the PV panels by more efficient panels in the future. The difference of stress distribution in punctiform versus linear supports is compared and the conclusion is made that linear supports distribute the stress across the whole section and is, therefore, more desirable.

Two linear connections are studied, The connection of the TU Delft Dome and The graduation project of Niki Nikalaou, and the advantages and disadvantages are mentioned. For a dome-like shape, the connection of the TU Delft Dome is sufficient, however, for a free form structure, the connection of Niki Nikalaou is more favorable due to the possibility to alter the angle between two panes and the ability to also transfer tensile forces that are the result of the freeform shape.

In this research, the connection of Niki Nikalaou is chosen for further development. The intended shape for the NS carport is a freeform structure, furthermore, the pilot study is a freeform structure.

## 4.6 MECHANICAL CONNECTION INTEGRATION IN PV

To integrate the connection into the PV structure multiple options are possible. In this section, two options are analyzed on their pro's and cons. The first option for the connection is when the embedded reinforcement is laminated in between the solar module itself. In the second option, another layer of glass is laminated below the solar module. In between the new layer of glass and the solar module the connection is laminated.

### 1. embedded reinforcement inbetween the solar module

As mentioned above, in this option the connection is laminated inside the solar module itself. This is done in the same layer as the solar cells. This results in the solar cells shifting back, to allow the connection to be implemented.

This option has the following pro's, the first being that the solar cells are in the zero bending stress level. Which results in lower stress on the fragile solar cells. although the normal stresses will still affect the solar cell. The second benefit is that the connection can be laminated at the solar cell manufacturer. This allows for a better end product since the lamination of the connection and the solar module is done at the same location.

The cons of this option are that there is less area available for the implementation of solar cells. This is due to the connection shifting back the cells. Another cons is the placement of the junction box. The junction box cannot be placed on the side of the solar module since the connection is placed there. This results in the junction box penetrating the glass and thereby negatively influences its structural integrity. The last con is that even though the connection is laminated by the solar cell manufacturer, the solar cell itself is custom made. This will increase the costs and the complexity of the solar cell.

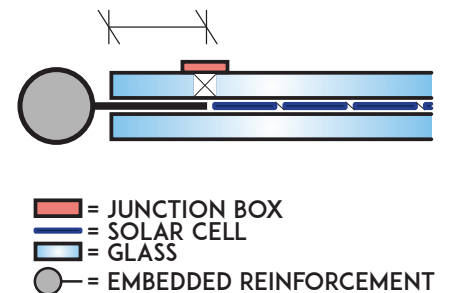


fig. 4.6.1: schematic drawing of option 1

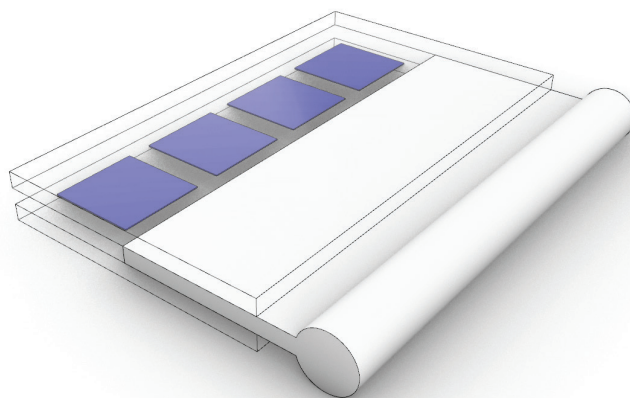


fig. 4.6.2: overview connection option 1

## 2. embedded reinforcement laminated below solar module

As mentioned above, in this option the connection is laminated below the solar modules. This is done by laminating an extra layer of glass below the solar module.

This option has the following pro's. The first pro is that by laminating the connection below the solar module, the solar module itself can be a standard module that is available on the market. This allows the price of the solar module itself to be as low as possible due to standardization. Another benefit is the maximum available area for solar cell implementation. This will result in a higher output of the design. The final pro is the placement of the junction box. This can be placed on the edge of the glass, without requiring a hole in the glass of the solar modules. This keeps the structural integrity of the solar module intact.

The con's to this option is that another layer of glass needs to be implemented in the design. This requires extra materials and another lamination process. Besides the extra energy required for the lamination, it adds more risk of delamination.

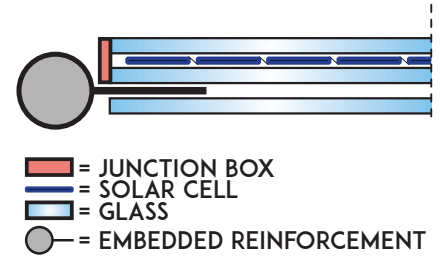
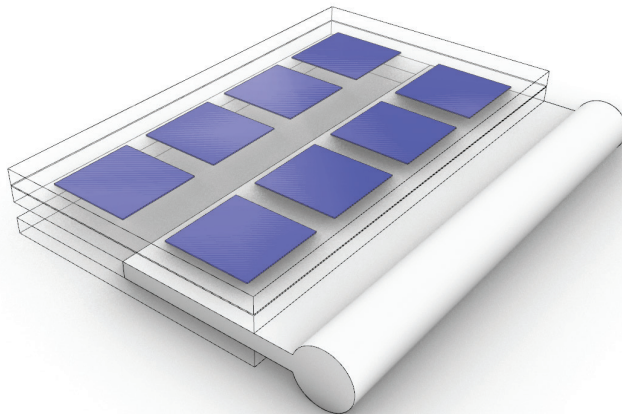


fig. 4.6.3: schematic drawing of option 2

## conclusion

In this section, two different options are analyzed for the implementation of the connection of Niki Nikalaou in solar cell modules. The first option is the integration of the connection between the solar modules, whilst the second option adds another layer of glass for the integration of the connection. The final decision is made to continue with the second option. The main factor's for this decision is the placement of the junction box and the maximum area of solar cell implementation. After a visit to a custom solar cell manufacturer, the first option wasn't possible to realize. The ribbons integrated into the solar cells wouldn't be able to gap the extra thickness of the connection. Therefore the second option will be further developed in this research.

## 4.7 BIBLIOGRAPHY

- [4.1] Gómez, G. (2017). BIPV: Modules Characterization. Delft: TU Delft.
- [4.2] Gabor, A., Janoch, R., Anselmo, A., Lincoln, J., Seigneur, H., & Honeker, C. (2018). Mechanical load testing of solar panels - Beyond certification testing. 2017 IEEE 44th Photovoltaic Specialist Conference, PVSC 2017.
- [4.3] Wurm, J. (2007). Glass structures: Design and Construction of Self-Supporting Skins. Basel: Birkhäuser Verlag AG
- [4.4] VGI (2010). DE VERSCHILLENDE TYPES VEILIGHEIDSGLAS. Retrieved from <https://www.vanpellicom.be/wp-content/uploads/2012/07/veiligheidsglas.pdf>hergebruik\_van\_spoorstaven/
- [4.5] S. Schoenfelder\*, A. Bohne, J. (2007). Comparison of test methods for strength characterization of thin solar wafer. Fraunhofer Institute for Mechanics of Materials
- [4.6] Hemmerle, C. (2017). Solar PV Building Skins – Structural Requirements and Environmental Benefits. JOURNAL OF FACADE DESIGN & ENGINEERING, 5(7), 93-106. <https://doi.org/10.7480/jfde.2017.1.1528>.
- [4.7] F.A.Veer, J Wurm, G.J.Hobbelman (2003).The Design, Construction and Validation of a Structural Glass Dome. Glass processing days 2003 Tampere, Finland.
- [4.8] N. Nikolaou (2015). Transparent enclosures; design strategies for free-form shell with structural glass. Delft



## **5. PILOT STUDY**

## 5.1 INTRODUCTION

To gain knowledge about integrating solar panels in a structural manner, a case study is done. A random complex design will be chosen for the integration of solar cells. The design that is chosen is the design of Brunier Ernst. This carport was designed for the architecture fair BAU 2013 in Munich. This carport was a prototype for “innovation in exploring the potential of sheet metal design and fabrication” as Brunier Ernst state on their website. It showed the possibilities of digital designing and structural form-finding methods.

The design will be adjusted to allow the solar panels to be structurally integrated. After the adjustments of the design, the structural connection will be discussed. The connection will be analyzed and discussed. The design will be simulated using Grasshopper with the following plug-ins: Karamba & Kangaroo.



fig. 5.1.1: carport case study by Brunier Ernst  
(source: Otto Wöhr GmbH, Frießheim)

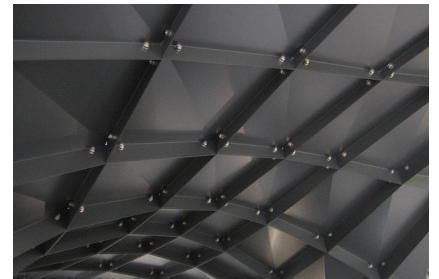


fig. 5.1.2: close-up inside  
(source: Otto Wöhr GmbH, Frießheim)



fig. 5.1.3: close-up connection  
(source: Otto Wöhr GmbH, Frießheim)



fig. 4.1.4: design render

## 5.2 DESIGN

The design concept is shown in (fig 5.2.3). The base shape is a rectangle where two points on the corner of the shape are elevated to get an arc. Two cantilevering shapes are added on the design to create the final shape. Finally, the two corners are further elevated whilst the arc in the middle of the design remains at the same height.

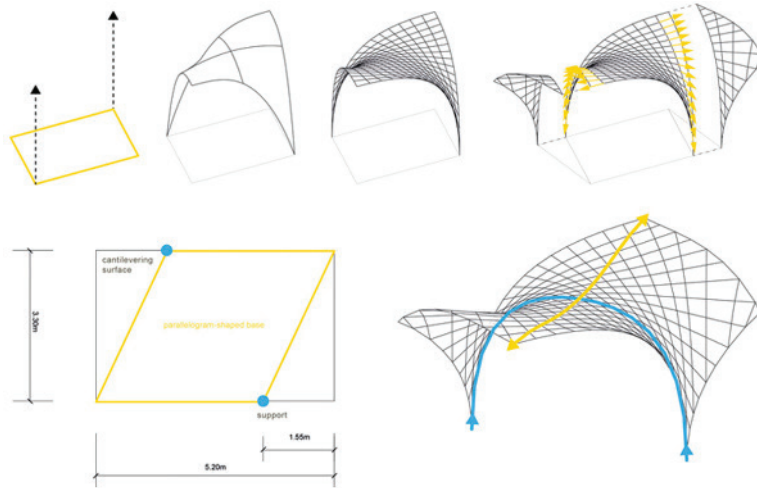


fig. 5.2.1: design concept  
(source: Brunier Ernst)

### design analysis

The design is composed of quadratic elements. These elements are slightly bent diagonally to accommodate the curvature of the overall design. These elements are made out of sheet metal and connected at the edges as seen in (fig. 5.2.1). At the inside of the design thin sheet metal strips are applied that act as a support structure.

### design adjustments

The design is adjusted in a few points to make the integration of solar panels feasible. As seen in (fig 5.2.2) some shapes of the design are triangular. A triangular shape means that either the solar cells need to have custom shapes, which result in more waste during the production of the cell, or less pseudo square solar cells can be implemented in the area of the triangular shape. This leads to an insufficient shape and therefore the choice is made to make every shape either square for maximum implementation of solar cells. The second change made to the design is to planarize the elements. These changes will result in a design that is less complex.



fig. 5.2.2: close up of sheet metal  
(source: Brunier Ernst)

## 5.3 ANALYSIS DESIGN

The goal of this pilot study is to gain insight into the complexities of integrating solar panels into the structure. The focus of this analysis is on the structure. The following questions will be answered in this pilot study;

- Is a full structure of solar panels possible?
- Could the solar cell wafers cope with the internal stress in the structure?
- Are regular glass thickness solar panels sufficient?

During the analysis of the current design of Brunier Ernst, some alterations were made on the design. This resulted in the model as seen in (fig 5.3.1).

The analysis is done using Rhino6, Grasshopper and the plug-in Karamba. The model is made parametric meaning design alterations can be made to the model. The glass is seen as a shell element in Karamba with a mesh resolution of 0.2. Since the complete element is seen as one shell the assumption is made the connection between the solar panels can transfer loads on all directions and transfer moment forces.

In the analysis a 1 kN/m<sup>2</sup> wind load uniformly distributed load is modeled, meaning one side of the model is loaded with a wind load as seen in (fig. 5.3.2). The thickness of the glass used in the model is 8 mm at first and altered later to see the difference in strength. The density is set to include the weight of the EVA and solar cells, resulting in a density of 25,928 kN/m<sup>3</sup>. The Youngs modulus is set to 7000 kN/cm<sup>2</sup>, shear modulus to 2800 kN/cm<sup>2</sup>, yield strength to 12 kN/cm<sup>2</sup> (tempered glass)

The model is supported at the edges. The following support conditions are used: The support can transfer loads in the direction of Tx, Ty, Tz, Rx, Ry, Rz. This results in fixed supports at the bottom edge.

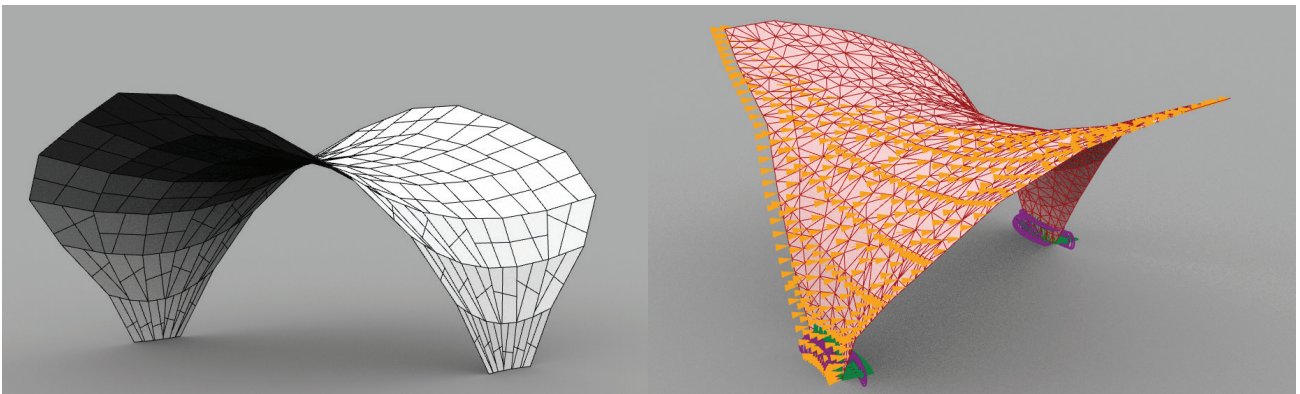


fig. 5.3.1

fig. 5.3.2

fig. 5.3.1: analysis model

fig. 5.3.2: analysis model incl. supports & loads

## analysis glass structure

The first analysis done on the pilot study is if it is possible to have a structure of PV panels. This results in a glass structure with a thickness of 8mm. This is then loaded with a wind load as described earlier.

The structure is analyzed on tensile stress and deformation. The tensile stress in the structure is concentrated around the supports, with a maximum of 20,7 kN/cm<sup>2</sup>, the model showing stress can be seen in (fig. 5.3.3). This exceeds the maximum tensile stress which glass is capable to absorb, Therefore the structure will fail when loaded in such a manner. Besides the tensile stresses, the deflection also exceeds a safe level. The upper edges of the structure show the biggest deflection being 10,3 centimeter, the model that shows the analysis of the deformation can be seen in (fig. 5.3.4). With these two factors in mind, the conclusion is made that a structure purely made out of PV panels is not possible.

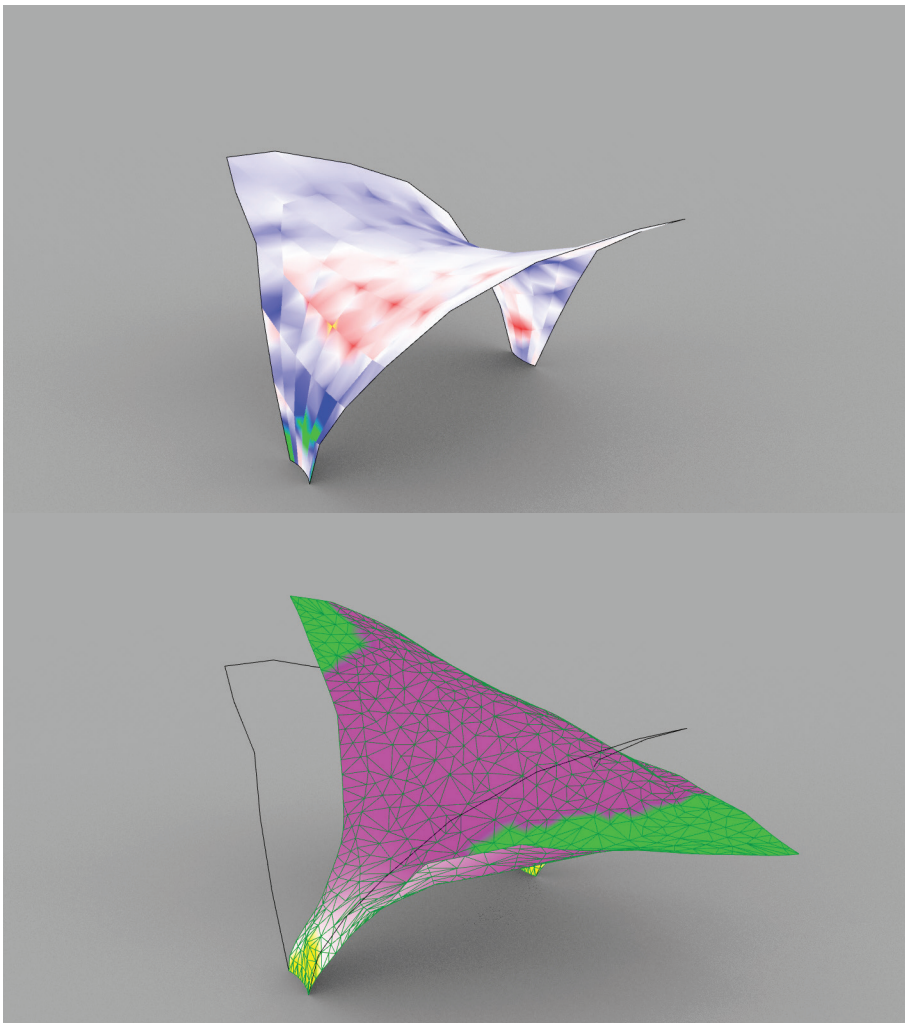


fig. 5.3.3: PV panels structure tensile stress analysis

fig. 5.3.4: PV panels structure deflection analysis

## analysis glass structure + edge beam

To gain an understanding of what is structurally needed to integrate solar panels into the structure of a carport an edge beam is added for additional strength. To assist the 8mm thick glass a 10 cm by 5 cm (height x width) steel edge beam with a thickness of 6mm is added along the edge of the carport, as seen in (fig. 5.3.5).

The tensile stress in the structure is concentrated around the supports, with a maximum of 2,4 kN/cm<sup>2</sup>, the model showing stress can be seen in (fig. 5.3.6). With the maximum tensile stress of tempered glass being 12 kN/cm<sup>2</sup>, this results in a structure that is able to withstand this load. Besides the tensile stresses, the deflection stays within a safe level. The upper edges of the structure show the biggest deflection being 1,15 centimeter the model that shows the analysis of the deformation can be seen in (fig. 5.3.7). With these two factors in mind, the conclusion is made that a structure that consists of PV panels and a steel edge beam can withstand the mechanical loading.

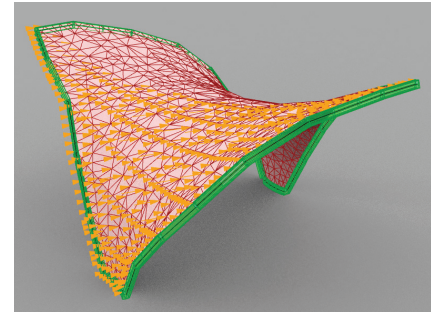


fig. 5.3.5: Analysis model including edge beam

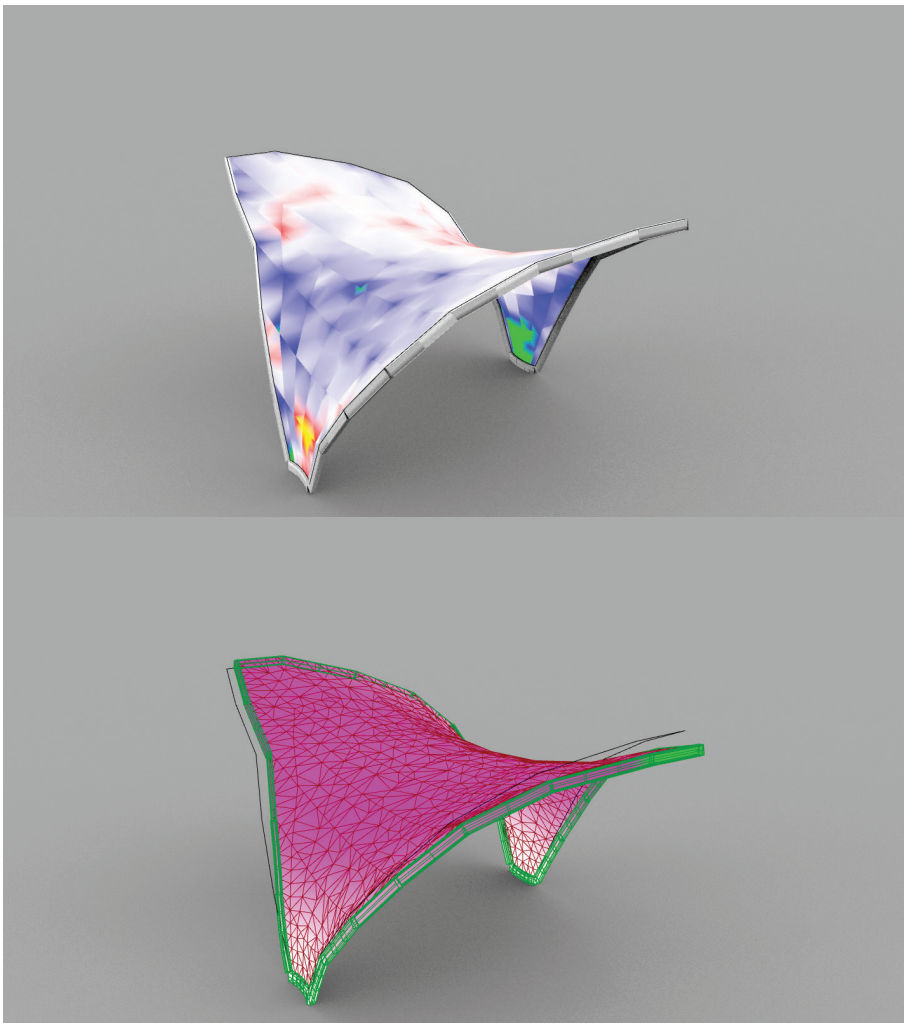


fig. 5.3.6: PV panels + edge beam structure stress analysis

fig. 5.3.7: PV panels + edge beam structure deflection analysis

## analysis stress level at solar cell wafer level

The silicon solar cell wafer that is present in the core of the solar module is a fragile piece. In this analysis, the stresses on the level of the solar cells are simulated. Research shows that the maximum characteristic fracture stress of a silicon wafer in a twist test is 157 MPa (15,7 kN/cm<sup>2</sup>) (table 4.3.1).

The stresses in the structure at the level of the solar cells are concentrated around the supports with a maximum of 1,14 kN/cm<sup>2</sup>, the model showing stress can be seen in (fig. 5.3.8). This is below the characteristic fracture stress of a silicon wafer and therefore the silicon wafer will be able to resist the forces in this design.

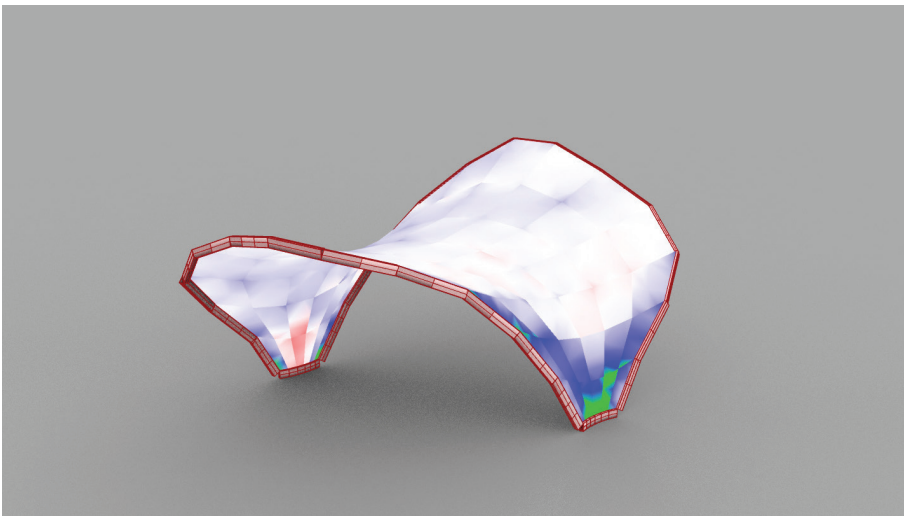


fig. 5.3.8: PV panels + edge beam structure stress analysis

## analysis regular thickness solar modules

The thickness used in the previous analysis was an average of the thickness found in regular solar cells and custom thickness solar cells. Therefore the next analysis is the use of regular thickness solar glass being two panes of 3,2 mm tempered glass, resulting in a total thickness of 6,4mm. The edge beam is still incorporated in the design because without the glass will fail.

The tensile stress in the structure is concentrated around the supports, with a maximum of 2,4 kN/cm<sup>2</sup>, the model showing stress can be seen in (fig. 5.3.9). With the maximum tensile stress of tempered glass being 12 kN/cm<sup>2</sup>, this results in a structure that is able to withstand this load. The deflection is a bit higher than the custom thickness glass as the upper edges of the structure show a deflection of 1,32 centimeter, the model that shows the analysis of the deformation can be seen in (fig. 5.3.10). With these two factors in mind, the conclusion is made that a structure that consists of regular thickness solar panels can be feasible.

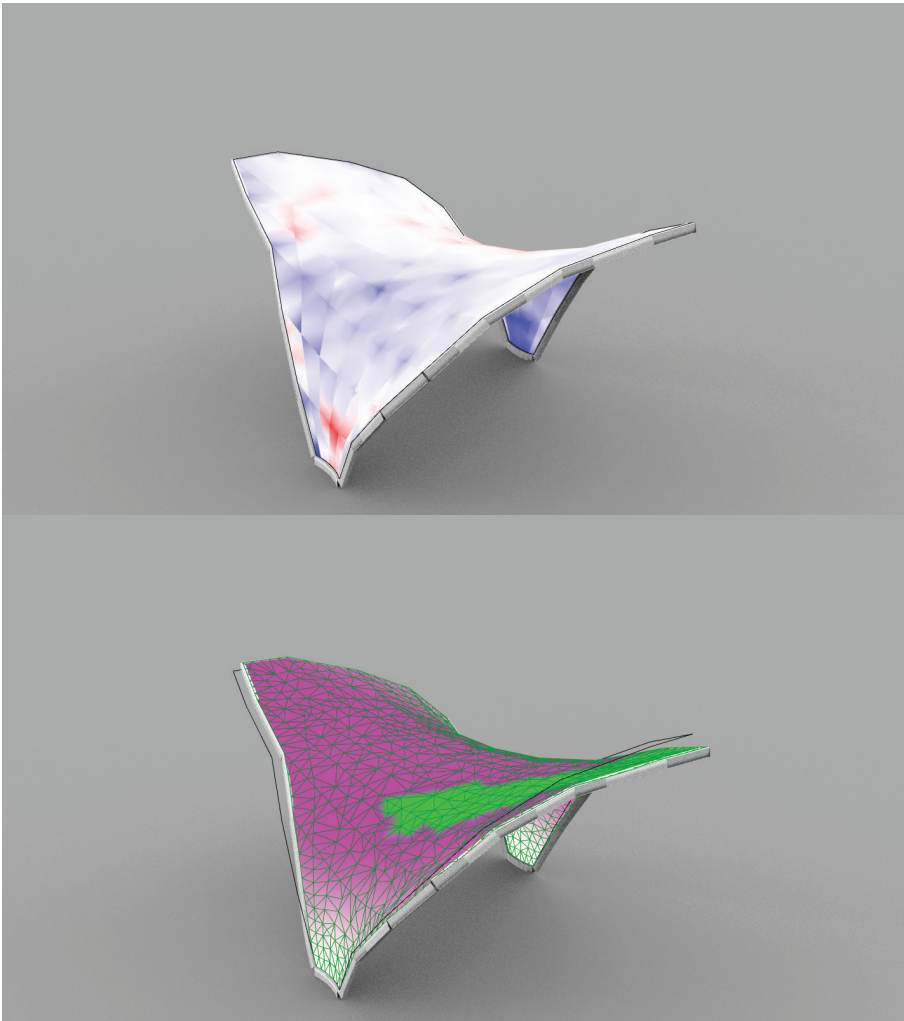


fig. 5.3.9: regular thickness pv glass structure stress analysis

fig. 5.3.10: regular thickness pv glass deflection analysis

## 5.4 CONCLUSION

A random complex design was chosen for the integration of solar panels into a structure. The overall design is adjusted to be suitable for the integration of these solar panels. The overall design was analyzed in Grasshopper to give insight into the stresses located in the design.

These analyses showed that a structure made only out of solar panels isn't possible. The stresses exceeded the maximum tensile stress of tempered glass, which will result in a failure of the glass elements. Besides the failure of the glass elements, the maximum deflection of the design is too substantial for a person to feel safe.

To allow the solar panels to be integrated into the structure an edge beam is implemented for added strength and stiffness. The analysis showed that with the edge beam implemented the stresses were significantly lower. The added strength of the edge beam resulted in stress which is lower than the maximum tensile stress of annealed glass.

In this analysis the solar panels are simplified to one shell. The result of this is that the connection between solar panels needs to be able to transfer load and bending moments in every direction. In the final design, the connection should be designed in such a manner that this is possible.

The silicon solar cell wafer inside the structure is a fragile piece. The analysis showed that, with edge beam implemented, the stresses at the level of the solar cell wafers were lower than the characteristic fracture stress found in the literature.

The last analysis on macro scale featured a design with regular thickness solar glass and edge beam. The stresses and deflection showed a slight increase when compared to the custom thickness solar glass used in the previous analysis. Even with the slight increase, the structure didn't exceed the limits set by the material properties of glass.



## **6.** CASE STUDIES

## 6.1 INTRODUCTION

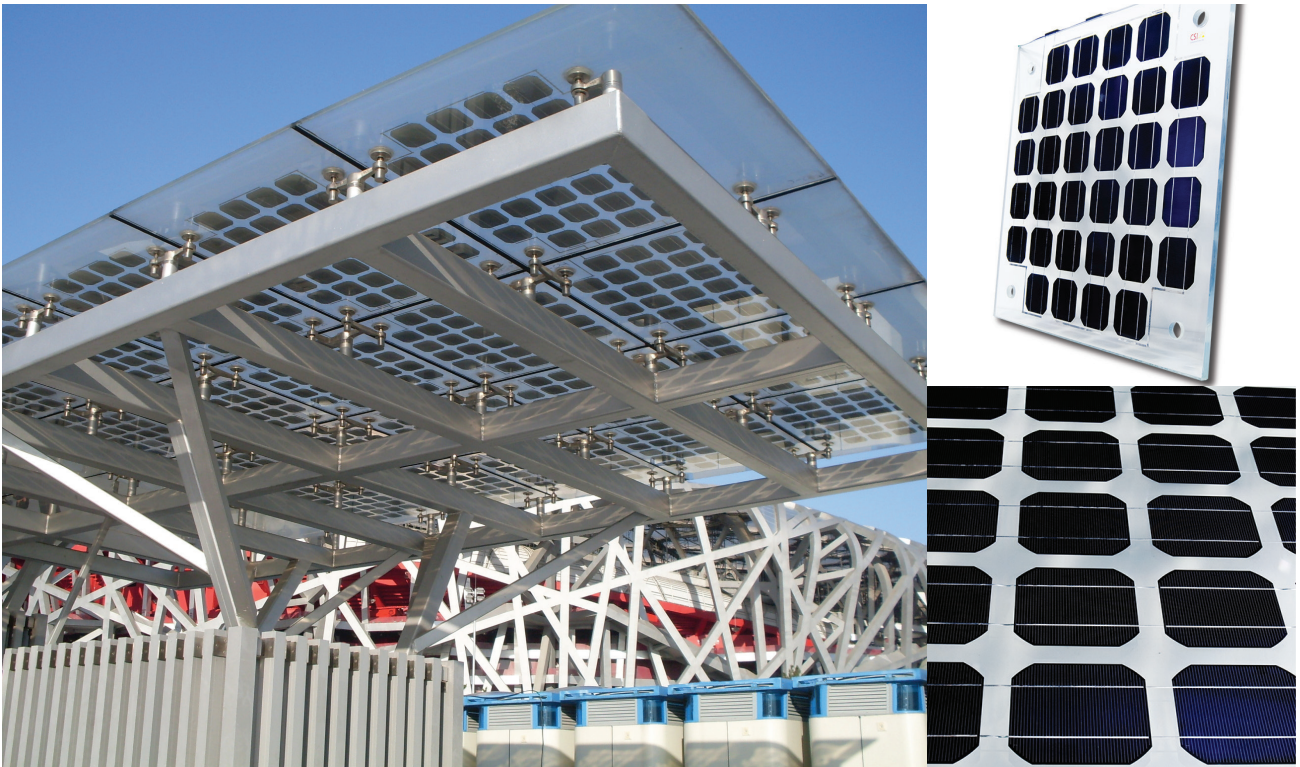
In this section selected novel PV designs are analyzed. The topics the designs are analyzed on are PV technology used, manner of integration, structural material, structural connection, smart design (meaning other functions added to the design) and when applicable other features.

The designs are selected on their novelties of PV use or structural materials. The designs are not only PV carport design but also other PV designs.

The goal of this analysis is to get a broader knowledge of what is already done and what is possible when designing with PV.

## 6.2 CASESTUDIES

### casestudy 1: Solar canopy Beijing Olympics Bird's nest



(source: Archello)

#### description

The Landscape Avenue lies between Beijing Olympics Bird's Nest and the National Sports Center. It features a solar canopy with transparent glass-glass modules. These solar tiles are mounted on top of a steel structure using a spider connection, where the connection protrudes the glass. The electrical connection between solar modules is hidden between the two modules.

#### analysis

pv tech:	mono silicon glass - glass structure
manner of integration:	enclosure
structural material:	metal
structural connection:	spider connection
smart design:	hidden electrical connections
other:	standardized module

## casestudy 2: ISFH Bifacial carport



(source: ISFH)

### description

As a case study, ISFH created a bifacial carport structure. The novelty of this design is the white reflective background. This background reflects the incoming light to the backside of the bifacial solar cell, which in return generates electricity. The distance between the solar cells is rather large and therefore not optimized for power generation.

### analysis

pv tech:	bifacial mono silicon glass - glass structure
manner of integration:	enclosure
structural material:	metal
structural connection:	unknown
smart design:	bifacial with reflective background
other:	n.a.

## casestudy 3: Wilmott Dixon Canopy



(source: PolySolar)

### description

The canopy was mounted on an existing wood laminate frame, utilizing the already existing glazing bar and clamp system to mount the solar glazing. The design uses transparent amorphous silicon modules to replace the originally placed polycarbonate sheets. By applying orange transparent modules the area below receives warm lighting and reduced heating by the sun because of the absorption of the solar modules.

### analysis

pv tech:	orange transparent a-Si modules
manner of integration:	enclosure & reduce light transmittens
structural material:	glu-lam
structural connection:	glazing bar and clamp system
smart design:	n.a.
other:	n.a.

## casestudy 4: FastNed fast charging station



(source: FastNed)

### description

This second generation of Fastned's fast-charging stations allows EV cars to be charged at a speed of 350 kWh. The design incorporates glass-glass solar modules. Optically the solar cells look horizontal but to accomplish this each cell is shifted to achieve this illusion. Incorporated into the modules is a solar optimizer. The geometry of the charging station allows the station to be orientation-independent, due to the solar modules being orientated in each direction. Another benefit of the geometry is the modularity. The edges of the design join together to form a larger station when needed. The structure is made out of steel, which is placed inside the CNC crafted hollow wooden beams and columns.

### analysis

pv tech:	mono silicon glass - glass structured
manner of integration:	enclosure
structural material:	steel with wood enclosure
structural connection:	mullion's and transom's
smart design:	orientation independent modular design
other:	n.a.

## casestudy 5: solar E carport



(source: MGT-esys)

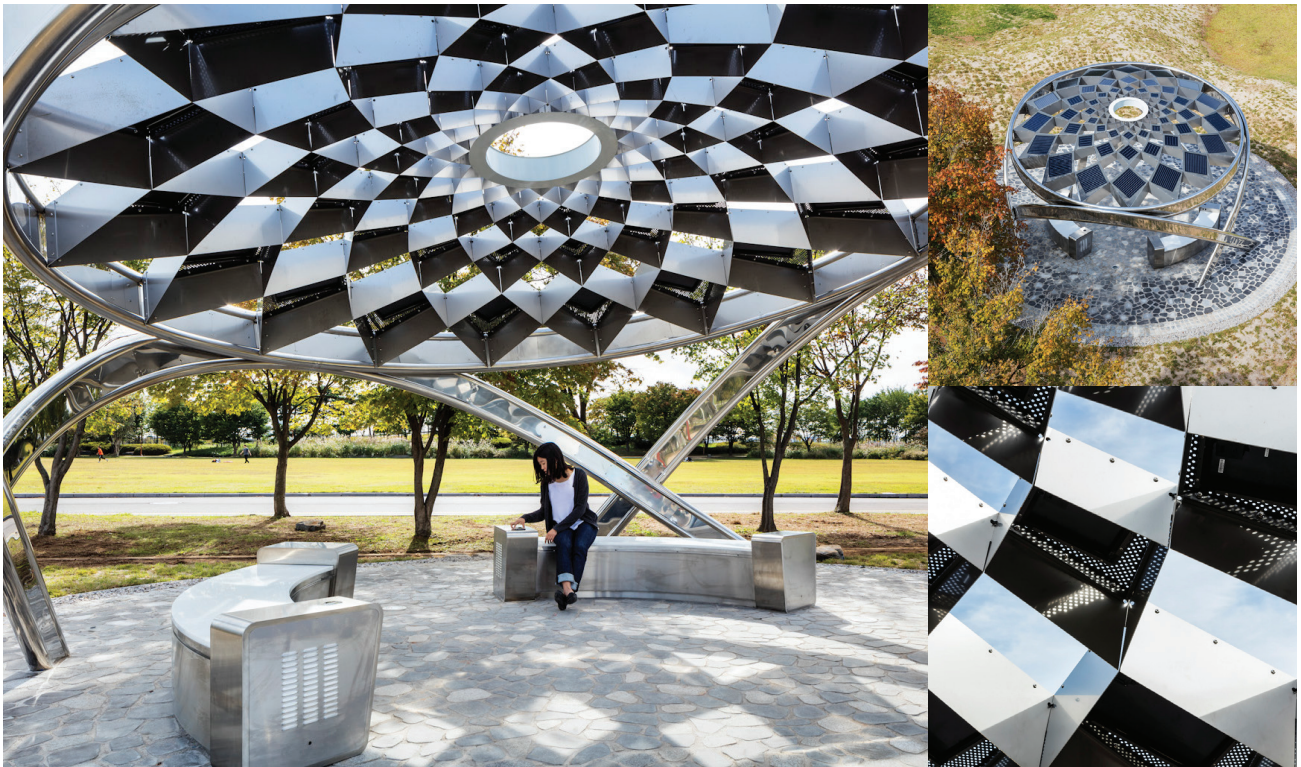
### description

This prototype carport is made by MGT-esys and incorporates glass-glass modules with a transparency of around 36%. The encapsulant in the glass-glass modules is PVB to meet the requirements for safety glazing in Germany. The construction of this carport is made out of steel with a glass crossbeams. These beams ensure an overall transparent design.

### analysis

pv tech:	mono silicon glass - glass structured
manner of integration:	enclosure
structural material:	steel & glass
structural connection:	n.a.
smart design:	n.a.
other:	n.a.

## casestudy 6: Solar Pine V2



(source: HG Architecture)

### description

This PV shelter design began with the geometric pattern of pine cones. The pattern of the pine cones is partially filled with solar modules and the other voids are left open. The tilt of the design is optimized to allow the maximum amount of sunlight to create a pattern of shade on the floor during the daytime, as well as generate the maximum amount of energy. The design integrates three different sizes of solar modules. The energy produced by the solar panels is max 1.2 kWh, which is stored in a battery and used for lighting the structure during the nighttime.

### analysis

pv tech:	unknown
manner of integration:	enclosure
structural material:	steel & glass
structural connection:	unknown
smart design:	n.a.
other:	create shadow pattern

## casestudy 7: La CUB



(source: ISSOL)

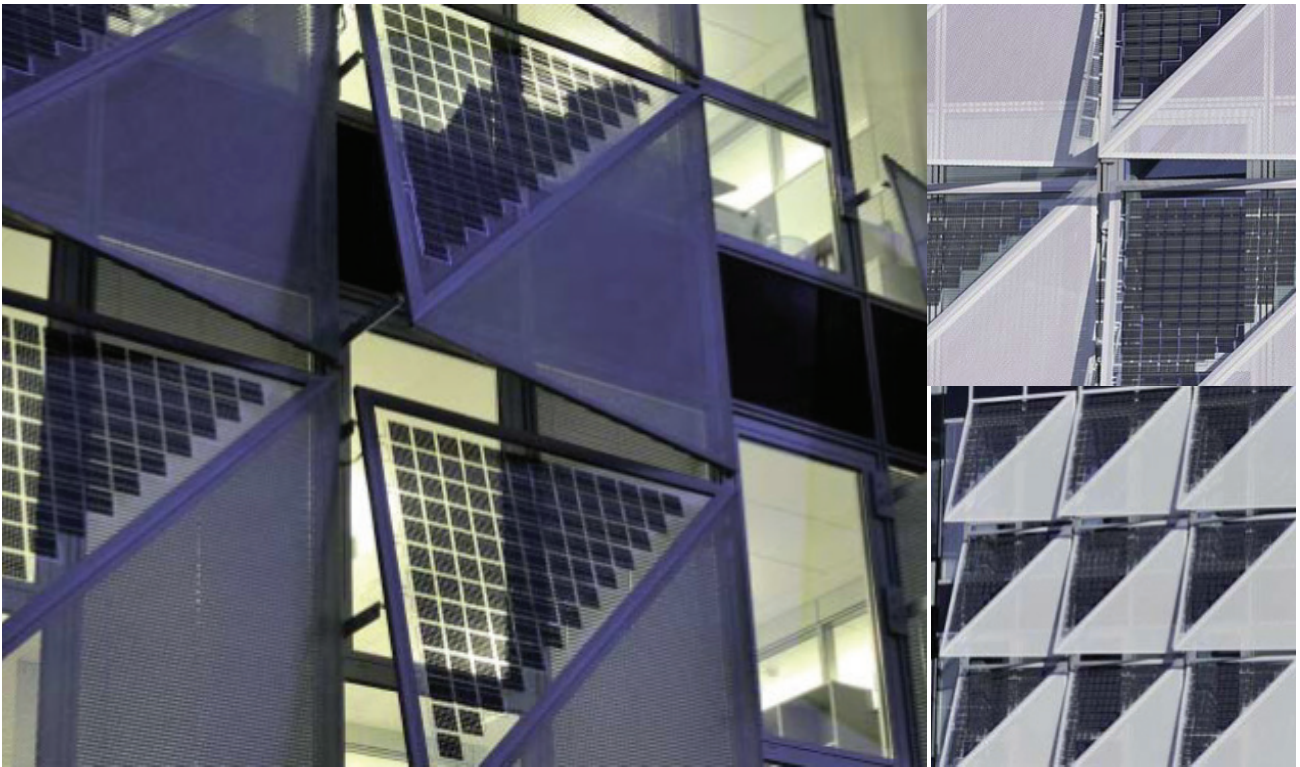
### description

This 9-story administrative building is the first public Plus Energy Building in Bordeaux. This is partly due to the colored PV modules on the south facade of the building. The modules differ in color to create a mosaic-like pattern. The serigraphy of the green tree on a pink and golden background, changing color depending on the received light, symbolizes the environmental approach of CUB.

### analysis

pv tech:	poly crystalline
manner of integration:	enclosure
structural material:	unknown
structural connection:	unknown
smart design:	n.a.
other:	artistic pattern

## casestudy 8: Facade study by Ertex



(source: source)

### description

This facade was created by Ertex, which incorporated crystalline glass-glass solar modules with a shading panel within the same system. The size of the panels is 2,3m by 2,3m with a separation diagonally between shading panel and solar module. The system is installed in front of the original facade of the building to acts as a shading element. The solar modules are angled upwards towards the sun to allow solar light to fall on the module.

### analysis

pv tech:	silicon glass - glass structured
manner of integration:	shading system
structural material:	unknown
structural connection:	unknown
smart design:	incorporated in shading system
other:	n.a.

## 6.3 CONCLUSION

In this chapter different PV designs are analyzed. They are analyzed on PV tech used, manner of integration, structural material, structural connection, smart design.

The designs analyzed showed variety in design possibilities. Some designs create an experience, others are modular in design. The case study of the FastNed fast charging station showed modularity in design. The solar modules are placed in such a way that the design is orientation independent. This aspect of the design is an input for the conceptual designs. These designs should be orientation independent.

La CUB shows how PV technology can also be artistic. The pattern created on the facade of the building show the possibilities with optical filters on solar cells.



## **7.** **CONCEPTUAL DESIGNS**

## 7.1 INTRODUCTION

The prior research done up to this point had the sole purpose to feed the designs of the solar carport for the NS. The outcome of the research form, together with the list of requirements of the stakeholder and the visit to the PV manufacturer, a design brief. In this design brief parameters are set for the three conceptual designs and eventually the final design.

For the conceptual designs and the final designs, five structural materials are researched. These materials are selected on either their sustainability (environmental impact) or due to their structural capabilities. The material properties will be highlighted.

The three conceptual designs consist of cost-effective design, sustainable design, and architectural design. The descriptions of the design themes are given in their chapter. Within the three conceptual designs, certain parameters set out of the design brief will be more highlighted whilst others might be of less importance.

After the three conceptual designs are set, they are evaluated on their design aspects and finally a design decision is made. In this decision, made by the student, a conceptual design is selected for further elaboration. The other designs will be analyzed for design aspects to be incorporated into the final design.

## 7.2 DESIGN BRIEF

The stakeholder has given the researcher a list of requirements for the design. This together with the requirements found in literature, pilot study and case studies will form the design brief. This list of requirements will act as a framework for the conceptual and final design(s). For the three extreme conceptual designs some requirements will be more dominant, others less relevant and some new requirements can be added. To give insight the source of the requirement is mentioned.

### stakeholder

#### **Modular design**

The design should be suitable for every P+R location of the NS.

#### **Suitable for different orientation**

Due to the big amount of different orientation of the P+R locations the design should be adaptable.

#### **Transparent design**

To discard the need for lighting during darker day's and to create social security.

#### **Flexible for replacement of PV**

The replacement of PV that is broken or the possibility of upgrading to newer more profitable PV panels should be taken into account

#### **Demountable elements**

Due to the possibility to recycle the elements when the structure is dismounted.

#### **Sustainable appearance**

The design should have a sustainable (green) appearance.

### pv research

#### **Minimal angle**

The minimal angle at which no dirt will build upon the module is 15 degrees.

#### **Blunt edges**

The design should avoid sharp edges of the glass modules to prevent lamination to occur on the edges.

#### **Rectangular shape**

The optimal shape for a PV panel is rectangular when diverted from this shape the biggest rectangular within this shape becomes the area at which PV cells can be implemented

#### **Avoid cutouts**

The module design should avoid cutouts since this is not possible to be manufactured.

### structural research

#### **Edge beam**

To allow a fully PV structure an edge beam is needed to lower the stress and deflection of the structure.

#### **Linear supports**

To distribute the stress over the whole cross sections of the glass

#### **Glass-glass modules**

For extra strength and protect the solar cells

## 7.3 STRUCTURAL MATERIALS

For the design of the carport, a structural material needs to be selected. In this chapter options for this material are explored. The following materials will be researched:

- Glued laminated timber (glulam)
- Recycled aluminum
- End of life rail tracks
- Hard wood (oak)
- Bamboo

Due to time constrain no more materials are researched. These materials are chosen for either their environmental impact or structural capabilities.

The properties of the materials will be taken from the program CES. CES is a program that acts as a database. In this database, almost all materials are mentioned, together with their typical use, properties, and description. The properties chosen represent the basic properties needed for understanding their structural capabilities. For each of the materials the following aspects will be discussed:

- Youngs modulus
- Compressive strength
- Tensile strength
- Density
- Recyclability
- Embodied energy
- Processability ( scale: 1 = impractical to 5 = excellent)

### glued laminated timber (Glulam)

Glued laminated timber is a structural timber product that is manufactured by bonding together individual pieces of timber under controlled circumstances with a durable, moisture resistant structural adhesive. It is widely used as a structural and architectural application. A benefit of glulam in comparison to conventional wooden beams is the use of smaller trees during manufacturing instead of processing a large tree as is done with conventional wooden beams. Glulam can be produced in a variety of shapes and curves.

Name	Values
youngs modulus	12000 - 14000 N/mm <sup>2</sup>
compressive strength	8,3 - 11 N/mm <sup>2</sup>
tensile strength	9,65 - 12,4 N/mm <sup>2</sup>
density	500 - 650 kg/m <sup>3</sup>
recyclability	no. downcycle yes
embodied energy (primary)	11,2 - 12,4 MJ/kg
processability	
moldability	3 - 4
machinability	4 - 5

table 7.3.1: properties glulam (source: bibliography 7.1)



fig. 7.3.1: close-up glulam (source: weekesforest)



fig. 7.3.2: bridge made out of glulam (source: biobasedbouwen)

## recycled aluminum (6061 T4)

Aluminum is the third most abundant metal in the earth's crust but extracting it costs a lot of energy<sup>[7.1]</sup>. Pure aluminum is a soft material, therefore it is mostly alloyed with different metals such as copper, zinc, magnesium, silicon. In current carport designs, aluminum is widely used as a structural material. Due to the large energy of extracting new aluminum, recycled aluminum becomes a more sustainable option, with recycled aluminum only having +- 16% of the embodied energy of new aluminum<sup>[7.1]</sup>. Aluminum can be made into profiles through extrusion. These extrusions can be curved in a later stage.

Name	Values
young's modulus	68000 - 71500 N/mm <sup>2</sup>
compressive strength	97 - 172 N/mm <sup>2</sup>
tensile strength	172 - 241 N/mm <sup>2</sup>
density	2700 - 2730 kg/m <sup>3</sup>
recyclability	yes
embodied energy (primary)	33,4 - 37 MJ/kg
processability	
castability	4 - 5
machinability	4 - 5

table 7.3.2: properties recycled aluminum (source: bibliography 7.1)

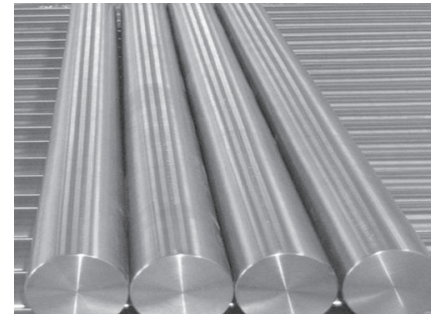


fig. 7.3.3: aluminum bars pre-processing (source: google images)



fig. 7.3.4 extruded aluminum profile (source: HenTec)

## end-of-life rail tracks

Throughout the Netherlands lies around 680.000 tons of end-of-life rail tracks, meaning 14.000 km of rail tracks<sup>[7.2]</sup>. These rail tracks can be melted to a new application but this takes a lot of energy. These rail tracks are made out of high-quality steel and therefore suitable for reintegration into a structure. These end-of-life rail tracks come in lengths of maximum of 6 meters<sup>[7.3]</sup>. From the current rail tracks, 67% and >90% of currently applied rail tracks are type 54E1 - 260Mn<sup>[7.3]</sup>. 54E1 describes the dimensions of the rail track, whilst 260Mn describes the steel quality used. This high carbon steel has a different chemical composition than regular steel. The following elements are present in the steel; Carbon, Silicon, Manganese, Phosphorus, Sulfur, Chromium, and Aluminum<sup>[7.5]</sup>. The shape of the rail tracks is suitable for integration into a structure, discarding the need for melting them into different shapes.

Name	Values
young's modulus	200000 - 215000 N/mm <sup>2</sup>
compressive strength	335 - 1160 N/mm <sup>2</sup>
tensile strength	880 N/mm <sup>2</sup> <sup>[7.4]</sup>
section weight	54,77 kg/m <sup>1</sup> <sup>[7.4]</sup>
density	7800 - 7900 kg/m <sup>3</sup>
dimensions	
height	159 mm
head width	70 mm
foot width	140 mm

note: properties are taken for "new" steel. The influence of age/wear isn't taken into account

table 7.3.3: properties end-of-life rail tracks (source: bibliography 3.35)



fig. 7.3.5: end-of-life rail tracks (source: Jeroen Mens)

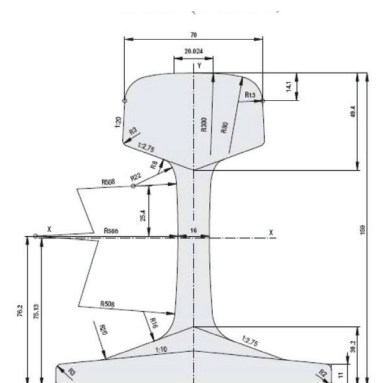


fig. 7.3.6: dimensions of 54E1 rail tracks (source: RailPro)

## bamboo

Bamboo is a hard grass species that has been used in construction for decades. It grows most commonly in Indonesia and some species can grow up to a meter a day, making it the fastest growing plant on earth. Bamboo has an extremely hard and durable outer surface. Its natural tubular structure gives it excellent bending stiffness and strength at low weight. Fasteners that require holes must be avoided. Bamboo that is intended for the use in structures needs to be treated against rot and insects.

Name	Values
young's modulus	15000 - 20000 N/mm <sup>2</sup>
compressive strength	50 - 100 N/mm <sup>2</sup>
tensile strength	36 - 45 N/mm <sup>2</sup>
density	600 - 800 kg/m <sup>3</sup>
recyclability	no, downcycle yes
embodied energy (primary)	32,9 - 35,9 MJ/kg
processability	
Moldability	1 - 2
machinability	4

table 7.3.4: properties bamboo (source: bibliography 7.1)



fig. 7.3.7: bamboo stem  
(source: google images)



fig. 7.3.8: bamboo construction  
(source: Chang Mai Life Architecten)

## hardwood (oak)

Wood is one of the world's major structural materials, as well as more delicate objects like furniture. Wood is renewable material as long as it is grown in a sustainable way, meaning there is a balance between harvesting and planting new tree's. Reason hardwood and in particular oak is selected is it's hardness, durability, and strength. Oak has sustainability class II, meaning it can last for 15 to 25 years when fully exposed in an outdoor application<sup>[7.6]</sup>. It typical uses varies from flooring to window framing and many more. The dimensions of the oak beams are standardized, 50x150mm, 100x100mm, 200x200mm, and 300x300mm to name a few, custom sizing is possible but adds to the cost. Natural materials like wood show greater deviation in strength than man-made materials like steel.



fig. 7.3.9: Oak beam  
(source: Hout Vakman)

Name	Values
young's modulus	20600 - 25200 N/mm <sup>2</sup>
compressive strength	68 - 83 N/mm <sup>2</sup>
tensile strength	132 - 162 N/mm <sup>2</sup>
density	850 - 1030 kg/m <sup>3</sup>
recyclability	no, downcycle yes
embodied energy (primary)	11,6 - 12,8 MJ/kg
processability	
Moldability	2 - 3
machinability	5

table 7.3.5: properties bamboo (source: bibliography 7.1)



fig. 7.3.10: Oak construction  
(source: Oakmasters)

## 7.4 CONCEPTUAL DESIGNS

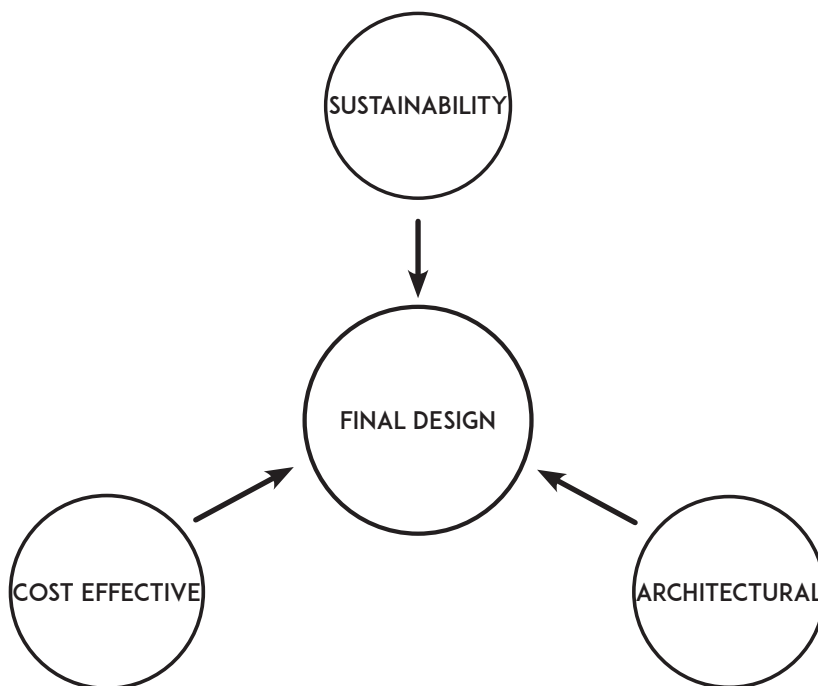
The main goal of the conceptual designs is to widen the scope of the final design. To accomplish these three different concept topics are chosen. The three different topic being:

- Cost-effective
- Sustainability
- Architectural design

The goal of these topics is to make an extreme design related to the topic. These extreme designs then feed as input for the final design. The final design will be based on one of the conceptual designs but will have influences from every conceptual design.

The detail in which these conceptual designs will be is on a concept level. The overall shape and concept behind it will be defined, same with the structural material. The conceptual designs will not include the calculations of structural behavior and details of the construction.

The eventual conceptual design will be evaluated on their pro's and con's to give insight into the final design decision.



## conceptual 'Cost effective' design

As the name of the concept suggest the focus of this conceptual design is to be cost-effective. In this research, a cost-effective design means the following: A design that is applicable in every orientation without altering the design. Therefore allowing the design to be mass-produced which will lead to a lower overall cost when compared to a design that needs to be altered for different orientations. The solar panels used in the design will focus on maximum output and minimal design and have standard dimensions to further lower the cost. The structure needs to be cost effective, meaning the material selected is well known in the industry and easy to manufacture.

This results in the following additions on the design brief:

- Design is effective in every direction
- Standardized dimensions solar panels
- Maximize output of design
- Cost effective structure

### design

The optimal angle for the PV panels when the orientation is unknown is flat. In this configuration, the solar panels still have an efficiency of 85%, as seen in (fig. 7.4.1.). Literature showed that in order to allow for minimum maintenance the minimal angle of solar panels should be 15 degrees or more. This to prevent water built up on the panels, this results in a solar module with dirt and other filth to accumulate on top of the panels which lowers the output.

The design features a group of 4 panels that are tilted 15 degrees in opposite directions, as seen in (fig. 7.4.2.). This results in an output of the design that is independent of orientation. The panels used are all the same size, 600mm by 1200mm. The layout of the solar cells inside the solar panels is performance based. This results in a maximum amount of solar cells per panel, which sacrifices the transparency of the design.

The structural material of choice is recycled aluminum. Reason for this being that in current carport designs all the structures are made out of aluminum and the market has experience with this material. Another reason why aluminum is selected, whilst cheaper materials are available is its durability. Aluminum has a long life span without the need of maintenance, therefore it is a cost effective choice.

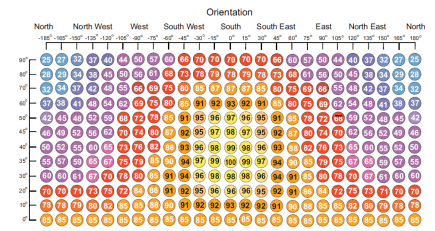


fig. 7.4.1.: solar module efficiency per orientation  
(source: EvoEnergy)

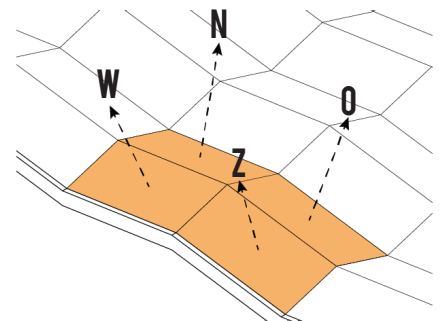


fig. 7.4.2: different orientations per panel



fig. 7.4.3: side elevation 'cost effective' conceptual design



fig. 7.4.4: birds eye view 'cost effective' conceptual design

To validate the design is orientation independent, its performance is simulated in Grasshopper, the script used can be seen in (fig. 7.4.5.). A weather data file from Amsterdam is used in the simulation. A two parking spot configuration of the design is simulated. The following orientations are simulated; N, NE, E, SE, S. The remaining orientations are not simulated since the design is mirrored and therefore will perform the same in the other directions. As can be seen in (fig. 7.4.6.) the performance of the design is in every orientation equal.

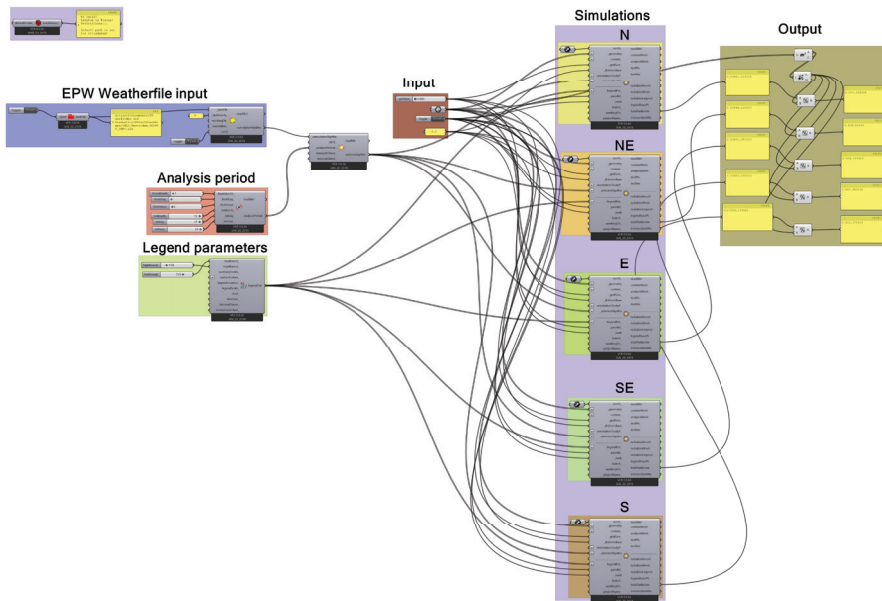


fig. 7.4.5: grasshopper script

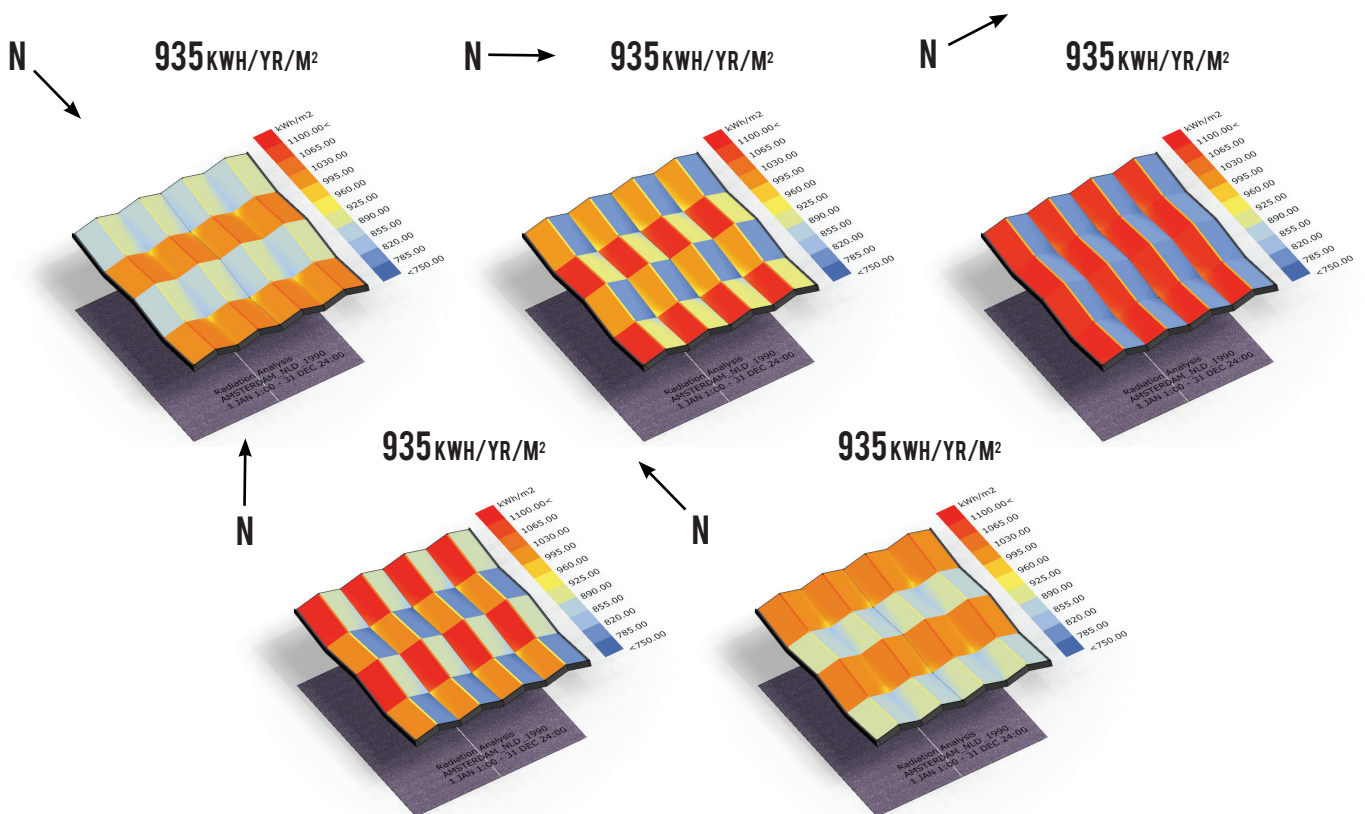


fig. 7.4.6: solar analysis simulation results

## design evaluations

The main challenge with this design is water accumulation on the design, as illustrated in (fig. 7.4.7). A change is made in the design to allow the water to fall off the design. This is done by shifting the second row half a panel (fig 7.4.8-9). This also allows more natural light to pass through the design and therefore lowering the need for lighting during darker days. The downside to this design alteration is that by shifting the panels the panels will shade the others and therefore lower the overall performance of the design. This is simulated in grasshopper and the overall performance for every orientation drops from 935 kWh/yr/m<sup>2</sup> to 922 kWh/yr/m<sup>2</sup>. Further design optimization will be done in a possible later stadium if this design is chosen for further elaboration in the design phase.

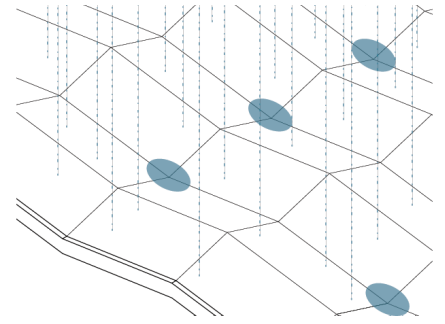


fig. 7.4.7: water accumulation points in design

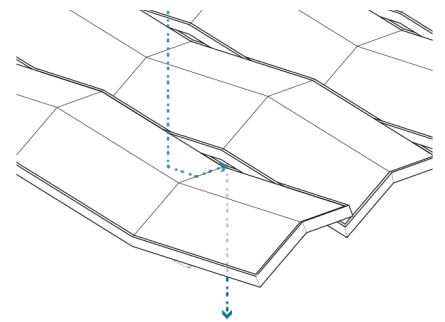


fig. 7.4.8: solution water accumulation



fig. 7.4.9: birds eye view design alteration cost effective concept

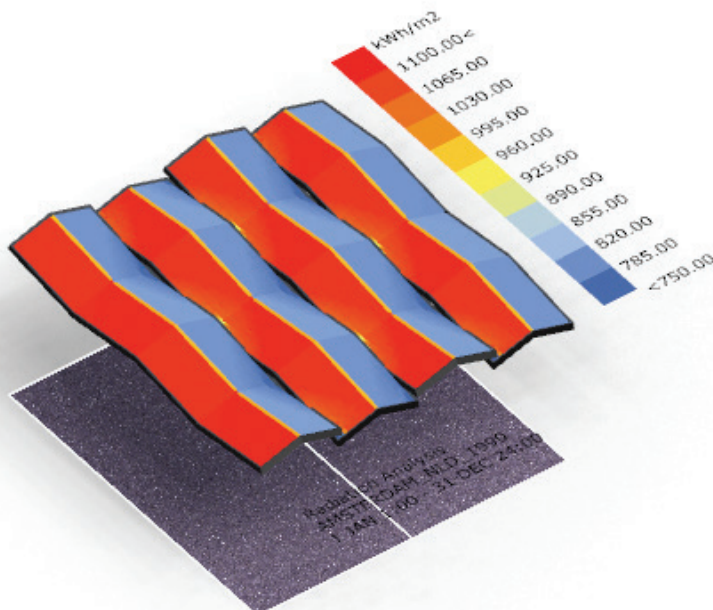


fig. 7.4.10: solar analysis design alteration cost effective

## conceptual 'Sustainable' design

The focus of this design is to be sustainable. In this research that means a low embodied energy structure and design. A different addition to this concept is that besides acting as a shelter for cars and generating electricity out of the sun another function should be added that benefits the surrounding of the design.

This results in the following additions on the design brief:

- Low embodied energy (construction)
- Additional function to the design

### design

To provide another function that benefits the surrounding of the design a green wall is added in between the two slopes. The slopes will transfer the water into the green wall, which will absorb this water and eventually evaporate this water. This evaporation is beneficial for the solar panels since this will cool the panels and therefore boosting the output<sup>[7.7]</sup>. The emissions of the cars in the carpark are absorbed by the plants and converted into oxygen. The absorption of water also discards the need for adding sewer points in the P+R plots.

The green wall featured in this design will consist of a water reservoir. Water captured on the roof will be drained into the reservoir. Connected to the reservoir is the irrigation system for the plants. The type of plants and the detailing of the green wall will be further developed in a further design stage if this design is selected for the final design stage.

The design features two main tilts of 15 degrees that are opposite. In these main tilted panes, the solar panels have three different orientations. The concept uses a less dense solar cell layout to allow light to fall on the green wall.

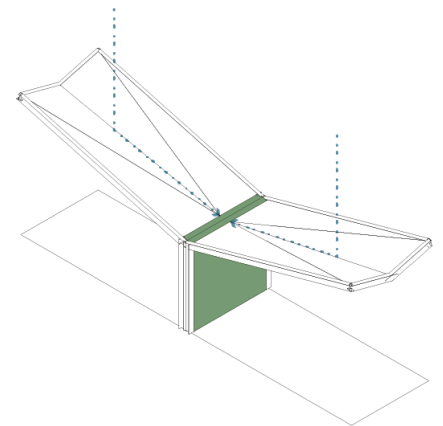


fig. 7.4.11: water transport sustainable concept



fig. 7.4.12: side elevation 'sustainable' conceptual design

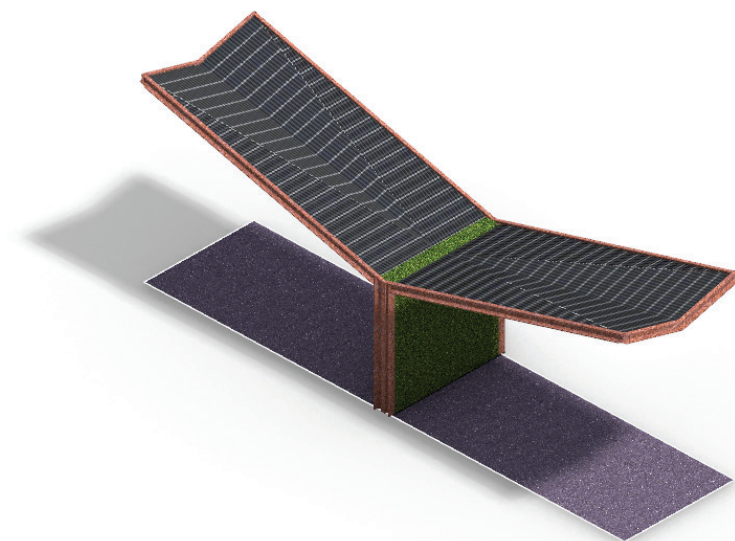


fig. 7.4.13: birds eye view 'sustainable' conceptual design

The structural material of choice is end-of-life rail tracks. Reason for this being that this material is already made and requires no additional energy to remake the material in construction material since the shape is already suitable to be integrated into the structure. Besides the sustainability reasoning behind the end-of-life rail tracks, the direct link with the stakeholder adds another layer to the design.



fig. 7.4.14: structural material sustainable concept, end-of-life railtracks

(source: Jeroen Mens)

## conceptual 'Architectural' design

In this design, the main focus is the social connections between the user and the design. Another aspect is the link between the stakeholder and the design.

This results in the following additions on the design brief:

- Social connection between design and user
- Connection between design and stakeholder

### design

Upon arrival in the P+R carpark, the user is in its own private bubble, represented by their private car. The user transitions between the private car to public transport. This is symbolized in the design by lifting the corners up, which results in a design that gradually opens at the edges.

The design features two different structural materials. The main wall being concrete, while the spine of the design is made from Glu-lam timber. These materials create a link to the NS by symbolizing the transition to sustainable energy that the NS is undergoing with this design.

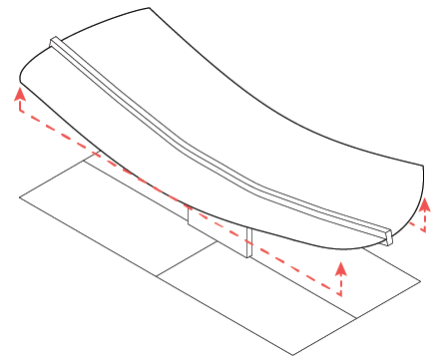


fig. 7.4.15: design diagram architectural concept

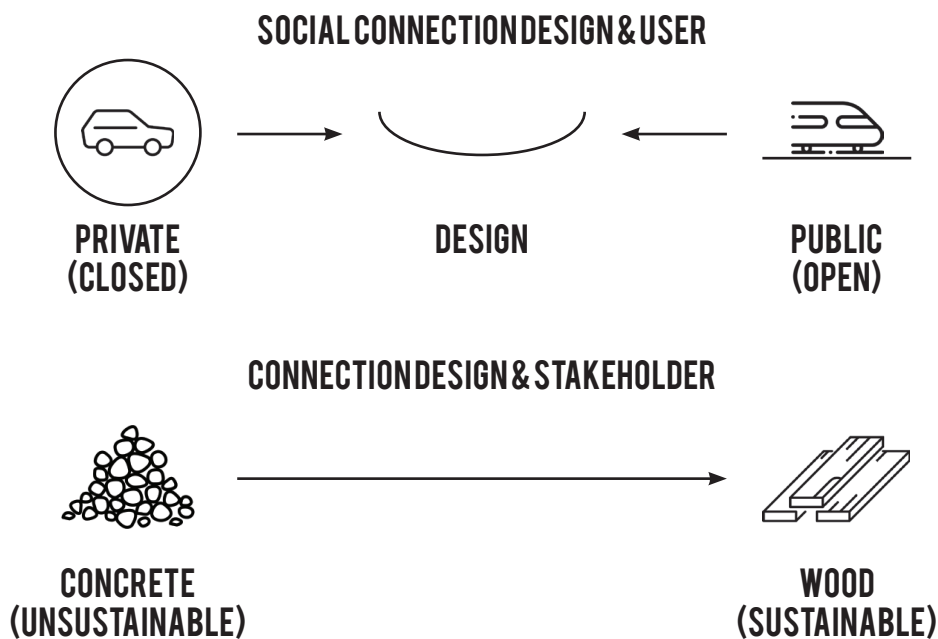


fig. 7.4.16: side elevation 'sustainable' conceptual design

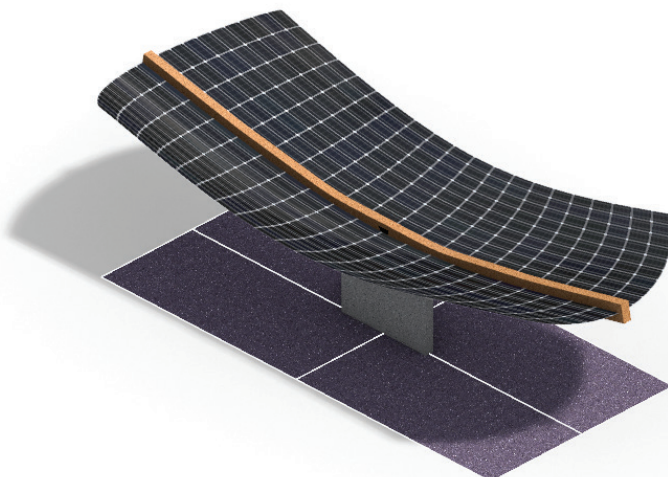


fig. 7.4.17: birds eye view 'sustainable' conceptual design

## 7.5 DESIGN EVALUATION & CHOICE

In this chapter, the three conceptual designs will be evaluated. The goal of this evaluation is to gain an understanding of the pros and cons of the designs. This information can, later on, be used to improve the final design and to make certain design choices retractable.

### conceptual 'Cost effective' design

The final version of the cost-effective design has a drawback. The voids created by shifting the second row, essentially create a leakage where water can freely pass through and fall on the area below. The carport then effectively loses its function as a shelter. Another drawback of shifting the second row is the increase in material use and complexity of the structure. The major benefit of this design is the orientation independence, as proven by the simulations made in Grasshopper. Due to the structural layout of the columns, the function of the parking lot isn't compromised.

### conceptual 'Sustainable' design

The challenge moving forward with this design is the incorporation of the end-of-life rail tracks. Since they are made out of high-grade steel the weight of this element can provide a challenge. The direct link between the rail tracks and the stakeholder is a pro. The design is inherently not orientation independent. East-West orientation is favored with this design. By implementing a wall on the short side of the parking spot, in between two spots, negatively influences the usability of the parking space. The absorption of water into the green wall is a benefit that needs further exploring in the final design stage.

### conceptual 'Architectural' design

The design features an arc with solar panels that cantilever out. In the current design, no edge beam is implemented and therefore the solar panels would need extra reinforcements. The placement of the wall parallel to the parking spot is a pro. With this, the functionality of the parking spot isn't compromised. The main challenge with this concept is water drainage. A solution for this could be similar to the sustainability concept.

### design choice

The concept that is chosen for further elaboration during the design stage is the sustainable concept, with some design influences from the architectural design. The reasoning behind the choice for the sustainability concept is the additional function of rainwater collection. During a visit with the stakeholder, the problem was mentioned that not every P+R plots have sufficient sewer points for water drainage. To further minimize the impact on the functionality of the parking plot, the positioning of the wall is taken from the architectural design. Together with the shape of the solar panels to create an orientation independent design that has a social connection to the user.

## 7.6 BIBLIOGRAPHY

- [7.1] Granta (2018). CES EduPack 2018 (18.1.1) [Software]
- [7.2] Roufs, D. (2018, May 07). Nieuw erin, oud eruit - what to do met gebruikte spoorstaven? Retrieved from [https://www.voestalpine.com/railpro/nl/nieuws/hergebruik\\_van\\_spoorstaven/](https://www.voestalpine.com/railpro/nl/nieuws/hergebruik_van_spoorstaven/)
- [7.3] ProRail (2010). CO2 ketenanalyse spoorstaven. Retrieved from [https://www.prorail.nl/sites/default/files/ketenanalyse\\_spoorstaven.pdf](https://www.prorail.nl/sites/default/files/ketenanalyse_spoorstaven.pdf)
- [7.4] Britishsteel (2017). Steel compositions and properties. Retrieved from <https://britishsteel.co.uk/media/40810/steel-grade-dimensions-and-properties.pdf>
- [7.5] Tatasteel (2014). Rail technical guide. Retrieved from [https://nanopdf.com/download/rail-technical-guide-tata-steel-in-europe\\_pdf](https://nanopdf.com/download/rail-technical-guide-tata-steel-in-europe_pdf)
- [7.6] Appropedia (2013, April 06). Durability classes of wood. Retrieved from [https://www.appropedia.org/Durability\\_classes\\_of\\_wood](https://www.appropedia.org/Durability_classes_of_wood)
- [7.7] Hui, S. C. M. and Chan, S. C., (2011). Integration of green roof and solar photovoltaic systems, In Proceedings of Joint Symposium 2011: Integrated Building Design in the New Era of Sustainability, 22 November 2011 (Tue), Kowloon Shangri-la Hotel, Tsim Sha Tsui East, Kowloon, Hong Kong, p.1.1-1.10.



8.

## **FINAL DESIGN**



## 8.1 INTRODUCTION

Chapter 8 focusses on the final design and the elaboration of the design. As mentioned previously the sustainable concept is chosen for further elaboration. Influences from the architectural concept are clearly visible in the final design. Extra attention goes into the detailing of the design.

The first parts consist of the MCA AHP method. The different technologies are compared to each other with the information found in the literature. For the concept, the final priorities for the MCA are set to choose the correct technology for the design. After the MCA the final design and design choices are discussed. Then the detailing and materials are discussed followed by the analysis of the construction, on the level of the complete structure and the connection. After the analysis, additional recommendations for improving structural performance are given for further development. A final analysis is done for the solar performance of the shape, showing if the design is orientation independent.

This chapter ends with the general conclusion and recommendations for further development of the presented research.

## 8.2 MULTI CRITERIA ANALYSIS

To compare the research solar cell technologies to each other a multi-criteria analysis (MCA) is used. The MCA methodology chosen is an analytical hierarchy process (AHP). This form of MCA technique is commonly used in cases with different criteria's and alternatives such as this case. The goals of the MCA AHP method is to assess the suitability of solar technologies for the final design.

The following Multi-level analytical hierarchy process (AHP) structure will be used to select the criteria for this project:

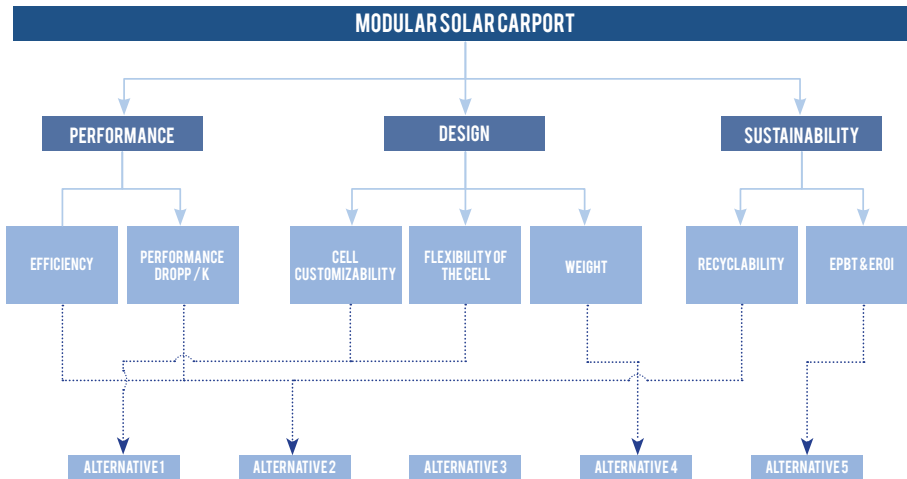


fig. 8.2.1: AHP structure

To compare the different criteria to each other a pairwise comparison is used. For each technology (alternative) is compared to each sub-criteria. This will result in a matrix to calculate the different preferences. To make the comparison measurable the fundamental scale is used<sup>[8.1]</sup>, see (table 8.2.1).

intensity of importance	definition	explanation
1	equal importance	Element 1 and 2 are equally important
3	moderate/weak importance	Experience and judgment slightly favors 1 over 2
5	essential or strong importance	Experience and judgment strongly favors 1 over 2
7	demonstrated importance	1 is favourite over 2 and has been demonstrated in practice
9	absolute importance	The evidence clearly shows that 1 is preferred over 2
2,4,6,8	An intermediate value between the judgments presented above	Compromise between 2 intensities of importance
reciprocals	If 1 over 2 has a value of 7, then 2 over one must have a value of 1/7	

table 8.2.1: Fundamental scale for pairwise comparison (source: bibliography 8.1)

For every conceptual design different preferences of criteria are set and this will result in different pairwise comparison scores. An example of a pairwise comparison can be seen in (fig. 8.2.2).



fig. 8.2.2: AHP pairwise comparison

When comparing the different technologies in relation to a criteria a matrix will be made. This will result in the following matrix:

$$A = \begin{pmatrix} x_{11} & \cdots & x_{1m} \\ \vdots & \ddots & \vdots \\ x_{l1} & \cdots & x_{lm} \end{pmatrix}$$

This means that when  $x_{lm}$  is the evaluation of the alternative  $l$ th in relation to the criterion  $m$ th. This will produce the following symmetry matrix:

$$\begin{pmatrix} 1 & x_{12} & x_{13} \\ x_{21} & 1 & x_{23} \\ x_{31} & x_{32} & 1 \end{pmatrix}$$

This results in the following:

$$x_{12} = \beta, \text{ then } x_{21} = \frac{1}{\beta}$$

Z. Haghghi et. al <sup>[8.2]</sup> mentions that the number of alternatives has a great influence on the reliability of the method. Therefore each element of a column is then normalized by dividing each entry in the columns by the total of that column. This is done by the following equation:

$$x_{11n} = \frac{x_{11}}{\sum_1^l x}$$

By averaging each row the weighing factor will be calculated.  $W_m$  is the normalized average of the row of criteria  $M$ .

$$A_n = \begin{pmatrix} x_{11n} & \cdots & x_{1mn} \\ \vdots & \ddots & \vdots \\ x_{l1n} & \cdots & x_{lmn} \end{pmatrix}$$

To check the consistency of the decisions maker comparisons, the following four step procedure is used:

1. Compute AWT, WT being the transpose vector W.
2. Calculate the value of  $\lambda_{max}$  by:

$$\lambda_{max} = \frac{1}{m} \sum \frac{\text{ith value of } AW^T}{\text{ith value of } W^T}$$

3. Consistency is then defined as:

$$CI = \frac{\lambda_{max} - m}{m - 1}$$

The number of alternatives used in the comparison dictate the random index (RI). This random index can be selected using (fig 8.2.3) <sup>[8.3]</sup>

ALTERNATIVES	2	3	4	5	6	7	8	9	10	11	12
RANDOMINDEX (RI)	0.00	0.58	0.90	1.12	1.21	1.32	1.41	1.45	1.49	1.51	1.48

fig. 8.2.3: random index per number of alternatives

San Cristobal Mateo (2010) states that if  $CI/RI = < 0,10$ , the degree of consistency is satisfactory. When the value of  $CI/RI$  is higher than 0,10 serious inconsistencies may exist

4. To make the final decision for the best alternative one more matrix needs to be formed.

To make the final decision for the best alternative one more matrix needs to be formed. This matrix composes of the vector W and the values of  $CI/RI$ . By multiplying the weighing factor with the  $CI/RI$  value the final score of the alternative will be calculated.

$$\begin{pmatrix} C_1 \\ \vdots \\ C_m \end{pmatrix} \times \begin{pmatrix} W_{11} & \dots & W_{n1} \\ \vdots & \vdots & \vdots \\ W_{1m} & \dots & W_{nm} \end{pmatrix} = \begin{pmatrix} A_1 \\ \vdots \\ A_m \end{pmatrix}$$

The alternative with the greatest score is the best suitable option for this application.

# Comparison solar technologies

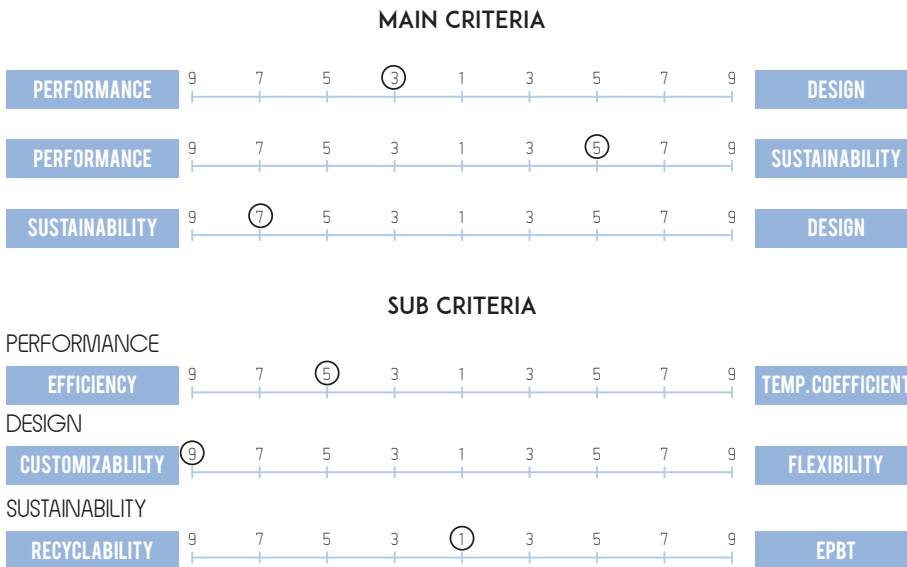
The comparison between technologies is based on literature research. At the end of each chapter in the literature research regarding solar technologies, a concluding table is produced. This is the information used for the comparison between technologies.

The results are checked on consistency. The outcome is consistent when the consistency factor is  $>0,1$ . After calculating the consistency factor of every comparison, the conclusion can be made that the comparisons are consistent

	PAIR-WISE COMPARISON MATRIX					NORMALIZED					RESULT		
	mono c-Si	poly c-Si	CdTe	a-Si	CI(G)S	mono c-Si	poly c-Si	CdTe	a-Si	CI(G)S			
EFFICIENCY	mono c-Si	1	3	7	9	7	mono c-Si	0,58	0,67	0,49	0,31	0,49	0,51
	poly c-Si	1/3	1	5	9	5	poly c-Si	0,19	0,22	0,35	0,31	0,35	0,29
	CdTe	1/7	1/5	1	5	1	CdTe	0,08	0,04	0,07	0,17	0,07	0,09
	a-Si	1/9	1/9	1/5	1	1/5	a-Si	0,06	0,02	0,01	0,03	0,01	0,03
	CI(G)S	1/7	1/5	1	5	1	CI(G)S	0,08	0,04	0,07	0,17	0,07	0,09
													consistency consistent? 0,08 yes
PERFORMANCE DROP OFF / CELSIUS	mono c-Si	1	1/3	1/7	1/6	1/5	mono c-Si	0,05	0,03	0,07	0,04	0,03	0,04
	poly c-Si	3	1	1/5	1/4	1/2	poly c-Si	0,14	0,08	0,09	0,06	0,07	0,09
	CdTe	7	5	1	2	3	CdTe	0,32	0,41	0,46	0,51	0,45	0,43
	a-Si	6	4	1/2	1	2	a-Si	0,27	0,32	0,23	0,26	0,30	0,28
	CI(G)S	5	2	1/3	1/2	1	CI(G)S	0,23	0,16	0,15	0,13	0,15	0,16
													consistency consistent? 0,02 yes
CUSTOMIZABILITY	mono c-Si	1	1	1	1	1	mono c-Si	0,20	0,20	0,20	0,20	0,20	0,20
	poly c-Si	1	1	1	1	1	poly c-Si	0,20	0,20	0,20	0,20	0,20	0,20
	CdTe	1	1	1	1	1	CdTe	0,20	0,20	0,20	0,20	0,20	0,20
	a-Si	1	1	1	1	1	a-Si	0,20	0,20	0,20	0,20	0,20	0,20
	CI(G)S	1	1	1	1	1	CI(G)S	0,20	0,20	0,20	0,20	0,20	0,20
													consistency consistent? 0,00 yes
STIFFNESS	mono c-Si	1	1	1	1	1	mono c-Si	0,20	0,20	0,20	0,20	0,20	0,20
	poly c-Si	1	1	1	1	1	poly c-Si	0,20	0,20	0,20	0,20	0,20	0,20
	CdTe	1	1	1	1	1	CdTe	0,20	0,20	0,20	0,20	0,20	0,20
	a-Si	1	1	1	1	1	a-Si	0,20	0,20	0,20	0,20	0,20	0,20
	CI(G)S	1	1	1	1	1	CI(G)S	0,20	0,20	0,20	0,20	0,20	0,20
													consistency consistent? 0,00 yes
RECYCLABILITY	mono c-Si	1	1	9	3	7	mono c-Si	0,39	0,39	0,33	0,4	0,38	0,38
	poly c-Si	1	1	9	3	7	poly c-Si	0,39	0,39	0,33	0,4	0,38	0,38
	CdTe	1/9	1/9	1	1/5	1/3	CdTe	0,04	0,04	0,04	0,03	0,02	0,03
	a-Si	1/3	1/3	5	1	3	a-Si	0,13	0,13	0,19	0,13	0,16	0,15
	CI(G)S	1/7	1/7	3	1/3	1	CI(G)S	0,06	0,06	0,11	0,04	0,05	0,06
													consistency consistent? 0,02 yes
EPBT	mono c-Si	1	1/5	1/8	1/3	1/7	mono c-Si	0,04	0,02	0,07	0,02	0,03	0,04
	poly c-Si	5	1	1/5	3	1/3	poly c-Si	0,21	0,10	0,11	0,20	0,07	0,14
	CdTe	8	5	1	6	3	CdTe	0,33	0,52	0,55	0,39	0,64	0,49
	a-Si	3	1/3	1/7	1	1/5	a-Si	0,13	0,03	0,09	0,07	0,04	0,07
	CI(G)S	7	3	1/3	5	1	CI(G)S	0,29	0,31	0,18	0,33	0,21	0,27
													consistency consistent? 0,06 yes

## design priorities

Before the selection of the technology can be accomplished, the priorities of the criteria's need to be set. This is done by the needs the design has for the technology. The priorities can be seen below.



As this design is an evolution of the sustainable conceptual design, the main criteria's favor sustainability. When performance is compared to design the comparison slightly favors performance since the higher the performance of the PV technology, the sooner the energy invested in realizing the design is paid back. For this reason, sustainability is of strong importance when compared to performance. Even though the design is based upon the sustainability concept, performance is also an of the sustainability of the design. When the design is compared to sustainability, sustainability is of demonstrated importance.

For the sub-criteria's of performance, the efficiency is of strong importance. The reasoning being the temperature of the solar panels are not going to be high since the climate where the design is going to be placed is moderate. For the sub-criteria's of design, customizability is of absolute importance when compared to flexibility. The design can act as a showcase for PV technology and the flexibility isn't important in the design since the panels need to be rigid in order to be implemented into the structure of the design. For the sub-criteria's of sustainability, both are equal. Since both contribute to a sustainable design. The matrix and weighting vectors can be found below

PAIR-WISE COMPARISON MATRIX				NORMALIZED				WEIGHTING VECTOR	
	performance	design	sustainability		performance	design	sustainability		
performance	1	3	1/5	performance	0,16	0,27	0,15		0,19
design	1/3	1	1/7	design	0,05	0,09	0,11		0,08
sustainability	5	7	1	sustainability	0,79	0,64	0,74		0,72

**WEIGHTING VECTOR INCL. SUB-CATEGORIES**

performance		design		sustainability	
efficiency	temp. coeff.	customizability	flexibility	recyclability	E.P.B.T.
0,13	0,06	0,07	0,01	0,36	0,36

# Selection of technology

The results of the comparison between the alternatives are multiplied by the weighting factor of each criteria. This results in a final score for each technology. Every score for each criteria of each technology is added to get the final score overall criteria's.

When the final scores are evaluated, surprisingly the second generation CdTe technology comes seconds. This is due to the thin application of solar cell and the relatively high efficiency, resulting in a low EPBT. Since sustainability is an important criteria in this design, CdTe scores high. EPBT is also the reasoning behind the first place of poly c-Si and the third place of mono c-Si. Due to the lower EPBT of poly, the technology comes in first. Therefore the technology applied in this design will be poly c-Si.

## FINAL SCORE

mono c-Si	0,238
poly c-Si	0,247
CdTe	0,242
α-Si	0,116
Cl(G)S	0,157

	RESULT COMPARISON	WEIGHTING FACTOR	RESULT
EFFICIENCY	mono c-Si	0,12	0,069
	poly c-Si		0,039
	CdTe		0,012
	α-Si		0,004
	Cl(G)S		0,012
PERFORMANCE DROP OFF / CELSIUS	mono c-Si	0,06	0,002
	poly c-Si		0,005
	CdTe		0,025
	α-Si		0,016
	Cl(G)S		0,009
CUSTOMIZABILITY	mono c-Si	0,07	0,015
	poly c-Si		0,015
	CdTe		0,015
	α-Si		0,015
	Cl(G)S		0,015
STIFFNESS	mono c-Si	0,01	0,002
	poly c-Si		0,002
	CdTe		0,002
	α-Si		0,002
	Cl(G)S		0,002
RECYCLABILITY	mono c-Si	0,36	0,136
	poly c-Si		0,136
	CdTe		0,012
	α-Si		0,053
	Cl(G)S		0,023
EPBT	mono c-Si	0,36	0,013
	poly c-Si		0,050
	CdTe		0,176
	α-Si		0,026
	Cl(G)S		0,036

X

=

## 8.3 FINAL DESIGN

In the previous chapter, the conceptual designs are discussed. The conceptual design that is chosen for further elaboration is the sustainable concept (fig. 8.3.1). This concept sets the final design brief of the concept. Some design requirements are taken from the architectural concept (fig. 8.3.2).

During a visit to the stakeholder, the problem of drainage of water arose. This concept tries to fix this challenge by adding a green wall in the middle of the design. The solar panels are angled towards the green wall to guide the water into the green wall. This green wall is two way beneficial since the plants incorporated into the design evaporate water. This evaporated water cools down the solar panels, which results in a higher efficiency of the panels. The green wall is placed parallel to the parking place to allow the function of the parking plot to be uncompromised. By placing the wall in this manner, cars still have the possibility to cross from one parking place to another when they want to exit/enter the parking spot. The ends of the solar panels are lifted upwards as is described in the architectural design. The reasoning behind this is to create an inviting design that opens in the edges, symbolic for the transition of the user.

As a result of the MCA, the technology poly c-Si is integrated into the structure. To extend the green wall into the solar panels an optical filter is used to generate a green solar cell, as seen in (fig. 8.3.3). One of the characteristics of an optic filter is when the angle of light changes, it gives a different shape of color. This mimics the green wall since this also produces different shades of green when the sunlight hits the wall, creating high and low spots. The low embodied energy of the end-of-life rail tracks ensures the overall energy used to produce the design is kept to a minimum. The goal of the detailing of the design is to be able to dismount the structure at the end of its life, allowing the materials to be reused.

In the next chapter different renders and elevations of the design are shown.

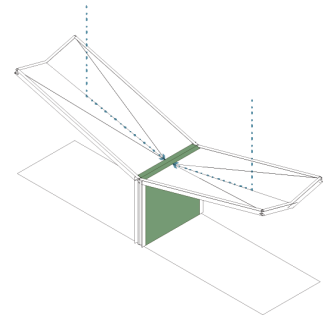


fig. 8.3.1: Sustainability concept illustration

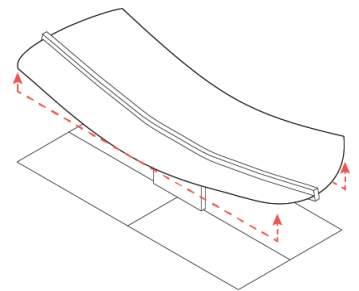


fig. 8.3.2: architectural concept illustration



fig. 8.3.3: optical filter used in design  
(source: Kameleon solar)

## design overview

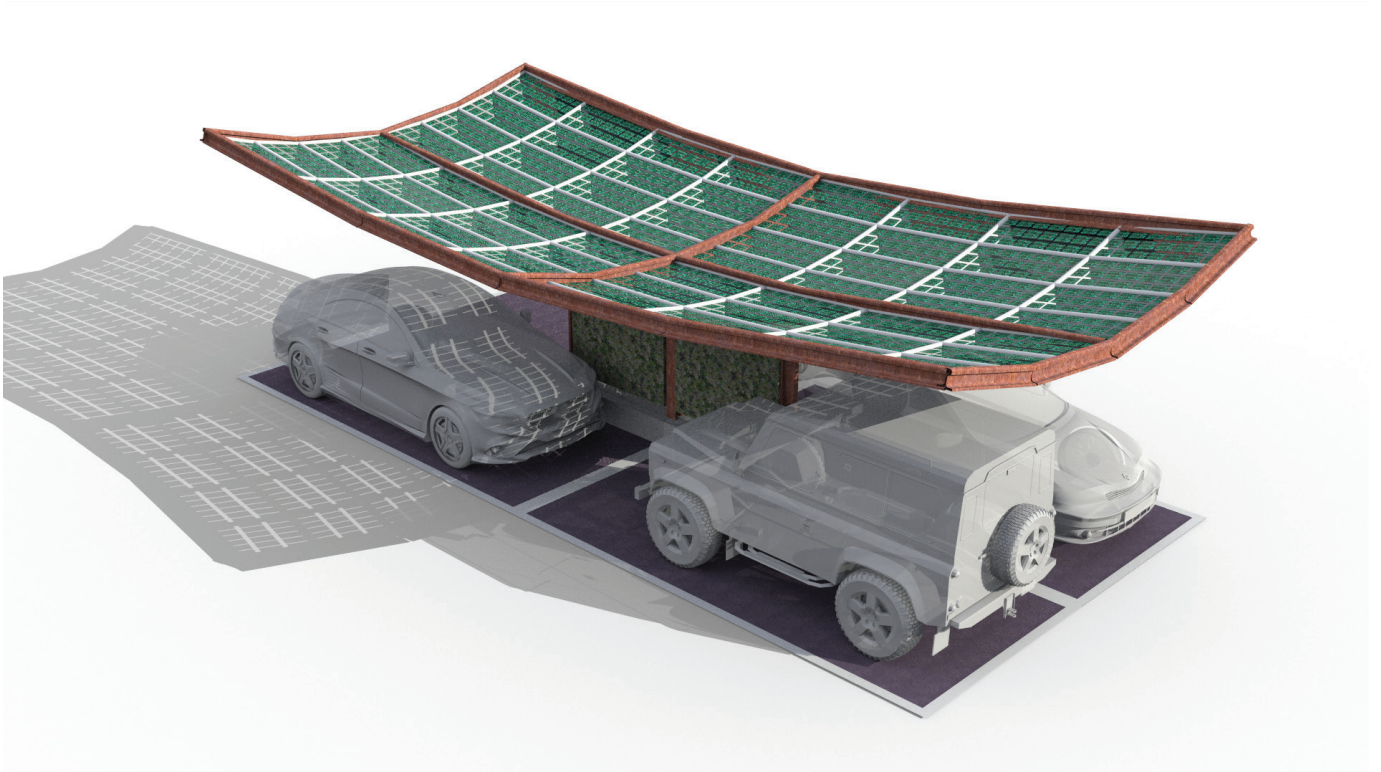


fig. 8.4.4: design birds eye view

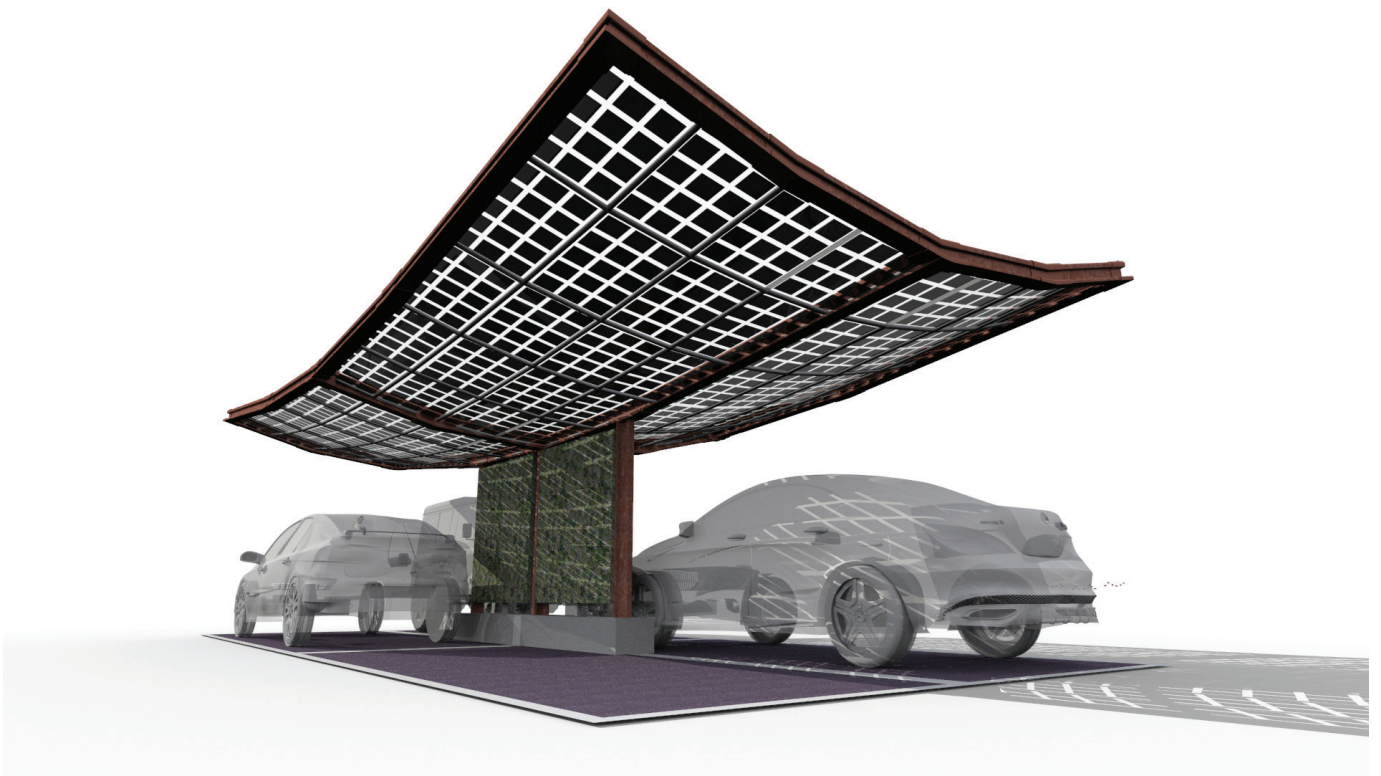


fig. 8.4.5: design eye height view



fig. 8.4.6: design eye height view 2



fig. 8.4.7: design side elevation

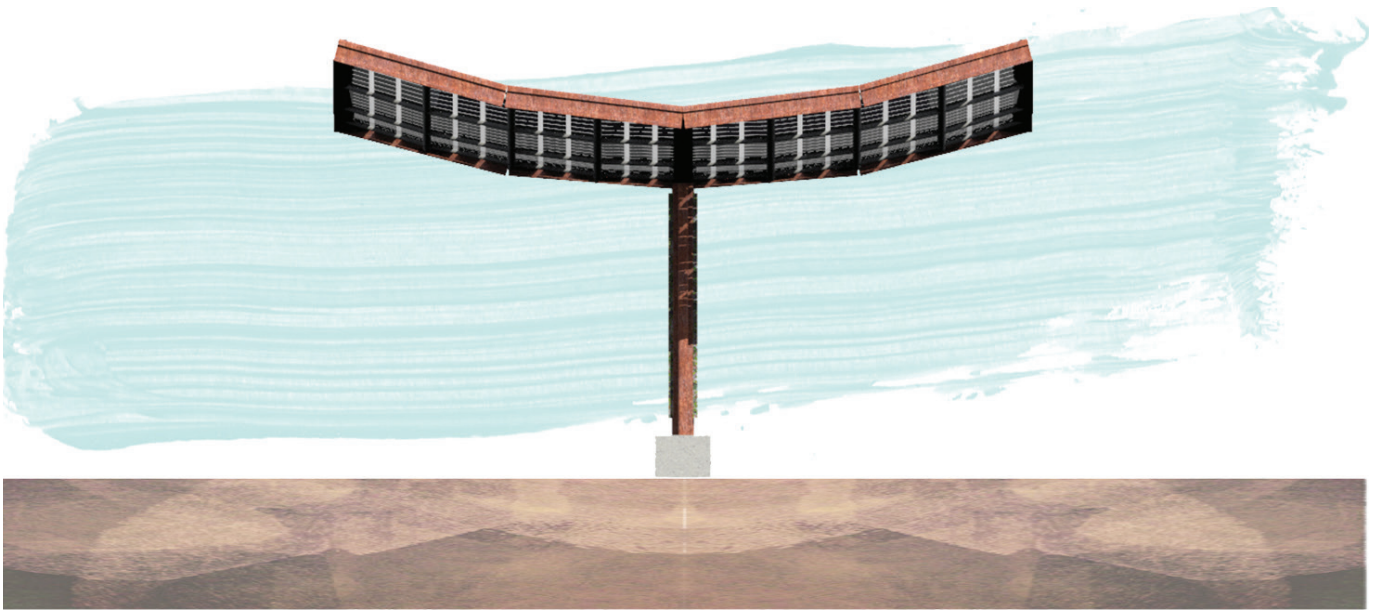


fig. 8.4.8: design front elevation

## modularity

As mentioned in the design brief a requirement for the design is to be modular. This is due to the varying sizes of the P+R plots. The stakeholder provided a list of requirements they apply when designing the P+R plots. The sizing of the parking spots is mentioned in this document. The measurements will be mentioned below (fig. 8.3.9.)

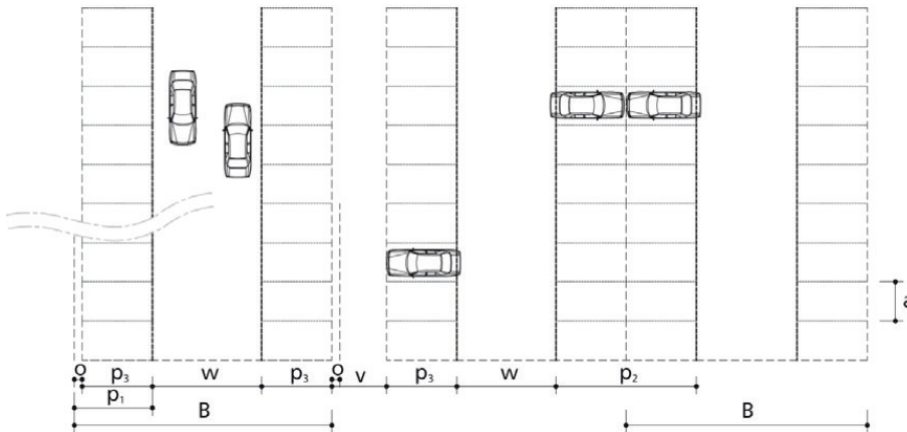


fig. 8.3.9: sizing parking spots  
(source: NS)

- a: width of parkingspot: 2,40 meter
- p1: length single parkingspot: 5,13 meter
- p2: length double parkingspot: 10,26 meter

The design takes these dimensions of the parking spot into account. To allow the design to be modular, the design block is based on one parking spot. This design block is then expendable in the x and y-direction. This allows for endless possibilities of parking plot size. Even and uneven parking spots can be realized with this design

In (fig. 8.3.10-12) possible configurations of the design are shown. How the structure is connected to allow for modularity is mentioned later on in the research

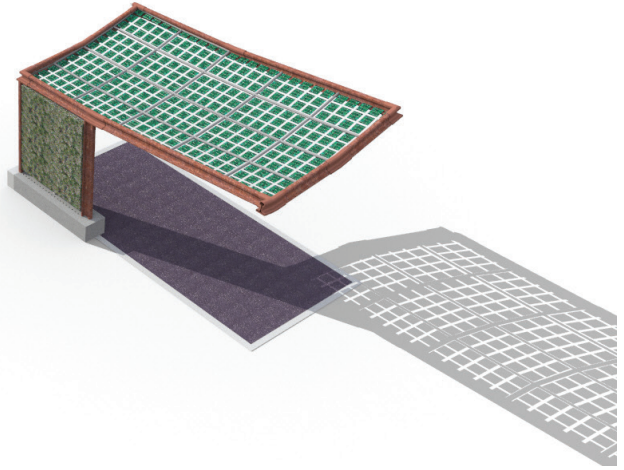


fig. 8.4.10: single parkingspot configuration

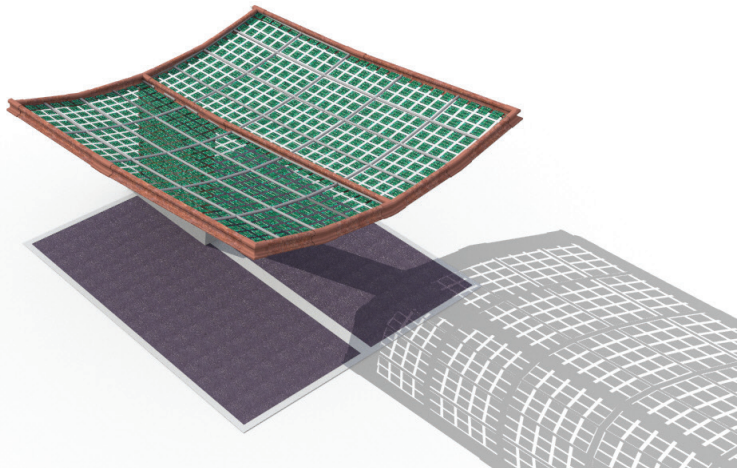


fig. 8.4.11: double parkingspot configuration

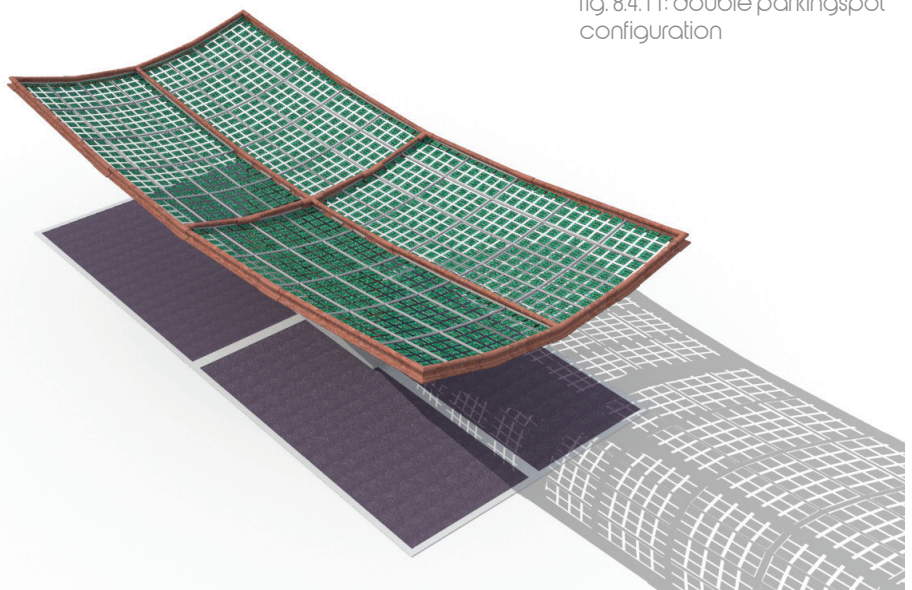


fig. 8.4.12: double row parkingspot configuration

## solar modules & electrical connection

The final design features 156 mm by 156 mm poly c-Si cells, as decided by the MCA AHP method. The panels have a double curved arrangement. The double curvature helps to collect and transport rainwater to the green wall. To allow for better manufacturability the panels are planarized, meaning that flat solar panels create the double curved arrangement. The planarization is done to allow the solar panels to be flat instead of skew, which is harder to manufacture and makes the design unnecessarily difficult. The size of the solar module is depended on the partition of the design. Since the edge beams have a kink in the middle of the design, the choice is made to only have an even number of solar cells in the design. This results in the kink of the solar panels following the kink of the edge beam. This leads to the following option for the design;

Amount of solar panels (WxL)	Dimensions (WxL)
2 x 2	1220 x 2565 mm
2 x 4	1220 x 1285 mm
2 x 6	1220 x 855 mm
4 x 2	610 x 2565 mm
4 x 4	610 x 1285 mm
4 x 6	610 x 855 mm
6 x 2	408 x 2565 mm
6 x 4	408x 1285 mm
6 x 6	408 x 855 mm

table 8.3.1: solar cell partitions and dimensions

The solar panel partition with 2 solar modules in the length is not an option since those solar panels have a length that is too substantial and negatively influences the rounded shape of the design. The partitions with 2 solar modules in the width also negatively influences the rounded shape of the design and therefore are discarded. This still leaves a number of options, but within these options, the biggest size is selected to allow the minimum amount of connection to be implemented. This results in a 4 by 4 solar modules partition with a dimension per solar module of 610mm by 1285 mm. Within this solar module, the maximum amount of solar cells is placed, with keeping in mind the minimal distance to the edge being 2 cm. This results in 3 solar cells being implemented in the width and 7 in the length. The dimensions of the solar module can be seen in (fig. 8.3.13). This still allows for enough transparency since this is what the stakeholder mentioned in the design brief. In this design brief, the requirement was noted that the design should be transparent to discard the need for lighting below the design during darker days. Also, social security was a theme which a transparent design influences.

The transparency of the design in combination with reflective cars parked below the design results in reflected sunlight on the backside of the panel. With this in mind, bifacial cells will be implemented to generate extra electricity.

4x4 (W x L) of solar modules  
In 1 parking spot conf.  
Max. amount of solar cells  
336 solar cells in 1 park conf.  
34,8% glass

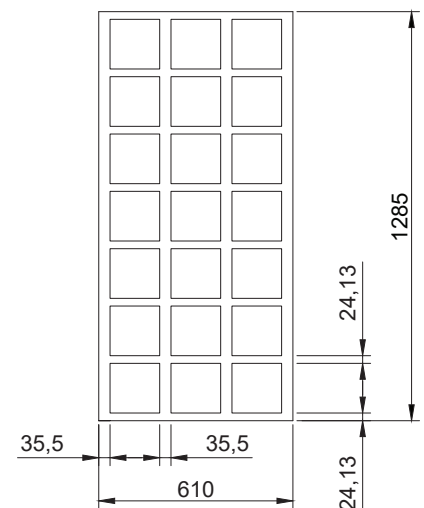


fig. 8.3.13: solar module dimensions

The modules are connected to each other using a junction box. To keep the structural integrity of the glass used in the solar panels, the junction box is placed on the edge of the glass. The design of the junction box is the pen-shaped junction box, as seen in (fig. 8.3.14). The cabling will be hidden behind the connection between the solar panels. The connection between solar panels will be discussed in a later chapter of this research.

Due to the orientation independent origin of the design, some panels in the string will generate less power than others with better orientation. Therefore power optimizers are applied at cell and panel level to allow the string of cells/panel not to be influenced by the lesser generating cell/panels. Even though these tools are implemented to allow for a better overall input, for each orientation different solar panels need to be connected in series to allow for the maximum overall output per orientation.

The diagonal angle of the solar modules is 15 degrees. Meaning the center and the most outer edge of the design have a 1,52m height difference. This results in an average angle of 15 degrees.



fig. 8.3.14: edge junction box  
(source: staubli)

## structure & structural connection

The structure is made out of the end-of-life rail tracks. This material supports the concept of the sustainable design by re-using “waste” materials into the structure to keep the embodied energy of the structure as low as possible. The shape of the rail tracks is similar to that of an I beam, therefore it is suitable to be integrated into the structure. To make the design modular, the connection between the rail tracks is bolted. To accomplish this a recycled aluminum extruded connection piece is designed. The connection piece is slightly larger than the rail tracks. This allows the rail tracks to be slide into the connection piece where it is bolted together. There are two different types of connection pieces. A 90-degree bend, and a T connection. This allows the design to be expandable and thus modular. By applying bolts, the design can be demounted and the materials applied in the design can be reused in a second life for another application. The connection is painted in a color that matches the color of the rail tracks to assure the connection blends in with the design, as seen in (fig. 8.3.15-16).

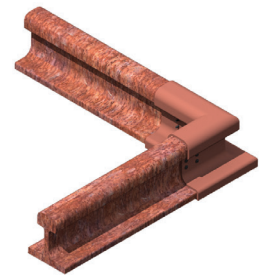


fig. 8.3.15: connection railtracks 90 degrees

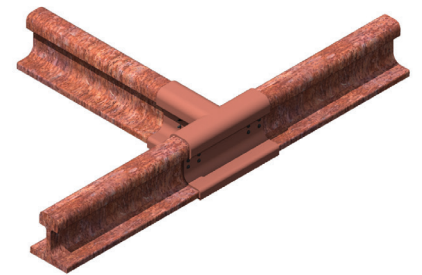


fig. 8.3.16: T connection rail tracks

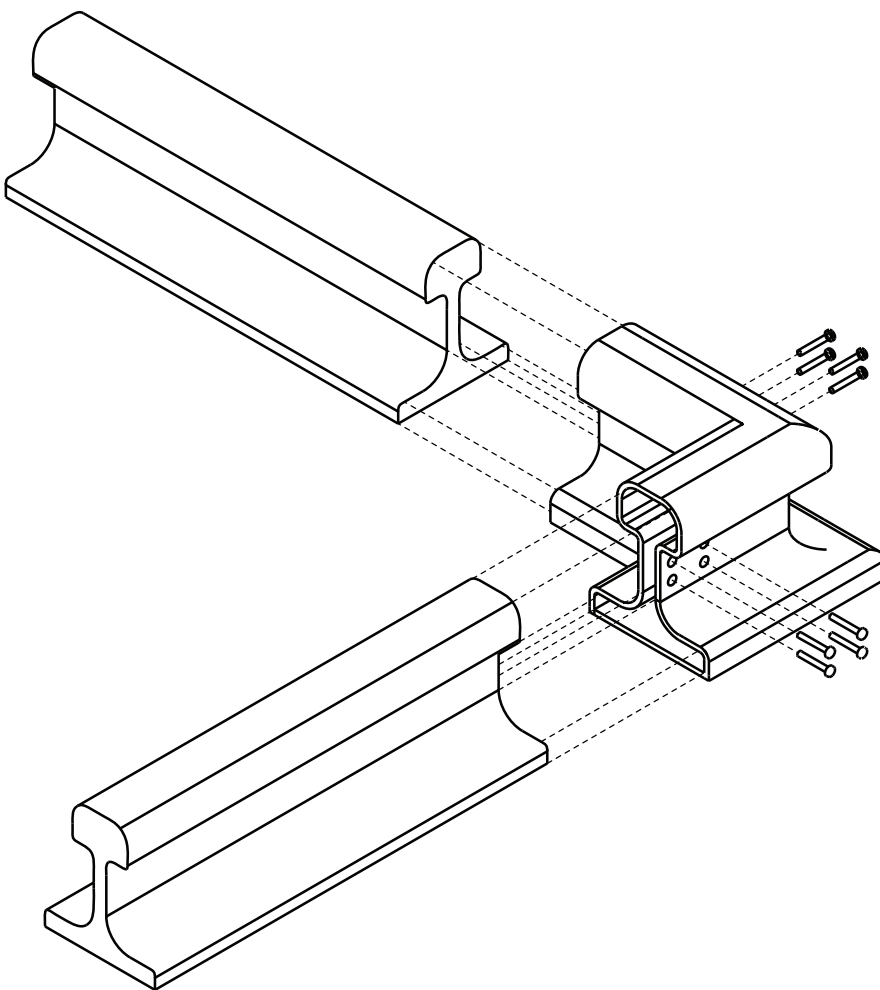


fig. 8.3.17: exploded view connections

## rail tracks connection evaluation

The aluminum extruded connection between the rail tracks is evaluated. In this evaluation, three major disadvantages were discovered. The topics of these disadvantages are; make ability, material properties and combination of connections. These disadvantages result in this type of connection being nonrealizable for this project. The details of the disadvantages will be discussed below.

### makeability

The initial extruded aluminum profiles are made by extruding aluminum through a mold. These molds are made out of a hard metal that is altered by an extensive manufacturing process to create the desired shape. Due to the material used and the difficulties altering the shape of the mold, they cost a lot of money to produce. When an aluminum profile manufacturer needs to make a special mold, there needs to be a lot of offset of extruded aluminum profiles to justify the costs of these molds. Although there are a lot of P+R carports the total length of aluminum profiles that are needed might be below the threshold of the manufacturer. This either results in a significant rise in costs or the manufacturer decides it is not in his interest to make the aluminum profiles.

### material properties

The material of choice for the profiles is aluminum. The reasoning behind this is that the intended outline of the profiles mimics the shape of the rail tracks. Aluminum is a great material to make into profiles since it can be extruded as mentioned above. Steel cannot be extruded and therefore it cannot be made into the rail track shape of the profiles. The main disadvantage of this choice of materials is its stiffness. Aluminum has a Youngs modulus of 70000 N/mm<sup>2</sup>, whilst the steel used in the rail tracks has a Youngs modulus of 210000 N/mm<sup>2</sup>, which is a multiplication of three times. To give some insight, to make aluminum as stiff as steel (in the same shape) three times more material needs to be used in order to achieve the stiffness of steel. This will result in thick aluminum profiles that connect the steel rail tracks to each other, to make sure the aluminum profiles aren't the weak link in the structure. This is not the intended shape of the profiles. The idea behind the connections was to make them blend in with the rail tracks when these profiles are too thick this idea is absent.

### combination of connections

The major disadvantage of this connection is at the intersections where the connection of the rail tracks interference with the connection between the rail tracks and the solar panels. The problem area is highlighted by the red rectangle in (fig. 8.3.18). The problem with this interference is that the connection of the solar panels doesn't allow for a local differing of the contactblock location.

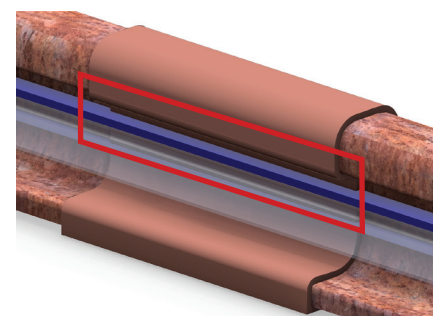


fig. 8.3.18: problem area connections  
blue: solar panels connection  
red: rail track connection

## rail tracks connection evolution

To make sure the design is realizable a different connection is designed for the reasons mentioned in the previous chapter. The following requirements are set for the connection;

- Demountable; to allow the materials of the structure to be reused
- Not interfere with the connection of the PV panels
- Make use of the material steel; to make sure the stiffness material used is the same as the stiffness as the rail tracks.

Since the connection needs to be made out of steel, complex shapes cannot be designed. In (fig. 8.3.19) the area where the connection of the solar panels with the edge beam is shown. In this area, no connection between rail tracks can be made. Therefore in the new connection, the material is placed on the top side and bottom side of the rail track. This makes sure the connection does not interfere with the connection of the solar panels and as an additional benefit, the material is placed at the maximum distance of the center point. This allows the material to be used in a more efficient way when compared to placing the material closer to the center point. This does result in a hole through the middle of the upper-, lower flange and a mouse hole through the web to allow the bolts to be inserted. A detail of the new connection is shown in (fig. 8.3.20). The amount of bolts, dimensions of bolts and steel plate will be calculated in a later phase of this report.

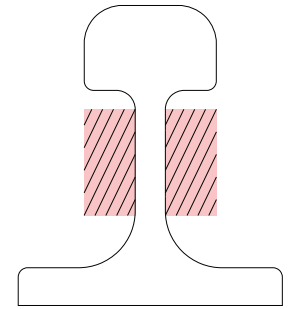


fig. 8.3.19: Zone of solar panel connection

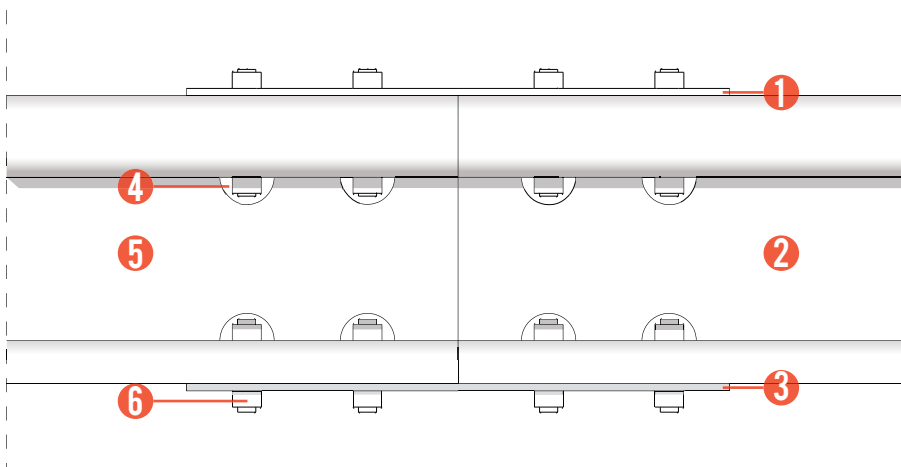


fig. 8.3.20: Detail of new connection  
 1: Upper steel strip  
 2: Rail track 1  
 3: Lower steel strip  
 4: Mouse hole through rail track  
 5: Rail track 2  
 6: Bolt & nut connection



fig. 8.3.21: isometric view of new connection

## solar panel connection

The connection between the solar panels can be seen in (fig. 8.3.22). The connection is an evolution of the graduation project of Niki Nikalaou. The main advantage of this evolution of the glass connection is the improved transparency of the design. This is done by reducing the size of the contact block by alternating the panels in the same contact block, as discussed in the pilot study case. The solar panels are made out of two sheets of 3 mm tempered solar glass laminated together with EVA. Inside this EVA layer, the 0,2 mm thick solar cells are placed. A layer of 3 mm tempered glass is laminated onto the solar panels using sentry glass. In between the glass and the solar module, the embedded composite connection is laminated. During the engineering of the connection, the problem occurred when one side was clamped in the contact block the other side would have a gap where rainwater could pass through. The solution to this problem is the implementation of a rubber gasket. The force that the clamping block provides will make sure no water can pass through. A benefit of applying a rubber gasket on the end of the opposite element is when the angle is altered between the two panels the rubber gasket will mold into the correct shape.

The connection relies on friction to transfer the forces from one element to the other. To add extra friction a protective sleeve made of POM coated with rubber is applied in between the composite element and the contact block.

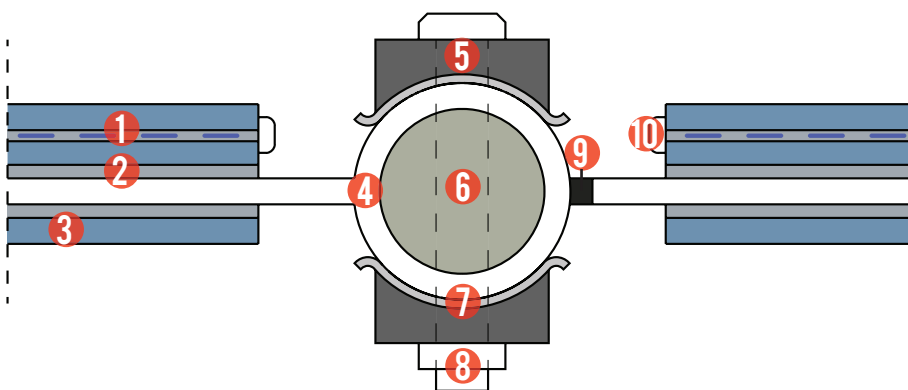


fig. 8.3.22: proposed connection detail

1. solar module, 2 x 3mm tempered glass
2. Sentry glass for lamination, 1.52mm
3. 3mm tempered glass
4. phenolic/E-fiber woven fabric composite biaxial lamina, 3mm thickness
5. 7mm steel linear contact block
6. pultruded glass fiber composite tube with 20mm diameter
7. protective sleeve made of POM coated with rubber for extra friction
8. prestressing bolt
9. sealing rubber gasket
10. junction box

To connect the glass to the edge beams made out of rail tracks, a different contact block is used. In basis, the concept is the same as the connection between glass to glass elements. The contact block covers one side of the connection. Within the contact block, a recess is made to allow a bolt connection to be applied between the connection block and edge beam. A detail of the connection can be seen in (fig. 8.3.23).

When the design is continuous two elements are connected to the edge beam. This is done in a similar manner as the single element connection. Instead of the bolt and nut connecting to the edge beam, it passes through the edge beam to the other contact block. Here a bolted connection is applied. A detail of the connection can be seen in (fig. 8.3.24).

The edge beams don't follow every kink of the solar modules. This allows longer rail tracks to be applied without negatively influencing their structural integrity. The more the edge beams follow the kinks of the solar modules, more connections need to be applied. Therefore the edge beam has one kink. To accommodate the curvature of the solar modules the contact blocks differs in placement amongst the web of the rail track. The design is engineered in such a manner that when the contact reaches the highest maximum point of the web, the edge beam kinks to accommodate more space for the contact block. The change of the placement of the contact block is illustrated with the arrows in (fig. 8.3.23-24).

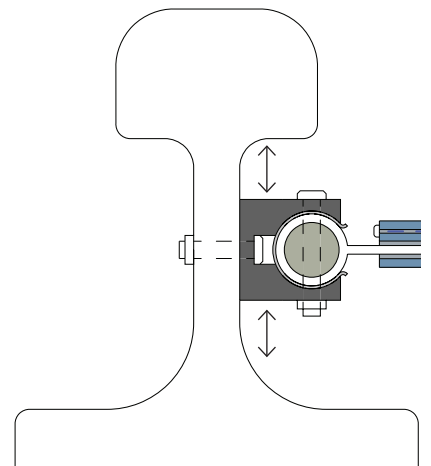


fig. 8.3.23: connection edge beam and single element

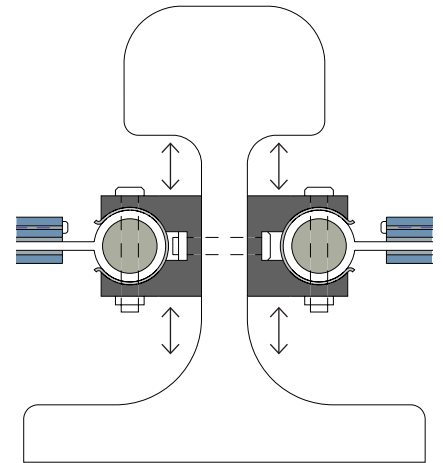


fig. 8.3.24 connection edge beam and double elements

# green wall

The design features a green wall perpendicular to the parking spot. The goal of this green wall is to capture the rainwater from the design. This water is then evaporated by the plants, this evaporated water then cools the solar panels. Research showed that when solar modules are placed above a green roof, the temperature of the upper soil layer is 5 to 11 degrees celsius less than a bare roof. This resulted in an output increase of the solar modules of 4,3%<sup>[8.4]</sup>. Although this research was conducted with a horizontal green roof, the green wall of the design will still have a cooling effect on the panels.

The green wall consists of green panels. The green wall panels themselves consist out of stonewool with at the level of the plants, earth implemented surrounding the roots of the plants. The green panels when places should consist out of different vegetation. The vegetation inside the panels should be carefully chosen for each of the different orientation. Reason for this being that some plant require direct sunlight, for example (fig. 8.3.26) , whilst some plants require shade, for example (fig. 8.3.27) . Since the climate in the Netherlands is moderate, the plants implemented in the green wall should be of the perennial type. This means that the plants in the greenwall will last for years with the correct maintaince, instead of the annual plants that require replacement every year. The design of the green wall can also include a design for the local partners of the stakeholder, like a municipality. The green wall panels are mounted on a steel substructure. This substructure is mounted on the concrete foundation of the structure and the rail tracks of the design.

As mentioned previously the green wall captures and stores the rainwater from the solar modules above. The rainwater goes through a void in the connection and enters the panels of the green walls (fig. 8.3.28). When the panels are saturated the water will go down to the panel below. This continues until the last panel is saturated. The water then falls on the concrete block on the bottom of the structure. This concrete block acts as the foundation of the columns. Between the two columns, the concrete block is hollow and acts as a water buffer for the green wall. An irrigation system is installed in the green wall and connected to the water buffer. The irrigation system is connected to the solar panels and when the output exceeds a certain amount (meaning a sunny day) the irrigation system should provide the plants with water.

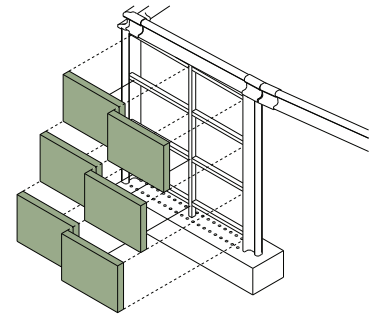


fig. 8.3.25: green wall panels on sub structure



fig. 8.3.26: Bacopa perennial plant (source: Nature & Garden)



fig. 8.3.27: Heuchera perennial plant (source: Bluestone perennials)

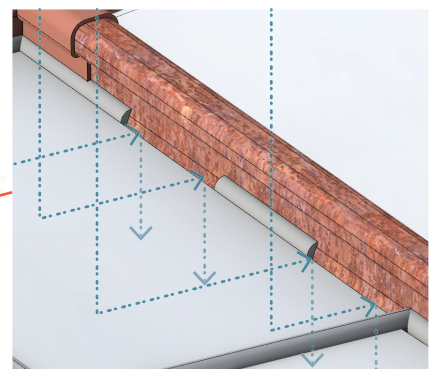
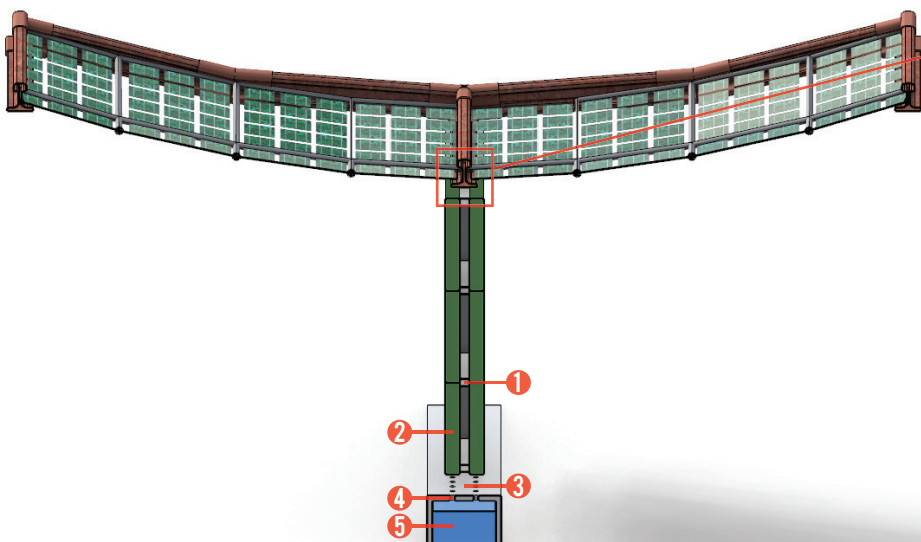


fig. 8.3.28: rainwater flow

fig. 8.3.29: section of green wall

1. steel sub structure
2. green wall panel
3. concrete block
4. drainage holes
5. water reservoir

The structure of the carport is placed on a concrete block placed on the ground below. The benefit of this foundation type, is that it does not require any piles. The exact dimensions of the concrete foundation block needs to be calculated in a later stage of the design.

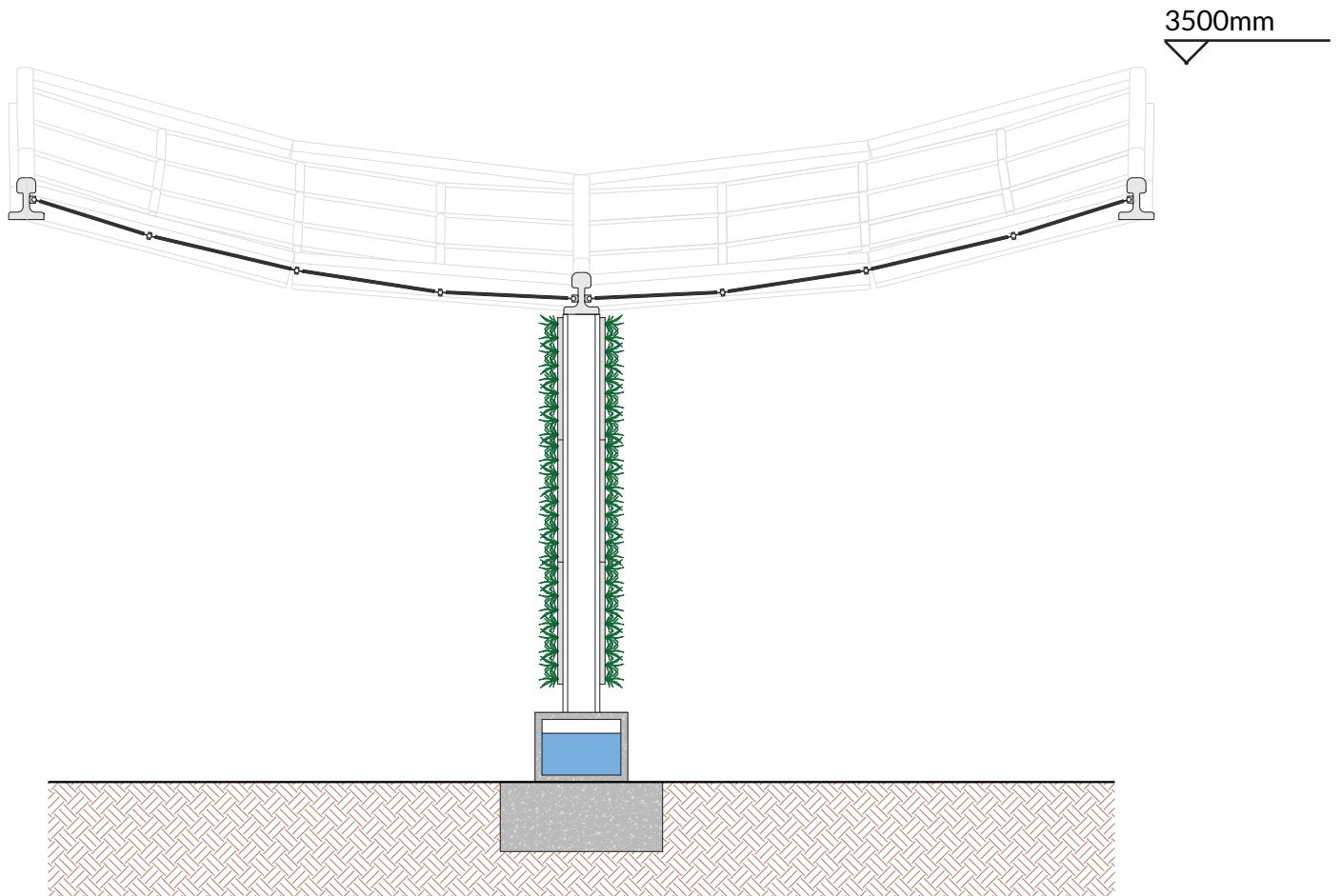


fig. 8.3.29: section of design

## 8.4 DESIGN ANALYSIS

In this chapter, the final design will be simulated for structural analysis and solar analysis. The assignment of this research was to create a design that was applicable in every orientation without significant loss in output. This is simulated and analyzed in this chapter. Then the structure of the design is simulated and analyzed. In this simulation, the stresses and the deflection of the surface are monitored to see if these values exceed either the maximum allowed stress in the glass or the maximum deflection.

### solar analysis

To validate if the design is orientation independent, it's performance is simulated in Grasshopper, the script used can be seen in (fig. 8.4.2). A weather data file from Amsterdam is used in the simulation. A four parking spot configuration of the design is simulated. The following orientations are simulated; N, NE, E, SE, S. The remaining orientations are not simulated since the design is mirrored and therefore will perform the same in the other directions. An overview of the model used can be seen in (fig. 8.4.1). In the first simulation, a double row configuration of the design is simulated. In the second simulation, a single row configuration is simulated to see the influence of applying the design in the least favorable conditions.

It is important to note that the solar irradiation calculated in kWh/yr/m<sup>2</sup> is for the surface, not for the final output of the solar modules. The efficiency of the solar cells, connection losses, and cell density need to be extracted from the calculated solar irradiation. The outcome of the calculation can be seen in (fig. 8.4.3). The final design in a double row configuration has a solar irradiation of 934 kWh/yr/m<sup>2</sup> that's independent of the orientation of the design. The single row configuration of the design is not orientation independent. The favorable orientation has 8,8% more solar irradiation when compared to the unfavorable orientation of the design.

As mentioned previously, due to certain modules getting less solar irradiation than others, a power optimizer is needed to make certain the string of solar modules aren't affected by the modules that get less sunlight.

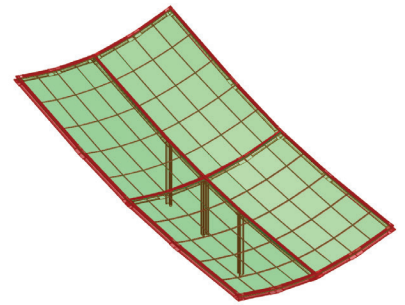


fig. 8.4.1: solar analysis model overview, green = radiation analysis surface red = context

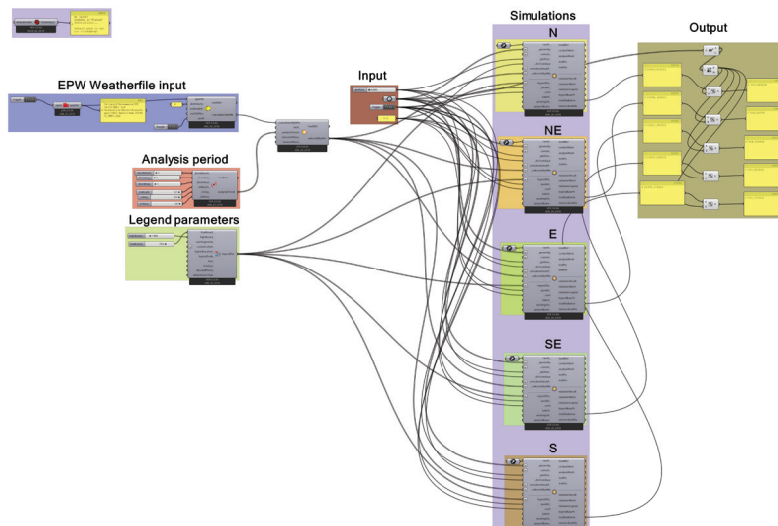


fig. 8.4.2: grasshopper script

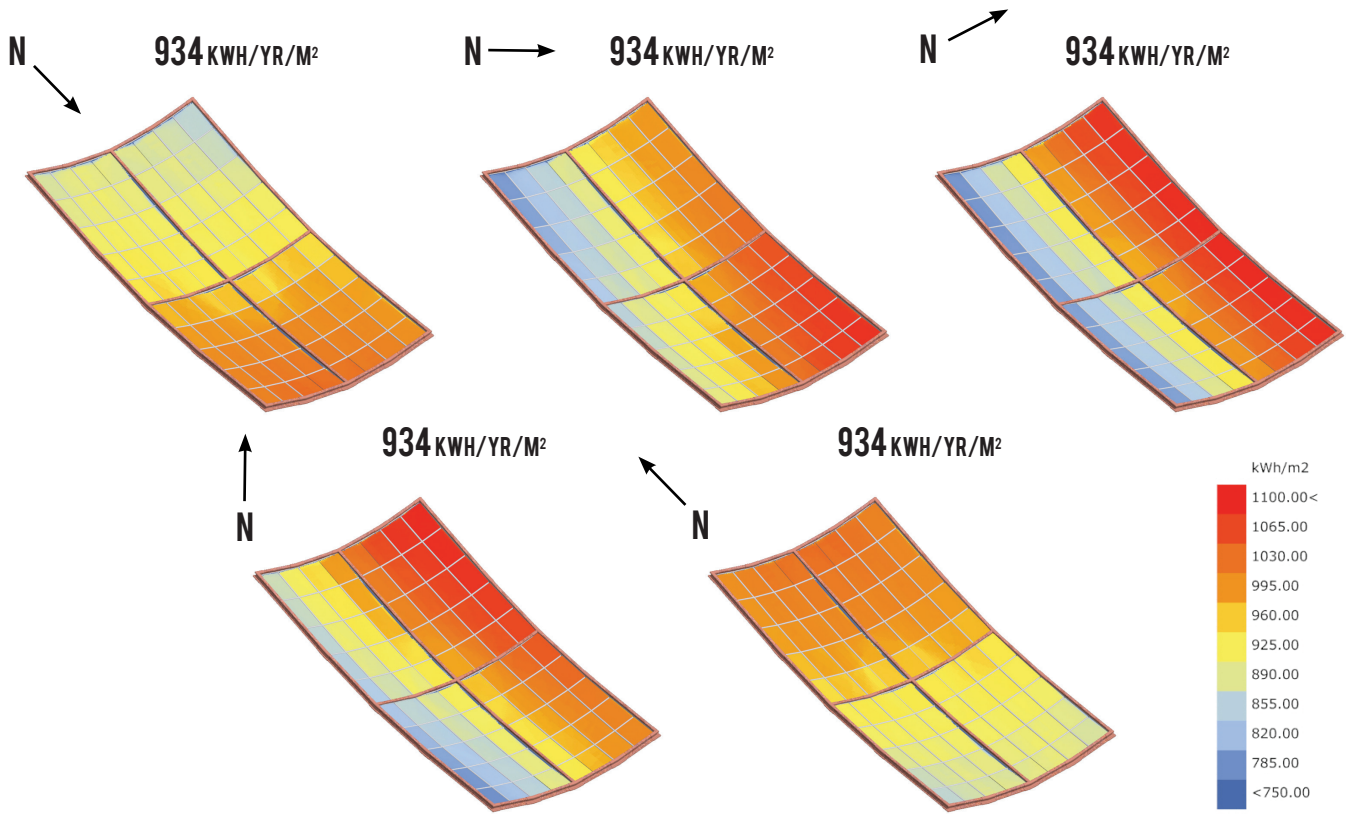


fig. 8.4.3: solar analysis different orientations

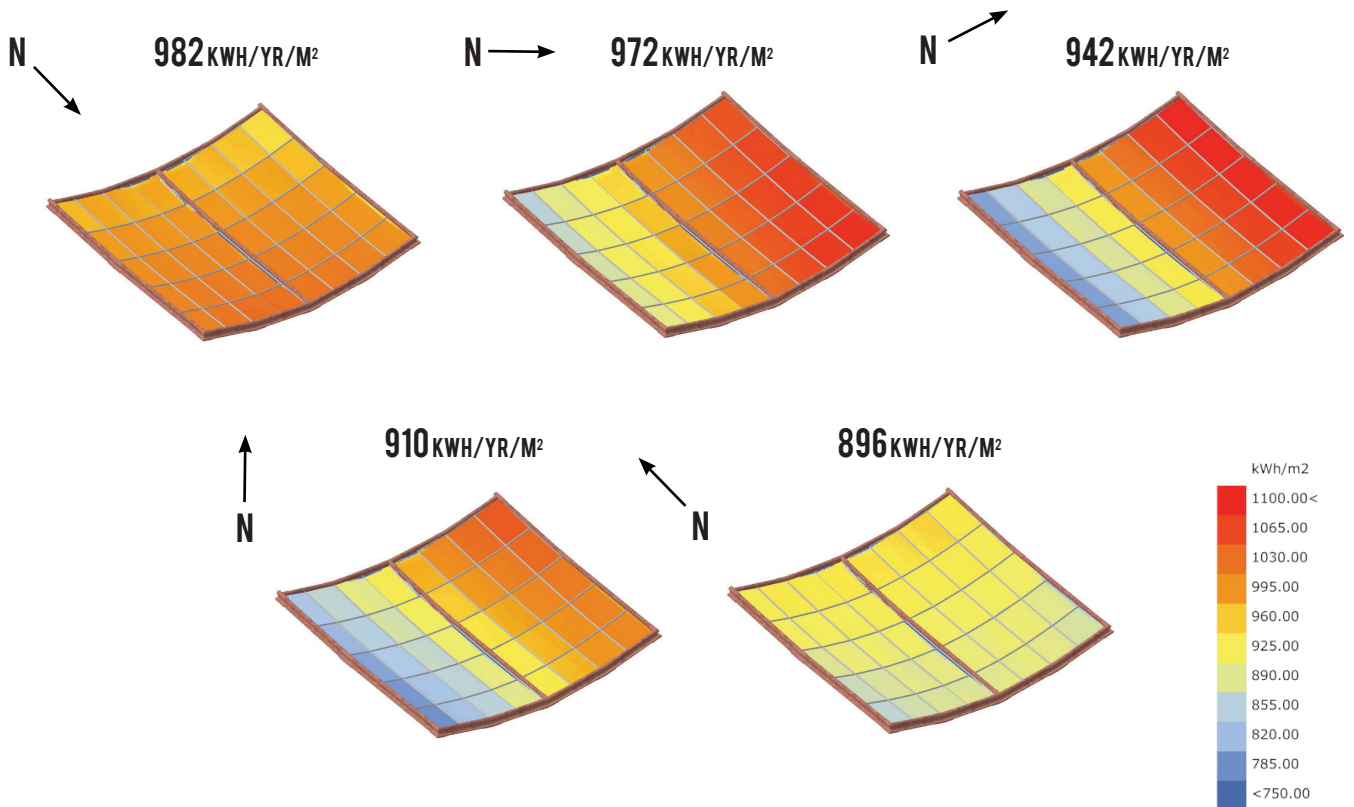


fig. 8.4.3: solar analysis different orientations

## structural analysis

The structural performance of the design is analyzed in this chapter. The analysis is done in Grasshopper with the plug-in Karamba. As previously mentioned the structural material used in the design are rail tracks. These rail tracks are modeled in Karamba as I beams with the same dimensions as the rail tracks (fig. 8.4.4). Karamba doesn't allow for this amount of fillet edges, the location where flange and web meet does have a fillet edge with a radius 16 mm. The steel used in Karamba is S235 steel. In the analysis, the glass has a thickness of 9mm with the properties of tempered glass.

The load is set to 1 kN/m<sup>2</sup> from in the Z-axis direction. This load can be a wind load, water load or a snow load. There are different configurations of the final design possible. The following configurations are modeled: 1 by 1 parking spot configuration, 2 by 1 configuration, 3 by 1 configuration and finally 2 by 2 parking spot configuration.

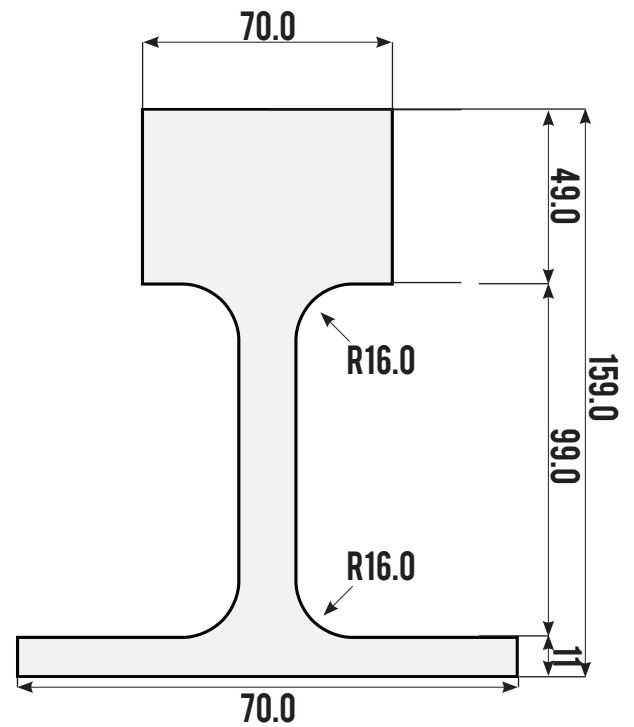
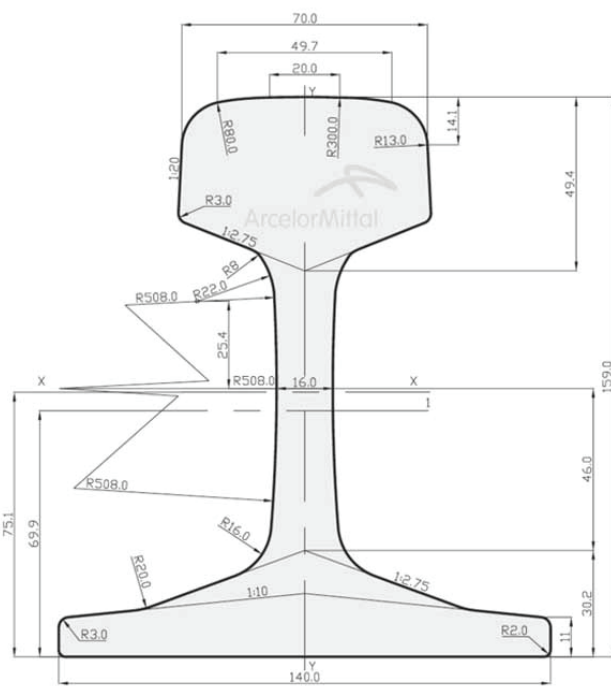


fig. 8.4.4: Railtrack dimensions  
left: original 54E1 rail track dimensions  
(source: Arcelor Mittal)  
right: karamba model dimensions

## 1 by 1 parkingspot configuration

1

max deflection: 39.6 cm

max tensile stress: 47.2 kN/cm<sup>2</sup>

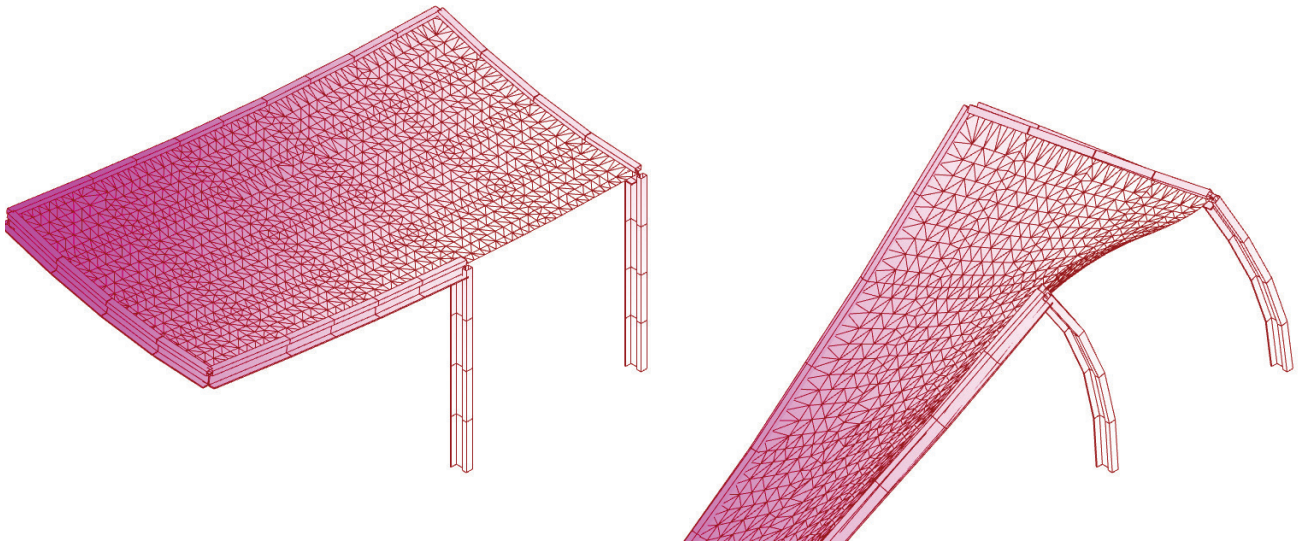


fig. 8.4.4: single carport analysis  
left: no deflection  
right: deflection (exaggerated)

2

max deflection: 25.4 cm

max tensile stress: 22.5 kN/cm<sup>2</sup>

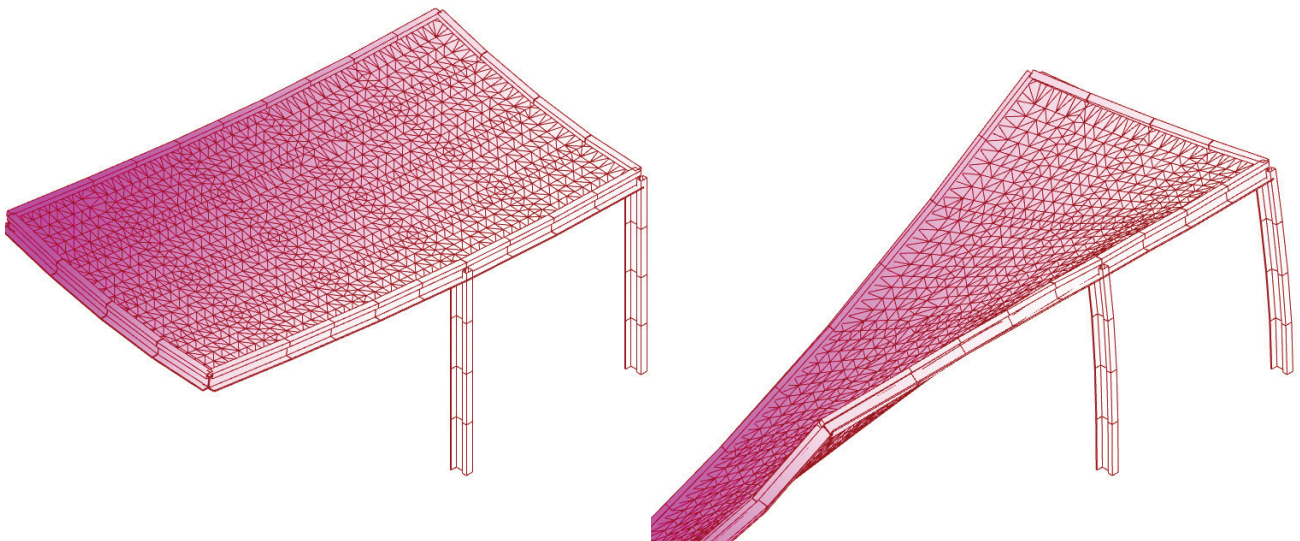
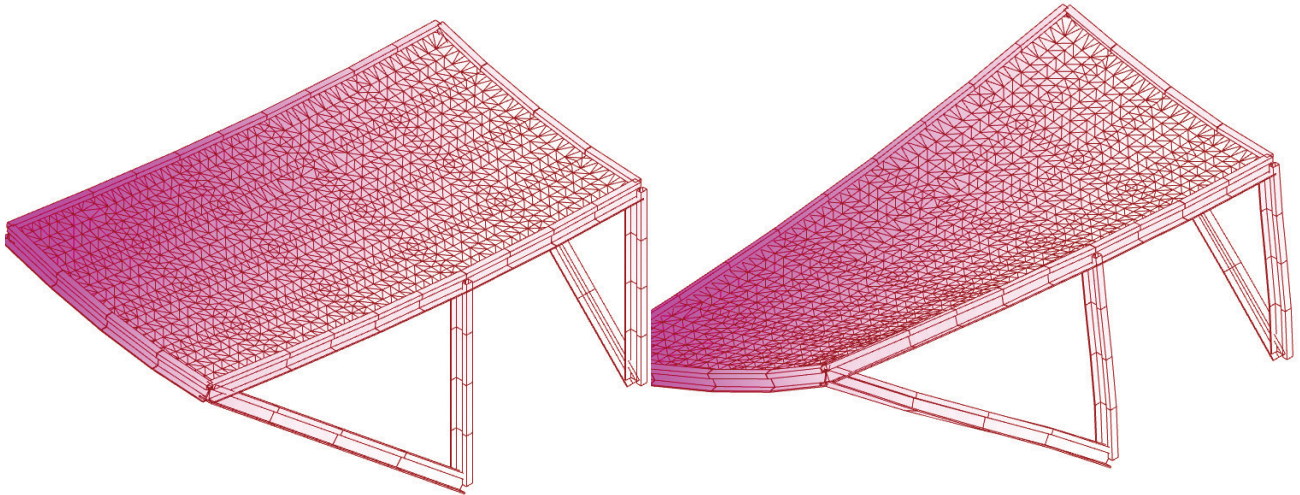


fig. 8.4.5: single carport, beam across  
green wall analysis  
left: no deflection  
right: deflection (exaggerated)

### 3

max deflection: 8.88 cm

max tensile stress: 6.83 kN/cm<sup>2</sup>



## analysis

fig. 8.4.6: single carport fully trussed  
left: no deflection  
right: deflection (exaggerated)

In the first simulation (fig. 8.4.4) the single configuration as designed is simulated. With a maximum deflection of 39,6 cm and a maximum tensile stress of 47,2 kN/cm<sup>2</sup>, it exceeds the maximum tensile stress that tempered glass is able to take. Besides the glass reaching its breaking point, the maximum deflection is also substantial. This deflection will result in the user of the carport feeling unsafe below the structure.

The design is then further evolved to see what measures are needed for this configuration to become viable. In the second simulation (fig. 8.4.5), a beam is added across the green wall for increased stiffness and strength of the structure. The maximum deflection, 25,4 cm, and the maximum tensile force, 22,5 kN/cm<sup>2</sup>, drop significantly, but still, the maximum tensile stress exceeds the maximum tensile stress tempered glass can absorb.

To make this configuration viable, the design needs to incorporate trusses as seen in the final simulation (fig. 8.4.6). The maximum deflection is still substantial with 8,88 cm but the maximum tensile stress drop below the tensile strength of tempered glass. The conclusion can be made that in this configuration the design needs to be fully trussed to be viable.

## 2 by 1 parkingspot configuration

1

max deflection: 4.67 cm

max tensile stress: 41.8 kN/cm<sup>2</sup>

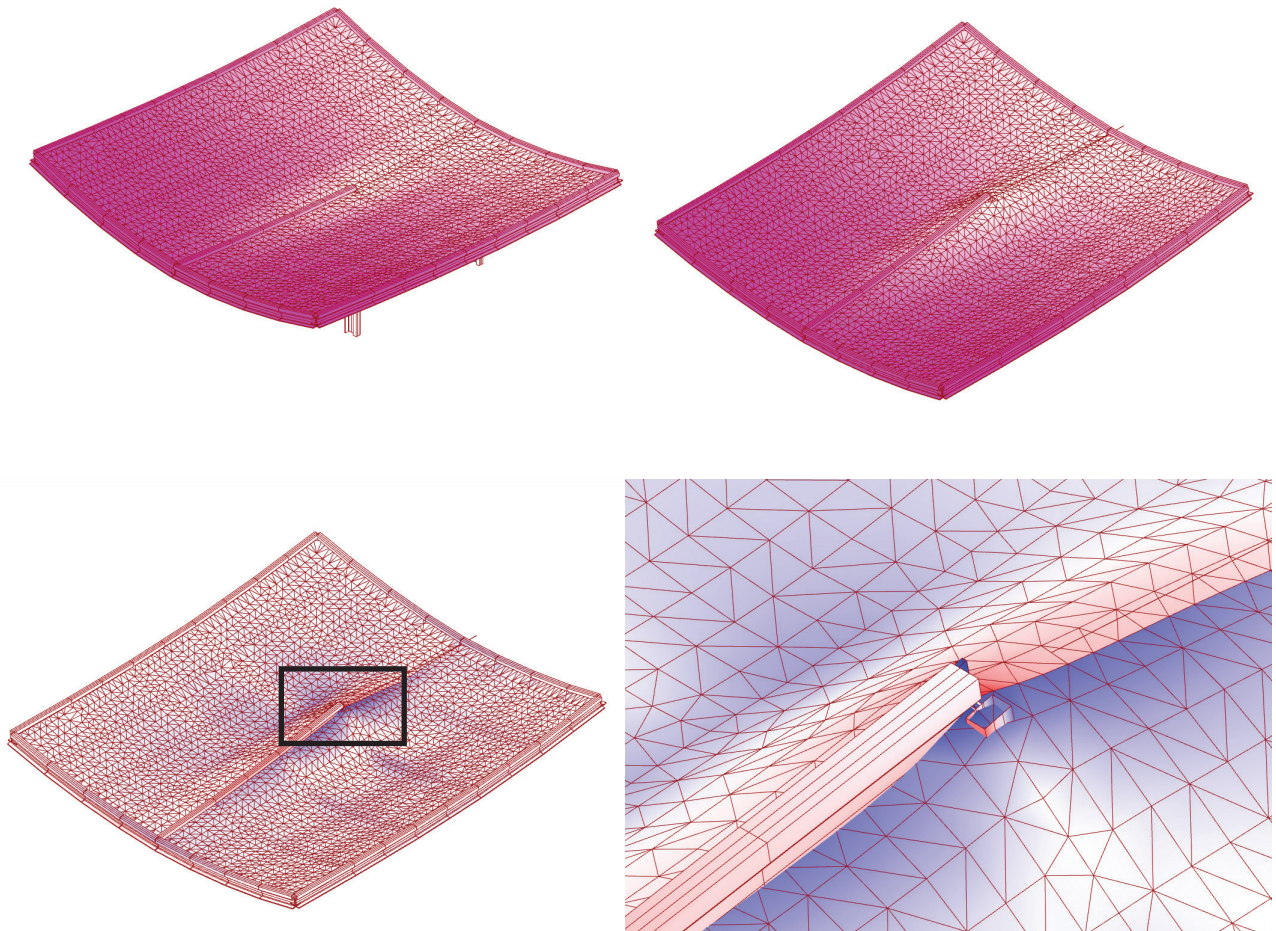


fig. 8.4.7: double carport analysis  
top left: no deflection  
top right: deflection (exaggerated)  
bottom left: stress simulation  
bottom right: stress zoomed in

### analysis

In the first simulation (fig. 8.4.7) of the double configuration as designed is simulated. With a maximum deflection of 4,67 cm and a maximum tensile stress of 41,8 kN/cm<sup>2</sup>, it exceeds the maximum tensile stress that tempered glass is able to take. As seen in the close up in the bottom right, the maximum tensile force concentrates around the column of the design.

## 2 by 1 parkingspot configuration

2

max deflection: 2.24 cm

max tensile stress: 13.6 kN/cm<sup>2</sup>

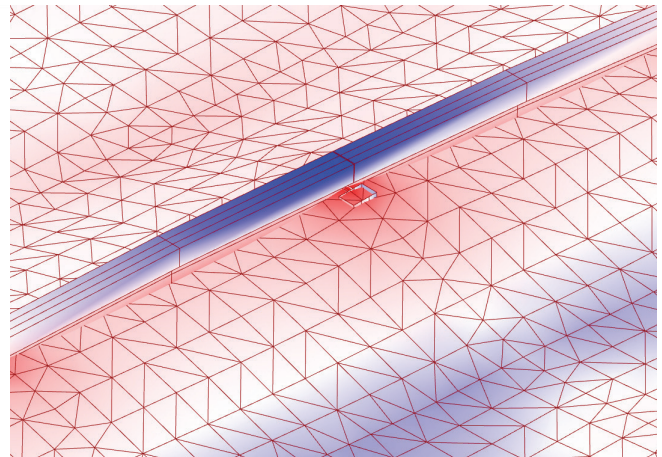
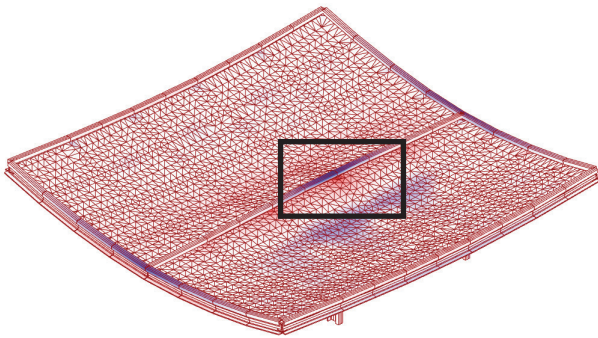
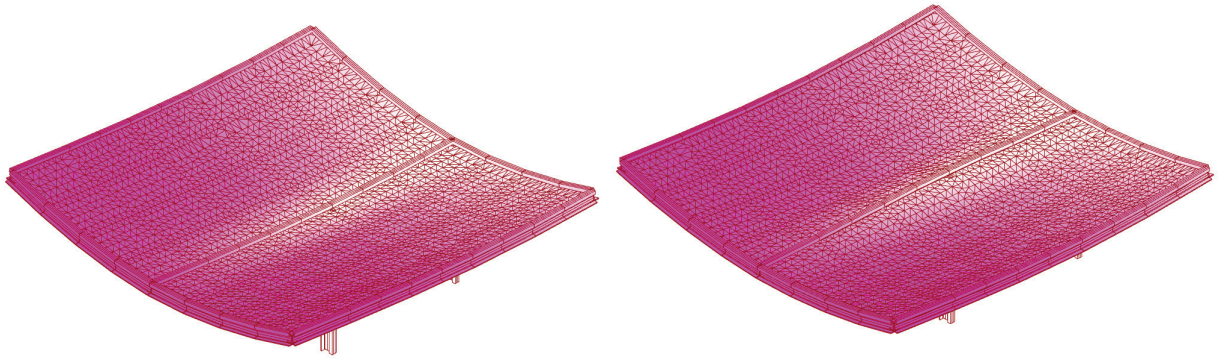


fig. 8.4.8: double carport analysis  
top left: no deflection  
top right: deflection (exaggerated)  
bottom left: stress simulation  
bottom right: stress zoomed in

### analysis

In the second simulation (fig. 8.4.8) of the double configuration, a beam is added across the green wall for extra stiffness and strength of the structure. With a maximum deflection of 2,24 cm and a maximum tensile stress of 13,6 kN/cm<sup>2</sup>, it still exceeds the maximum tensile stress that tempered glass is able to take. The stress concentrates around the column of the design. This can be solved with good detailing.

## 3 by 1 parkingspot configuration

max deflection: 2.58 cm

max tensile stress: 15.0 kN/cm<sup>2</sup>

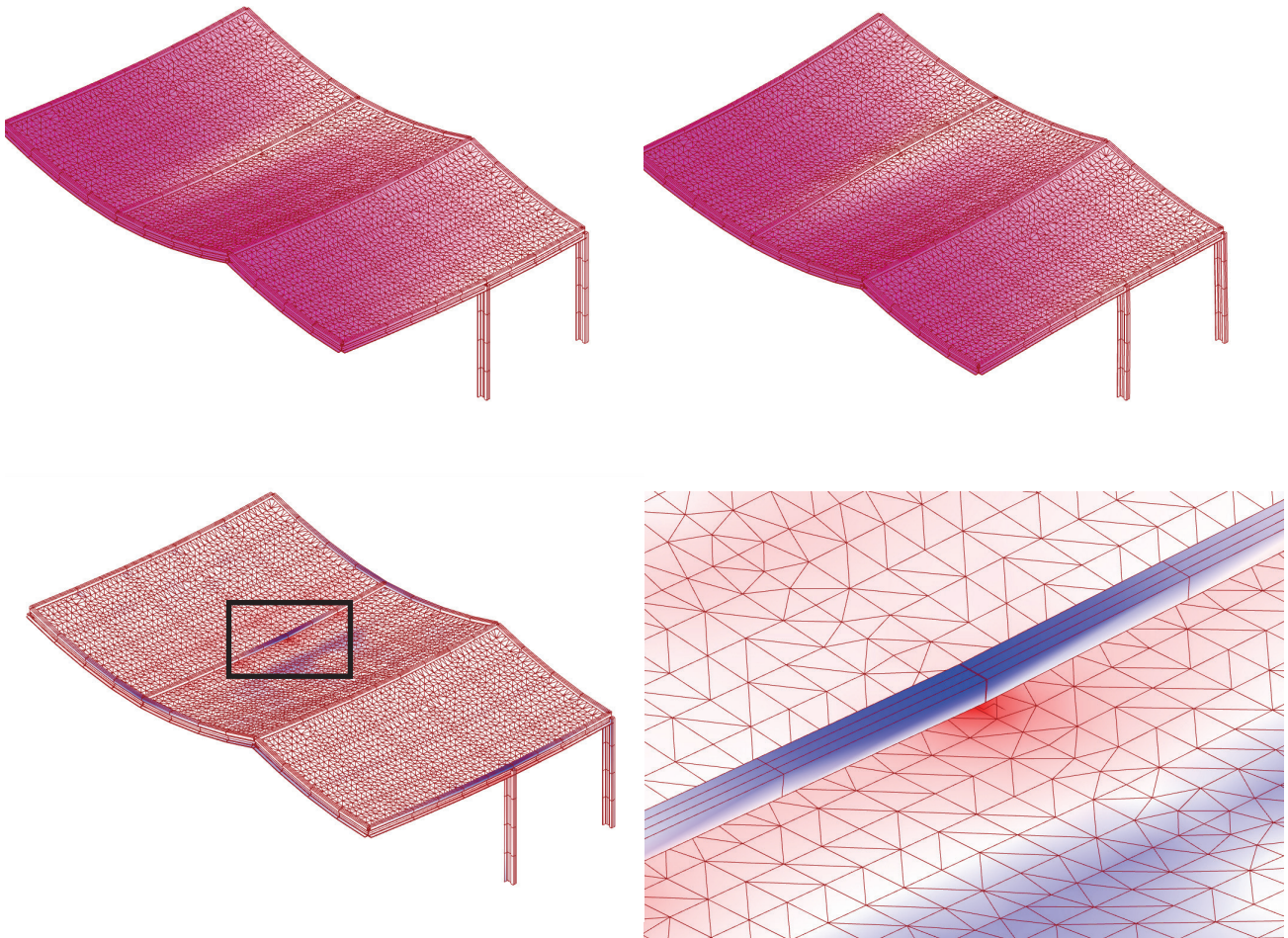


fig. 8.4.9: double carport analysis  
top left: no deflection  
top right: deflection (exaggerated)  
bottom left: stress simulation  
bottom right: stress zoomed in

### analysis

In this simulation (fig. 8.4.9) the triple configuration is analyzed. As concluded from previous simulations, the design needs a beam on top of the green wall to strengthen the structure. With a maximum deflection of 2,58 cm and a maximum tensile stress of 15,0 kN/cm<sup>2</sup>, it still exceeds the maximum tensile stress that tempered glass is able to take. The stress concentrates around the column of the design. This can be solved, as previously mentioned, by good detailing.

## 2 by 2 parkingspot configuration

max deflection: 0.53 cm

max tensile stress: 3.94 kN/cm<sup>2</sup>

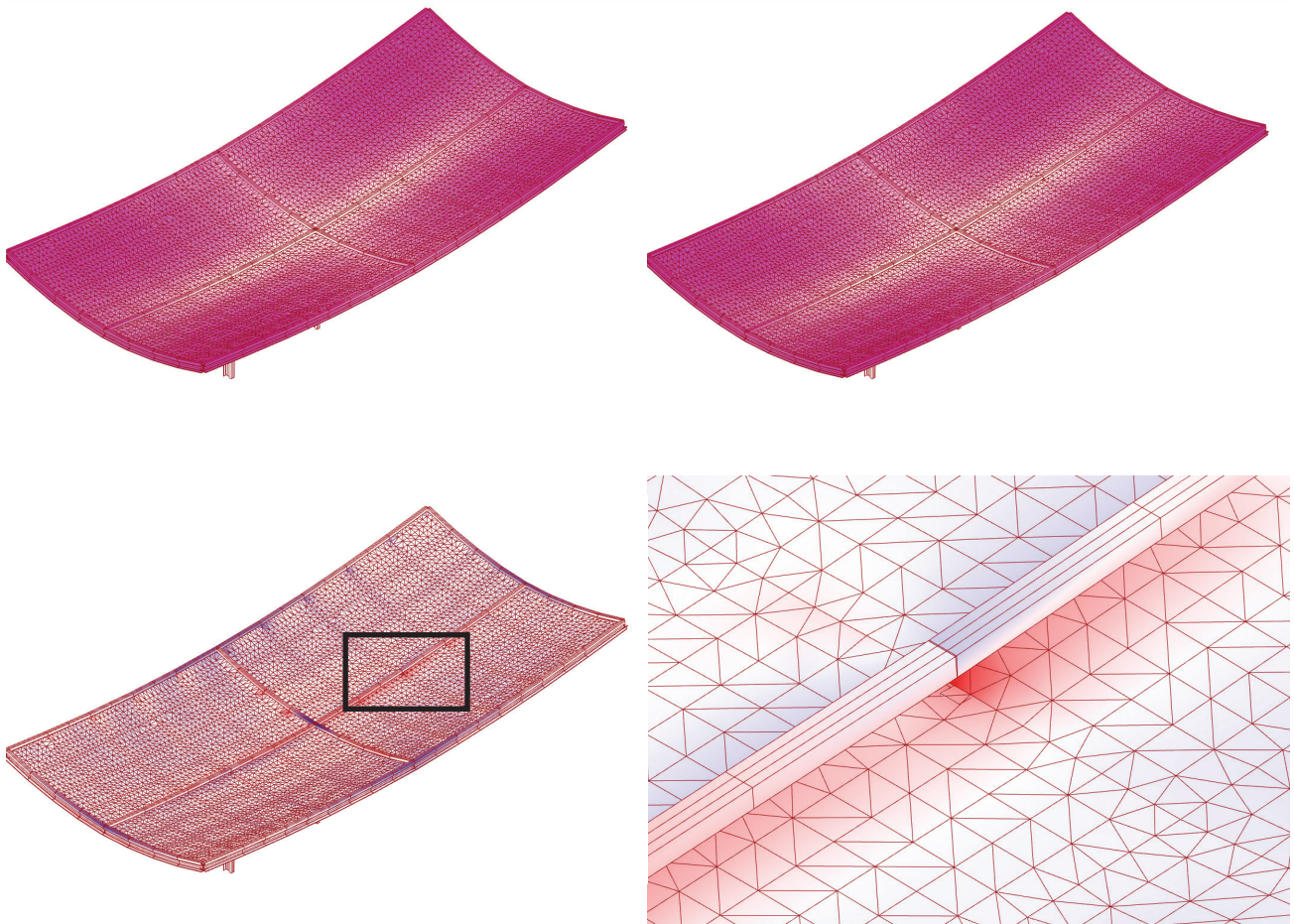


fig. 8.4.10: double carport analysis  
top left: no deflection  
top right: deflection (exaggerated)  
bottom left: stress simulation  
bottom right: stress zoomed in

### analysis

In this simulation (fig. 8.4.10) the 2 by 2 configuration is analyzed. As concluded from previous simulations, the design needs a beam on top of the green wall to strengthen the structure. With a maximum deflection of 0,53 cm and a maximum tensile stress of 3,94 kN/cm<sup>2</sup>. This is below the maximum tensile stress glass is able to absorb and therefore this configuration is viable. Even in this configuration, the stresses concentrate around the column of the design. This can be solved, as previously mentioned, by good detailing.

## 8.5 CONNECTION ANALYSIS

In this chapter, the connections in the structure will be analyzed. There are two types of connections recognized for this analysis, the first being the connection between the rail tracks and the second being the connection between solar panels. In the first analysis, the designed connection of the rail tracks will be calculated with hand calculations. In the second analysis, a FEM simulation is done to gain understanding about what influences the angular deflection of the connection between solar modules.

### rail track connection

As mentioned previously the connection between rail tracks is calculated through hand calculations. These hand calculations will determine the thickness of the steel plate used to connect the rail tracks and the amounts of bolts needed to transfer the load through the steel plate to the rail track. There are two ways of transferring the load from the plate to the rail tracks, one being via friction whilst the other relies on shear stress to transfer the loads.

The following loads are recognized at the level of the connection. One being the bending moment ( $M$ ), this bending moment will result in a torque force acting on the steel plate and the bolts, whilst the other is the shear force acting on the structure. The shear force ( $V$ ) acts on the two steel plates on the top and bottom side of the connection. The loads that are recognized are shown in (fig. 8.4.1).

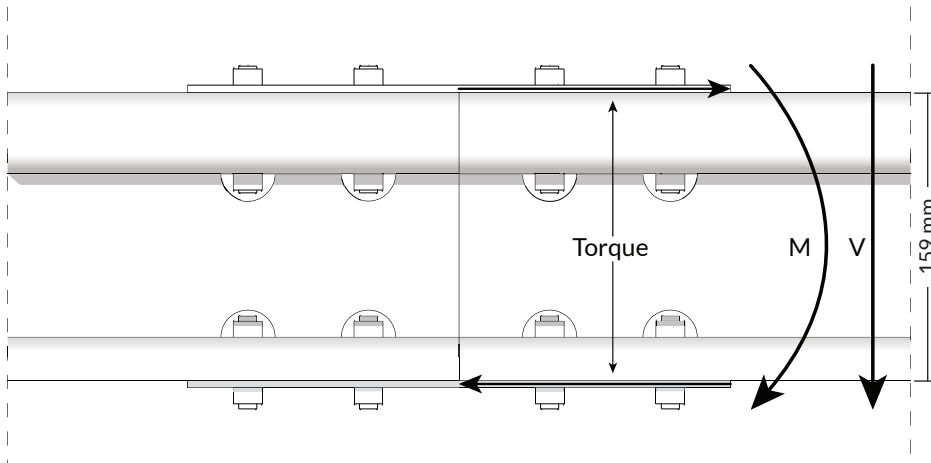


fig. 8.5.1: forces at connection level

The steel plates have two methods of transferring the loads from one rail track to the other, one being friction, whilst the other being shear force. In this analysis, both are calculated separately to show that in one load case the connection is able to transfer the load but also in the other load case. In reality, the force will be transferred via both friction and shear force. The result of designing the connection for either of the two loads is that the connection has a certain safety measurement built into it.

To determine the minimum thickness ( $t$ ) of the steel plates the bending moment is extracted from the Karamba simulation. The configuration of the design taken for this calculation is the design with the highest bending moment present in the rail tracks. The highest bending moment is present in the double row configuration of the design. The maximum bending moment in this design is 7,4 kNm located at the middle of the design where four beams come together. The location of the maximum bending moment is illustrated in (fig. 8.5.3). By dividing the maximum bending moment with the height of the rail track 0,159m, the torque can be extracted. The maximum torque ( $T$ ) is calculated to be 46,5 kN. The other force acting on the steel strips is the shear force. The maximum shear force ( $V$ ) in the simulation of the double row configuration of the design is 10,6 kN. Since this force acts on both steel strips it is divided by two to create the force that acts on one steel strip. The total force that acts on one steel strip is thereby set to 51,8 kN.

The next step in the calculation is to determine the width of the steel strips. Although the top flange of the rail track is 70 mm, this is not the maximum width of the steel strip. The ends of the flange have some curvature, as can be seen in (fig. 8.5.2), and therefore the maximum width ( $w$ ) of the steel strips is set to 50 mm. Although the bottom strip can be made wider, both strips are made identical to simplify the construction of the design. The steel that is chosen is widely used construction steel S235. S235 steel has a yield strength ( $f$ ) of 235 N/mm<sup>2</sup>. With all parameters known the thickness of the steel strip can be calculated using the following formula:

$$t = \frac{T + \frac{V}{2}}{w * f}$$

The calculated minimal thickness of the steel strip is 4,41 mm. In the design, this is rounded upwards to 4,5 mm. This gives the following dimensions of the steel strips: 50mm x 4.5mm. The length is not a crucial parameter for the strength of the strips. In the next calculation, the number of bolts is calculated/

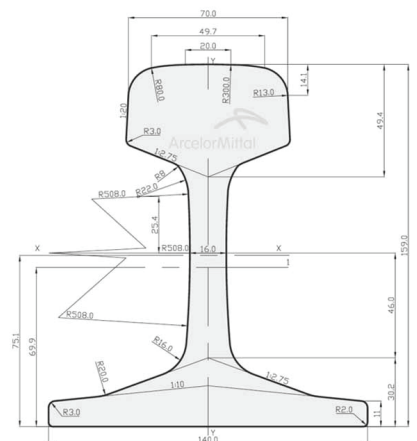


fig. 8.5.2: Railtrack dimensions  
left: original 54E1 rail track dimensions (source: Arcelor Mittal)  
right: karamba model dimensions

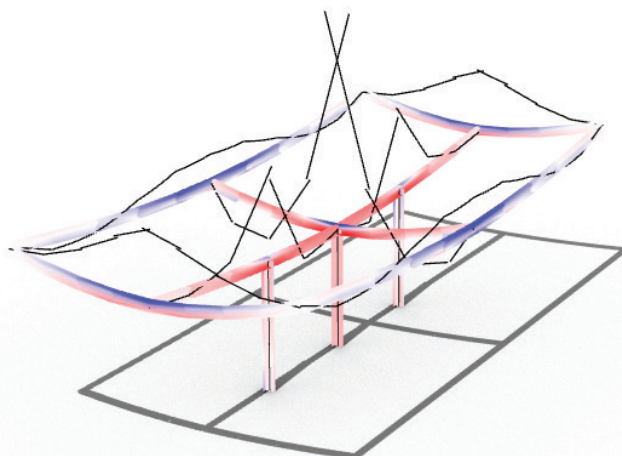


fig. 8.5.3: stress in beams with max bending moment lines

The first method of transferring the loads from one rail to the other to be calculated is via friction. To eventually get to the number of bolts needed the normal force ( $F_n$ ) needed to transfer the loads via friction needs to be calculated. To calculate the normal force a friction coefficient is needed. Each material has a different friction coefficient relative to another material. In the case of this connection, the two materials are steel and steel. The formula to calculate the force of friction is as follows:

$$F_f = \mu F_n$$

This formula is then re-written to give the normal force as a result of the formula, since the other elements of the formula are already known:

$$F_n = \frac{F_s}{\mu}$$

The force  $F_s$  is the force of the torque of the bending moment, resulting in a force of 46,5 kN. The friction coefficient of steel on steel is 0,7<sup>[8.5]</sup>. By dividing the  $F_s$  with the friction coefficient the following normal force is extracted; 66,5 kN. The number of bolts is set to 4. Reason for this being the force needs to be distributed over multiple bolts since if a since the bolt is used per side and the bolt fails, no force is able to be transferred. This number of bolts results in a force per bolt of 16,6 kN. The tensile force of the bolts is set to 300 GPa, this equals to AISI 403 Annealed steel<sup>[8.6]</sup>. To calculate the required area of the bolt, then the force per bolt is divided by the tensile force of the material. This results in a required area of 55,41 mm<sup>2</sup>. Following the required area, the required diameter is calculated to be 8,4 mm. The closest metric bolt size is M10 with a diameter of 10mm. By using this diameter it allows one bolt to fail, whilst the other still be able to transfer the load. If one bolt fails the force per bolt increases to 22,2 kN. Resulting in a required area of 73,87 mm<sup>2</sup> and a required diameter of 9,7 mm.

The other method of transferring loads, in this case, is via shear force. The force present in the beams is transported through the bolts in the steel plates to be transferred through the plate to the other rail track, as seen in (fig. 8.5.5). To calculate the shear stress in the bolts the torque force is added onto the shear force divided by the number of plates, 2, in the structure. This results in a force of 51,8 kN per side, divided by the number of bolts calculated in the friction method, this results in a force of 12,95 kN per bolt. With the following formula the shear stress is ca This is then divided by the tensile strength of the steel used in the bolts, 300 GPa, resulting in a required area of 43,20 mm<sup>2</sup>. This equals to a diameter of 7,42 mm, with the closest metric bolt being M8. When a bolt fails and three bolts need to handle the load the force per bolt is 17,28 kN, resulting in a required area of 57,60 mm<sup>2</sup>. This equals to a diameter of 8,56 mm, with the closest metric bolt being a M10.

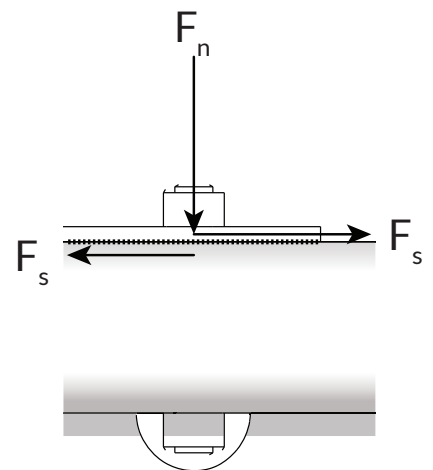


fig. 8.5.4: Zoom in friction load transfer

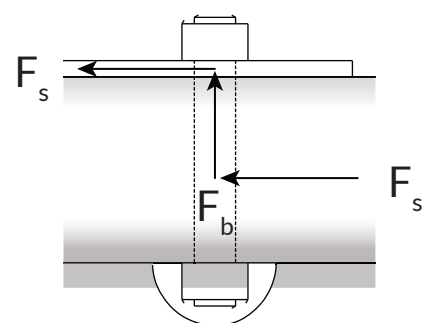


fig. 8.5.5: Zoom in shear force load transfer

The calculations both result in the use of four M10 bolts. This allows for one bolt to fail and the other bolts still are able to transfer the load to the other rail track. The result of this calculation is a connection where some safety margin is taken into account, as well as the dimensions of the bolts but also in the method of calculating. Since in reality, the forces are transferred via shear force and via friction, but by showing the connection is able to do it with either one of the methods there is a safety margin.

## connection solar panels

One of the drawbacks of the connection of Niki Nikalaou is the substantial size of the contact block. This contact block negatively influences the transparency of the structure. The design evolution proposed in this research reduces the size of the contact block to increase transparency.

In the old situation, the two panels would be placed opposite to each other in the contact block. In the new situation, the panels are placed alternately behind each other, see (fig. 8.5.6) for a simplification of the new situation. This allows the contact block to be more than half the size than the old situation and therefore increasing the transparency of the connection.

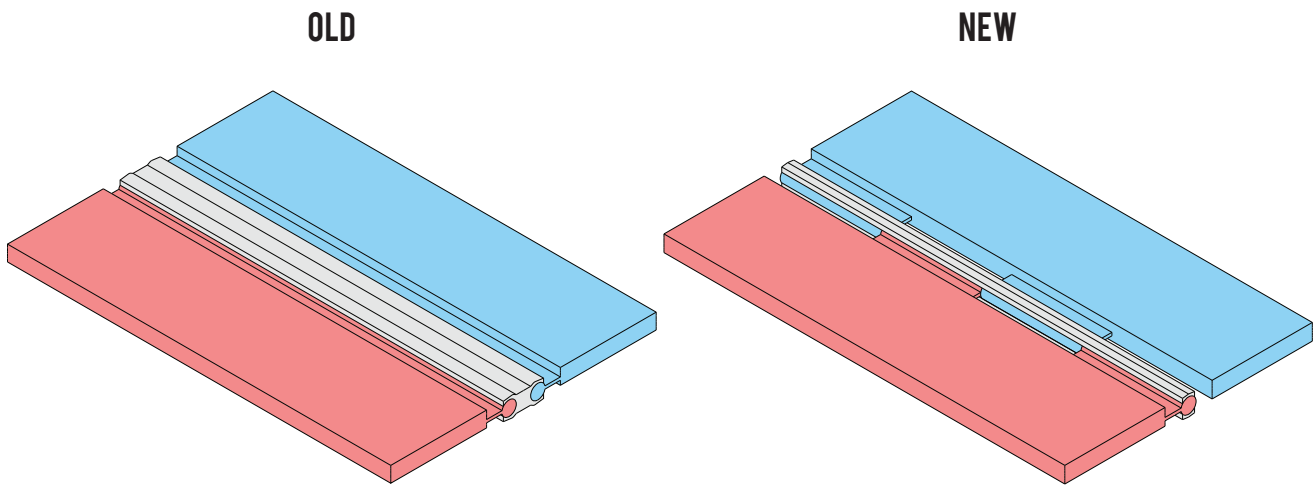


fig. 8.5.6: proposed evolution of mechanical connection  
red: panel  
blue: opposite panel  
grey: contact block

This evolution of the connection results in an altering bending moment on the contact block as illustrated in (fig. 8.5.7). As a result of this bending moment, the contact block will deflect. Due to the different direction of the bending moment, the contact block will deform in two directions as illustrated in (fig. 8.5.7).

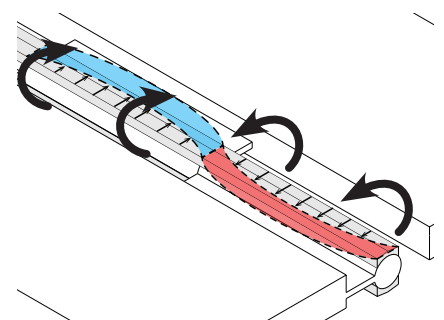


fig. 8.5.7: bending moment direction at contact block and resulting deflection

To understand the behavior of the connection under these circumstances, a schematic drawing is made (fig. 8.5.8). The bending moment results in the upper contact block deflecting to the left, whilst the bottom contact block deflects to the right. This deflection, also known as angular displacement, will result in a bigger deflection of the structure. When the angle increases, the total deflection of the structure increases. The angle can be calculated by the following formula:

$$\tan X = \frac{2\text{Deflection}}{\text{Height}}$$

To gain an understanding of what influences the angular deflection, a FEM simulation is made in Diana. In Diana one side of the contact block is modeled. The contact block is simplified to a rectangular block. The length of the contact block in the model is 1 meter, similar to the length of the solar modules used in the design. The thickness is set to 5mm, close to the original thickness of the contact block set by Niki Nikilauo. For a starter, the model is divided by 4 equal parts. Each part equals to a connection. At the end of the model, the contact block is supported, these supports are fixed in X, Y, and Z direction. This will cause a wrong deflection in the first part of the model, but in the middle, a deflection that is more closely matched to reality will show. The bending moment is extracted out of the Karamba simulation of the final design. In this Karamba model some peak bending moment of 0,4 kNm/m. These peak bending moments can be solved with good detailing of the structure, therefore the more representative bending moment of 0,29 kNm/m is taken instead. This bending moment is then divided by the length of the subdivision, in the first case, this is 250mm. The force on the area of the contact block is calculated by dividing the bending moment with the thickness of the total connection. This result in a force of 2,07 kN/ This is then divided by the area to create a force per mm<sup>2</sup>, 0,41 N/mm<sup>2</sup>. Aluminum is chosen as a material for the first simulation of the contact block.

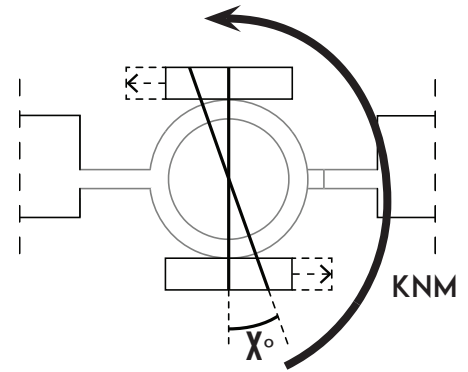


fig. 8.5.8: schematic drawing of connection and deflection



fig. 8.5.9: diana model overview

The first simulation (fig. 8.5.10) used an aluminum contact block with a thickness of 5mm and a subdivision length of 250mm. This resulted in a maximum deflection of 3,12mm to - 3,12 mm. This results in an angle of 10,1 degrees.

In the second model (fig. 8.5.11) the thickness of the aluminum contact block is increased to 7 mm, whilst retaining the 250 mm subdivision. This resulted in a maximum deflection of 2,23 mm to - 2,23mm. This results in an angle of 7,3 degrees.

In the third model (fig. 8.5.12) the material of the contact block is changed from aluminum to steel. The thickness of the steel contact block is set to 7 mm, whilst retaining the 250 mm subdivision. This resulted in a maximum deflection of 0,76 mm to - 0,76mm. This results in an angle of 2,5 degrees.

In the fourth and final model (fig. 8.5.13) the subdivision length is decreased to 166mm, resulting in 6 connections per meter. The material of the contact block is kept to steel and the thickness of 7 mm is used. This resulted in a maximum deflection of 0,23 mm to - 0,23mm. This results in an angle of 0,75 degrees.

The goal of this simulation was to gain an understanding of the parameters that influenced the angular deflection of the contact block. The parameters that were found to have influence are:

- Thickness of the contact block
- Material of the contact block
- Sub division length

In further research, this aspect of the improved connection must be further simulated and calculated to gain understanding about the impact of the angular deflection on the total structure and what thickness, material and subdivision length is needed. For this research 7mm steel is used in combination with 4 subdivisions.



fig. 8.5.10: diana simulation result, 5mm aluminum, 250mm length of sub division



fig. 8.5.11: diana simulation result, 7mm aluminum, 250mm length of sub division

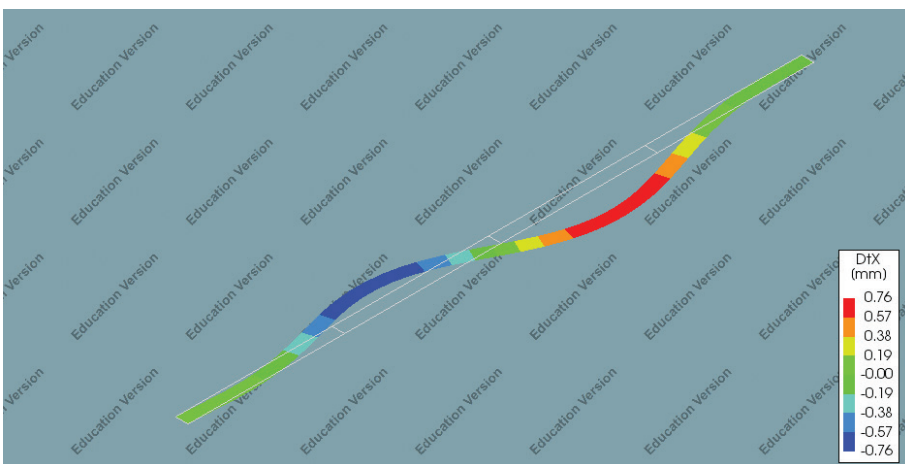


fig. 8.5.12: diana simulation result, 7mm steel, 250mm length of sub division



fig. 8.5.13: diana simulation result, 7mm steel, 166 mm length of sub division

## 8.6 COMPARISON CONNECTION WITH EXISTING CONNECTION

To gain insight into the sustainable material use of the connection, a comparison is made between a regularly used aluminum transom and mullion system and the designed connection in this report. A side by side detail is shown in (fig. 8.6.1). From the comparison, the difference in dimensions is clearly visible

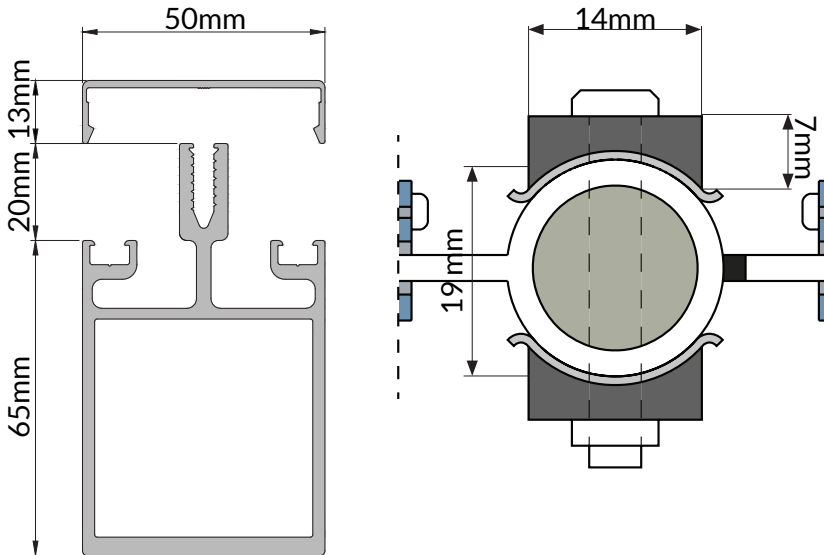


fig. 8.6.1: comparison connections (no scale)

For the aluminum transom and mullion system the following dimensions are chosen; 50 x 65. For the designed connection, the biggest dimensions analyzed in this report is chosen to give a true insight into the CO<sub>2</sub> footprint of the two designs. The CO<sub>2</sub> footprint will be calculated over one panel. This results in the materials partaking in this calculation as half of the connection around a panel and the glass in the panel, since the new connection requires an extra pane of glass. The rubbers and nuts and bolts are not incorporated in the calculation since for one the influence on the outcome is minimal and the amount of nuts and bolts is unknown in both connection types. In the table below the cubic materials integrated into the two connections are shown, together with the CO<sub>2</sub> footprint per material<sup>[7.1]</sup>. This leads to a total CO<sub>2</sub> footprint of both designs.

Material (CO <sub>2</sub> footprint kg/kg)	new connection		standard connection	
Aluminum (12,85 kg/kg)			0,00145 m <sup>3</sup>	50,48 kg CO <sub>2</sub>
Steel (1,81 kg/kg)	0,00011 m <sup>3</sup>	4,98 kg CO <sub>2</sub>		
Lam. glass (1,755 kg/kg)	0,00652 m <sup>3</sup>	27,45 kg CO <sub>2</sub>	0,00470 m <sup>3</sup>	19,81 kg CO <sub>2</sub>
Glassfibre (6,54 kg/kg)	0,00061 m <sup>3</sup>	7,02 kg CO <sub>2</sub>		
Total:		39,46 kg CO <sub>2</sub>		70,29 kg CO <sub>2</sub>

table. 8.6.1: CO<sub>2</sub> footprint calculation

This calculation shows that the newly designed connection, not only boosts the transparency of the design but also improves the CO<sub>2</sub> footprint of the connection by +- 30 kg footprint per panel.

Besides creating a more transparent design, the connection also proves to have a smaller CO<sub>2</sub> footprint than the more conventional aluminum mullion and transom system.

## 8.7 FINAL CONCLUSIONS AND RECOMMENDATIONS

The goal of this research was to create a solar carport with structurally integrated PV cells, that was applicable on every P+R parking plot with different orientations (without alterations), that was modular in design, represented of the NS whilst remaining the function as a parking lot.

To accomplish this a literature research in PV technology and the structural capabilities of PV pan-els was conducted. The goal of both topics was to generate design parameters for the final design. Research in PV technology showed three generations of PV technologies. The third generation was deemed to be out of the scope of the research due to market availability. The PV tech researched showed different characteristics from the various technologies. The structural capabilities of PV technologies showed that the solar cell within the module is a fragile piece. Extra precaution should be taken when designing with PV modules that the cells within the modules are subjected to as little stress as possible. Research showed that when a PV panel is mechanically loaded, the cells are subjected to cracking, however when the mechanical load has decreased the cracks that occurred in the cells closed again and were undetectable in a static state.

The image that the NS wanted to be represented by the design was noted by them in their design requirements. The design should be open, transparent (for social security and light savings), modular and flexible (to be applicable on every P+R plot), apply principles of circular material use and have a sustainable (green) appearance.

The best suitable technology for the design was selected via a multi-criteria method called the analytical hierarchy process. in this method, multiple criteria's and alternatives were compared to each other. The importance of the criteria's was set by the parameters for the final design appearance. As a result of the AHP, the poly crystalline silicon was selected to be the best suitable technology for the design. This technology showed great recyclability and efficiency, whilst still having a relatively low energy payback time.

One of the design requirements of the NS was a modular design. This was done by following the guidelines set by the program of requirements for parking spots of the NS. In this program of re-quirements, measurements were given for different layouts of the parking plot(double row and sin-gle row). The final design takes these measurements into account. By designing a connection that allows for either a 90-degree bend or a T connection the design can be expendable. The design also takes the different layouts into account. The design can be applied in a single row or double row configuration and an even or uneven amount of parking spots is possible.

Analysis of current carports showed that all of the designs have the structure placed parallel to the parking spot for minimal influence on the functionality of the parking spot. This is implemented in the final design.

Different options of manners to integrate the solar panels into the structure are researched. In the end, the product of a master thesis of the TU Delft is selected. The connection is analyzed and the conclusion is made that the transparency of the connection can be increased by decreasing the size of the contact block. This is done by altering the connection of opposite elements in the same contact block. The influence of the improvement of the connection is analyzed. This analysis showed that certain parameters have an impact on the angular displacement of the connection. These parameters are the Young's modulus (material), the thickness of the contact block and the length of the subdivision all have an influence on the angular displacement of the connection. The more substantial the angular displacement is the bigger the overall displacement of the structure. This aspect of the final connection requires further research. This research should show the maximum angular displacement that is allowed in the structure and what the parameters mentioned above should be.

The structural performance of the design is simulated. In this simulation, the different variations of the design are analyzed on their structural performance. This analysis showed that in a one parking spot configuration the design showed a substantial deflection. This deflection makes the user below feel unsafe and therefore the conclusion is made that the current design cannot be applied in a single parking spot configuration with the load set in the analysis. The P+R plots don't call for a single parking spot configuration and therefore no solution for this problem is researched. The other configurations of the solar carport showed small deflections but some peak tensile stresses. The main reason for this being that the model used in the analysis had a planarized panel configuration and the program only connects the edges of these panels to the edge beam. This results in peak tensile forces. The dimensions of the connection between the rail tracks is calculated via hand calculations, since this design step was made late in the research process. Therefore the recommendation is made to further simulate and analyze this connection.

The solar performance of the design is analyzed. This analysis showed that the design can be placed in any orientation whilst retaining the same solar radiation on the surface of the structure. The final solar radiation mentioned is not the final output of the design. The efficiency of the solar cells used, cable losses, etc. should be deducted from this number to gain a full understanding of the final output of the design.

The final design features a transparent PV panel design, that allows for light to pass through on darker days for light savings and social security. In the design bifacial solar cells are implemented. In this application bifacial cells are functional since the cars that are parked below the design reflect the light, that passes through the transparent solar panels, on the backside of the solar cells. When a bifacial cell is implemented this light will be converted to electrical energy. The end of life rail tracks implemented in the design applies the principle of circular material use. Besides the shape of the rail tracks being almost perfect I beam, the direct link to the stakeholder is an additional benefit of this material. The downside of the rail tracks is the weight of the material.

## 8.8 BIBLIOGRAPHY

- [8.1] Saaty, T. (1980). The analytical hierarchy process. New York: McGraw-Hill.
- [8.2] Haghghi, Z., Lizcano, J. C., van den Dobbelsteen, A., Isabella, O., Konstantinou, T., Klein, T., & Zeman, M. (2018). Assesment of the suitability of photovoltaic cell technologies for product development of building integrated solutions using the analytical hierachy process(AHP). Delft.
- [8.3] San Cristóbal Mateo, J. (2012). Multi-Criteria Analysis in the Renewable Energy Industry. New York: Springer-Verlag.
- [8.4] Hui, S. C. M. and Chan, S. C., (2011). Integration of green roof and solar photovoltaic systems, In Proceedings of Joint Symposium 2011: Integrated Building Design in the New Era of Sustainability, 22 November 2011 (Tue), Kowloon Shangri-la Hotel, Tsim Sha Tsui East, Kowloon, Hong Kong, p.1.1-1.10.
- [8.5] Robbins, M., Saronson, D., Szeto, G., Rozenberg, D. (2005). Coefficients Of Friction For Steel. Retrieved from <https://hypertext-book.com/facts/2005/steel.shtml>
- [8.6] Granta (2018). CES EduPack 2018 (18.1.1) [Software]



9.

## **PERSONAL REFLECTION**

## 9.1 PERSONAL REFLECTION

### aspect 1:

The relationship between research and design.

The starting point of my graduation project was a design question, what would the design of a modular shelter for cars be when taken into account the integration of solar panels into the structure with maximum solar gain, different orientations and the image of the NS whilst keeping the function as a parking lot? Partly this question originated from the stakeholder, the NS. They wanted to know what was possible for a solar carport design that is applicable on every P+R parking plots without the restriction of cost.

The final solar carport design is a product of a research on PV technology combined with a research into the structural behavior of PV modules. The literature studied directly fed the design (research for design). During the pilot study, a design was used to study the impact of integrating the solar modules into the structure (research by design). The literature study, case studies, and pilot study formed guidelines for the conceptual designs, where creative ideas and knowledge from the researched combined into three designs. Segments of these conceptual designs formed the final design concept. This concept featured a mechanical connection between glass panels found in the literature. This connection was evolved to increase the transparency of the design.

At the beginning of this research, I always found it hard to connect research with design and visa versa. The main reasoning for this is that some design decisions are made from within. In this research decisions and how to give insight into these design decisions. The main misstep I made during this graduation was that I spend too much time researching and as a result, the time for designing was less than I would have liked.

### aspect 2:

The relationship between the theme of the graduation lab and the subject/case study chosen by the student within this framework (location/object)

My graduation, the solar carport with structurally integrated solar panels, relates to the climate design and structural design chair of the sustainable graduation studio of the building technology track. Within the building technology track, there are four chairs, all of which are related to sustainability. Sustainability had a great influence on this graduation project. Within the project these topics touch upon sustainability: minimizing the required energy for the structure, generating energy in a sustainable manner and maximizing the structural use of materials. In addition, sustainability can also be found through material choice and designing with demountability of the design in mind to allow materials to be re-used in another life.

The building technology always has been focused around designing in combination with engineering. Due to my background in building engineering, I have always been more engineering-minded. During this graduation, I learned a lot about designing and this resulted in a more balanced interest in designing and engineering.

### **aspect 3:**

The relationship between the methodical line of approach of the graduation lab and the method by the student in this framework.

Within the building technology master track, a lot of research is done through design. This was applied in the pilot study and the design stage of this graduation project. During the pilot study, design parameters were found for the designs. However, some elements of the research are based on research for design, which has the goal to supply enough knowledge which can be used to make a design. An example of this is the literature study at the start of my graduation process about PV technologies and the structural behavior of solar modules. This literature study fed the final design with the knowledge to create a relationship between research and design.

The misstep I made when setting up the framework is that I miss judged the time it took to do the pilot study. Although it gave me some relevant information, the usefulness can be debatable. The questions answered in the pilot study could also be answered during the analysis of the final design.

### **aspect 4:**

The relationship between the project and the wider social context.

The energy transition is a social topic. To achieve the transition to sustainable energy, solar panels need to be integrated into the built environment. The placement of the solar carport design besides railway stations makes people aware of the energy transition that is needed to create a more sustainable planet. Besides the awareness the design creates for the energy transition, the design also acts as a showcase of how solar panels can strengthen a design instead of being an add-on onto a structure with no architectural impact. Showing passengers of the trains that there are other options regarding solar panels than the standard crystalline solar panels.

### **aspect 5:**

Discuss the ethical issues and dilemmas you may have encountered in (i) doing the research, (ii, if applicable) elaborating the design and (iii) potential applications of the results in practice.

During the research a NEN norm was consulted. The only problem with this NEN norm is that it was outdated. The applicable NEN norm was out of reach. The media library of the TU Delft didnt have excess to this document.